HYDROGEOCHEMICAL INVESTIGATION OF GROUNDWATER QUALITY IN ZING AND ITS ENVIRONS, PART OF JALINGO SHEET 236NE, NORTH-EASTERN NIGERIA

BY

HUSSAINI, Sunday Ushe
MTech/SPS/2018/8463

DEPARTMENT OF GEOLOGY
SCHOOL OF PHYSICAL SCIENCES
FEDERAL UNIVERSITY OF TECHNOLOGY
MINNA, NIGERIA

JUNE, 2023

HYDROGEOCHEMICAL INVESTIGATION OF GROUNDWATER QUALITY IN ZING AND ITS ENVIRONS, PART OF JALINGO SHEET 236NE, NORTH-EASTERN NIGERIA

BY

HUSSAINI, Sunday Ushe
MTech/SPS/2018/8463

A THESIS SUBMITTED TO THE POSTGRADUATE SCHOOL FEDERAL UNIVERSITY OF TECHNOLOGY, MINNA, NIGERIA IN PARTIAL FULFILMENT AND REQUIREMENTS FOR THE AWARD OF THE DEGREE OF MASTER OF TECHNOLOGY (MTech) IN GEOLOGY (HYDROGEOLOGY)

JUNE, 2023

DECLARATION

I hereby declare that this thesis titled **"Hydrogeochemical Investigation of Groundwater Quality in Zing and its Environs, Part of Jalingo Sheet 236NE, North-Eastern Nigeria"** is a collection of my original research work and has not been presented for any other qualification anywhere. Information from other sources (Published and Unpublished) have been duly acknowledged.

HUSSAINI, Sunday Ushe
MTech/SPS/2018/8463
FEDERAL UNIVERSITY OF TECHNOLOGY
MINNA, NIGERIA

…….
Signature and Date

CERTIFICATION

The thesis titled **"Hydrogeochemical Investigation of Groundwater Quality in Zing and its Environs, Part of Jalingo Sheet 236NE, North-Eastern Nigeria"** by HUSSAINI**,** Sunday Ushe (MTech/SPS/2018/8463) meets the regulations governing the award of the degree of Master of Technology (MTech) of the Federal University of Technology, Minna and it is approved for its contribution to scientific knowledge and literary presentation.

DR. MRS. S.H. WAZIRI ……
SUPERVISOR Signature & Date

DR. MRS. S.H. WAZIRI ……...
HEAD OF DEPARTMENT Signature & Date

PROF. M. JIYA ……
DEAN, SCHOOL OF PHYSICAL SCIENCES Signature & Date

ENGR. PROF. O.K ABUBAKARE …….
DEAN, POSTGRADUATE SCHOOL Signature & Date

DEDICATION

This reseach work is dedicated to the Almighty God for making it a reality despite challenges. Secondly, to my dear wife, Mrs. Geyok-Sharon Sunday and my Son, Master Elijah Sunday as well as the Management of the Nigeria Hydrological Services Agency (NIHSA).

ACKNOWLEDGEMENTS

My profound gratitude to God for the opportunity, grace and good health He has availed to me to undergo the postgraduate programme successfully. I also want to acknowledge the management of the Nigeria Hydrological Services Agency (NIHSA) for the unconditional approval and support to pursue and satisfactorily complete this programme without any incuberances. My appreciation is also extended to all staff of the Department of Geology, particularly my supervisor, Dr.Mrs.Salome H. Waziri for her resilience, tenacity and time invested to ensure that the completion of my research work was achieved in good time.

I will also want to appreciate the postgraduate lecturers of the Department of Geology for moulding me academically to independently carry out these research work without any hitch. I also acknowledge the Coordinator of Water Sanitation and Hygiene (WASH), Mr. James Koyumba and his Assistant, Mr. Jonathan Gabriel during the field work at Zing and the surrounding communities. The commitment and support channeled towards the success of the fieldwork will ever remain indelible in my mind. A very big thank you to my friends and colleaques for their unrelenting care and assistance throughout these years study.

Finally, to my beloved wife, Mrs. Geyok-Sharon Hussaini and my Son, Elijah Silazeka Sunday, I salute your patience and also appreciate your prayers and understanding through out these years of academic exercise.

ABSTRACT

The hydrogeochemical investigation at Zing and its Environs, North-Eastern Nigeria, aimed at determining groundwater quality characteristics has been carried out. Geological mapping was accompanied by sampling of 19 rocks out of which 12 representative samples were analyzed for elemental and mineralogical compososition using X-Ray Fluorescence (XRF) and X-Ray Diffraction (XRD) methods. Similarly, 28 groundwater samples were collected and analysed for their physicochemical parameters using standard analytical methods. The outcome of the study suggests that the area is underlain by granite, granodiorite, gneiss and pegmatite enriched with major elements such as aluminium and silicon including trace elements of strotium and barium compared to others. The bulk chemical composition of the rocks in weight (wt%) of SiO_2, Al_2O_3, K_2O and MgO indicates enrichment of felsic and mafic minerals with major species such as quartz, albites, microcline and biotites. Other associated minerals are actinolites, annites, sinidine, zircon, kaolinites, magnetite and phlogopite. Field observations, elemental and mineralogical composition of the rocks shows that the rocks are of I-Type granitic rocks while the Chemical Index of Alteration(CIA) of the rock samples infers that they are moderate to higly weathered. All measured physicochemical, parameters heavy and trace elements parameters in the groundwater samples shows elevated concentrations compared to others in few and most of the locations. The chemical characteristics of the groundwater of the area infers that Ca^{+2} and HCO_3^- are the most dominant ions. 75% of the water samples corresponds to earth alkaline water with prevailing HCO_3^-, 14.3% are alkaline with predominant HCO_3^- while 3.6% each corresponds to normal earth alkaline water with predominantly HCO_3^2 and SO_4^{2-} or Cl^-, and earth alkaline water with prevailing SO_4^{2-} and Cl^- water respectively. The hydrogeochemical facies of the groundwater system revealed four classification with 71.4% of the samples characterized as Ca^{2+}- Mg^{2+}- HCO_3^-, 14.3% as Na^+- K^+- HCO_3^- while the two other facies are of Na^+- K^+- Cl^- SO_4^{2-} and Ca^{2+}-Mg^{2+}- Cl^--SO_4^{2-} respectively. The chemical constituents in groundwater of the area are derived from chemical weathering of granitic rocks. Additionally,water rock interaction, a combination of evaporation and precipitation, ion exchange, dissolution and mixing have been identified as the main hydrogeochemical processes influencing groundwater chemistry of the study area.

TABLE OF CONTENTS

CHAPTER TWO

2.0 LITERATURE REVIEW

CHAPTER THREE

LIST OF TABLES

LIST OF FIGURES

LIST OF PLATES

LIST OF APPENDICES

CHAPTER ONE

1.0 INTRODUCTION

1.1 Background to the Study

Water is an essential component of life on earth which contains vital minerals extremely important in human nutrition (World Bank, 1997) and is very essential for sustaining life. Groundwater is one of the major sources of water supply for various uses globally because it is comparatively fresh and widely distributed unlike the surface water. However, the presence of certain chemical ions at a higher concentration has made groundwater unsuitable for utilization in some places (Brindha and Elango, 2011).

The geology of an area, the degree of weathering of rock types, chemical composition of precipitation, mineral composition of aquifer materials and the confining beds through which water flows, chemical reactions occurring on the land surface and in soil zones as well as anthropogenic activities is alleged to influence the chemistry of groundwater **(**Giridharan *et al.*, 2008; Aminu and Amadi, 2014). Hydrogeochemical processes are responsible for the seasonal, temporal and spatial variations of groundwater chemistry and subsequently their quality (Waziri *et al*., 2019).

The chemical composition of groundwater therefore is adjudged safe for utilization when it is within the permissible limit prescribed by the international and national water quality regulating agencies otherwise it becomes unsuitable for use and of great concern to human lives. Consequently, in response to the high demand for groundwater and the increased risk of contamination induced by natural or human factor, a better understanding of groundwater quality and its availability is needed for efficient management of the resource (Montcoudiol, 2015).

1.2 Statement of the Research Problem

The study area is underlain by the basement complex rocks that are weathered, jointed and fractured. These geological features and structures control the flow and distribution of groundwater which is one of the major sources of potable water supply in the area.

In view of the established geological environment, the quality of groundwater in the area is likely to be compromised as a result of likely geochemical processes within the aquifer materials resulting to concentration of chemical ions in groundwater. Furthermore, the recent increase in population due to migration from rural areas and high demand for groundwater as a result of urbanization has exerted pressure on the available resource and also increase waste generation and indiscriminate disposal. Hence, a potential threat to water quality degradation and consequential health challenge to inhabitants. Therefore, an effective groundwater development and management scheme will not be feasible without a comprehensive hydrogeochemical study of the area.

1.3 Aim and Objectives.

The aim of the research is to determine the groundwater quality characteristics of Zing and its Environs, North-Eastern, Nigeria. The objectives are to;

I. Produce a geological map on a scale of 1:30,000 for the study area.

II. Compare results of laboratory analysis of groundwater samples with the World Health Organization (WHO) and Nigerian Standard for Drinking Water Quality (NSDWQ) permissible limits.

III. Produce concentration maps of chemical elements identified to be above permissible limits and responsible for groundwater pollution the area.

IV. Determine the sources and processes influencing possible groundwater quality impairment in the area.

1.4 Justification for the Research

Water is vulnerable to contamination emanating from either geogenic, anthropogenic activities or a combination of both (Adedapo and Fokolade (2014). Studies revealed that 85% of all communicable diseases affecting humans are either water-borne or water-related (WHO, 2006; Amadi and Nwankoala, 2013a).

The increasing population and urbanization coupled with the nature of the geological environment may change the initial groundwater chemistry. Hence, the need to characterize the groundwater system towards providing the needed baseline data and information for development and management of groundwater in the area.

Prior to this study, there is no detailed hydrogeochemical investigations carried out in groundwater of Zing and its Environs. Hydrogeochemical study of the area will provide plausible insight on the status of groundwater quality and help create suitable management strategies to overcome any groundwater quality related issues in the area

1.5 Location, Description and Accessibility of the Study Area

Zing and its Environs, part of Jalingo Sheet 236NE, Taraba State, Northeastern, Nigeria has a total land area of about 1,052 square kilometres (Oruonye and Bange, 2015). However, the total land mass under investigation is estimated at 707 square kilometres and lies between Latitudes 08^0 44′.00” to 09^0 05′.00” and Longitudes 11^0 40′.0” to 11^0 52′.00”E (Figure 1.1) with a population of 170,600 (Nigerian Population Commission, 2006). It is bounded to the East by Mayo-Belwa Local Government Area, to the South by Jada Local Government Area (both in Adamawa State) and to the West by Yorro Local Government Area in Taraba State (Oruonye and Bange, 2015).

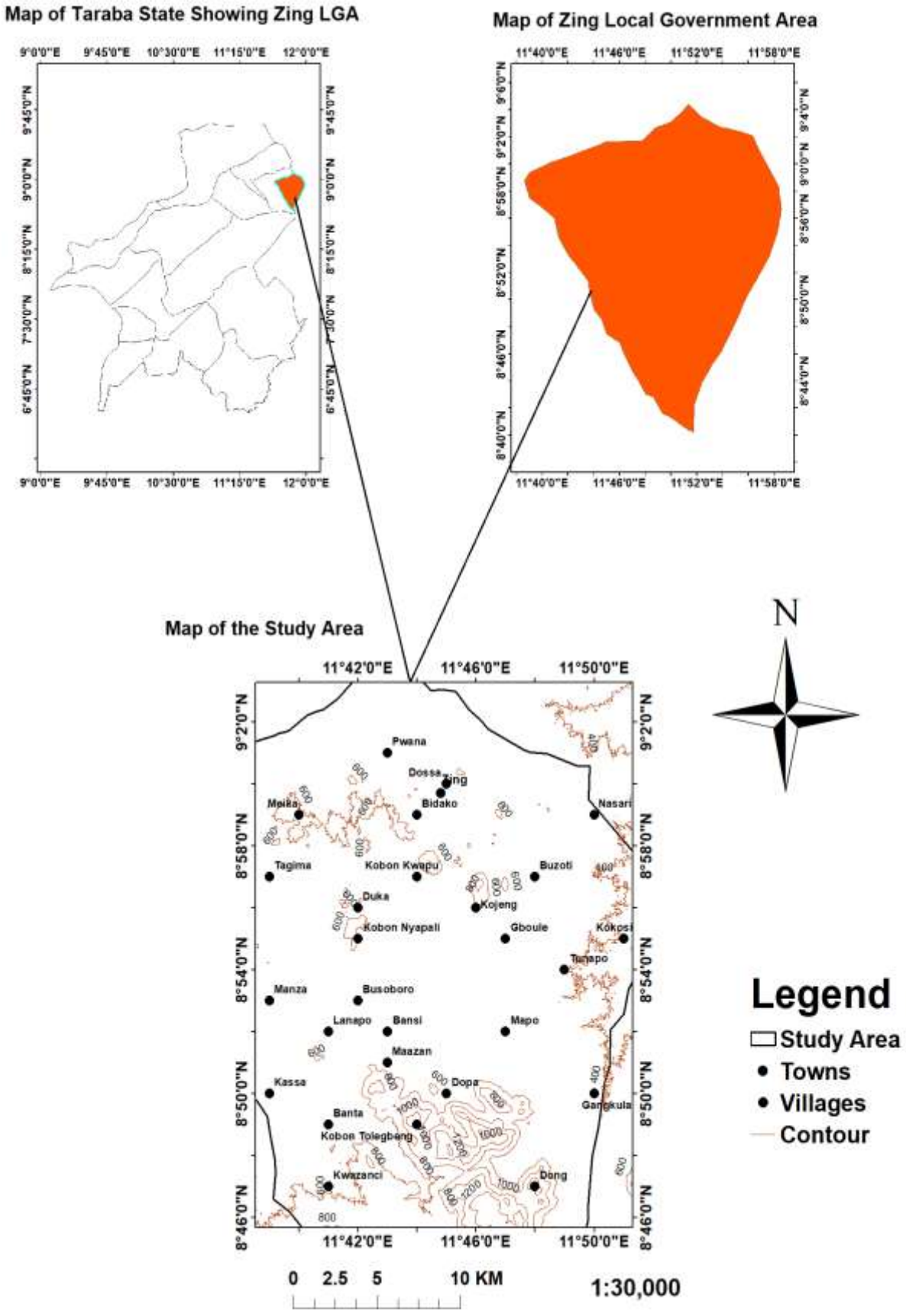

Figure 1.1 Topographic Map of the Study Area

1.6 Relief and Drainage

The study area is characterized by highlands/mountain ranges and lowlands. The highlands occupy the southern region stretching from the west to south in chains of mountain (shebshi mountains), with elevation ranging from 1,800 to 2,400 metres above sea level. This occupies 40% of the area while 60% of the landmass which is the lowland hosts most of the settlements in the area (Ray and Yusuf, 2011**).** The area is also endowed with natural resources such as rivers and streams such as Dingdin, Monkin, Kanini, Nyaho and Mayo Belwa flowing southwards draining the area (Plate 1 and Figure 1.2).

Plate I: Relief of Dinding, Southern Zing about 120m above sea level

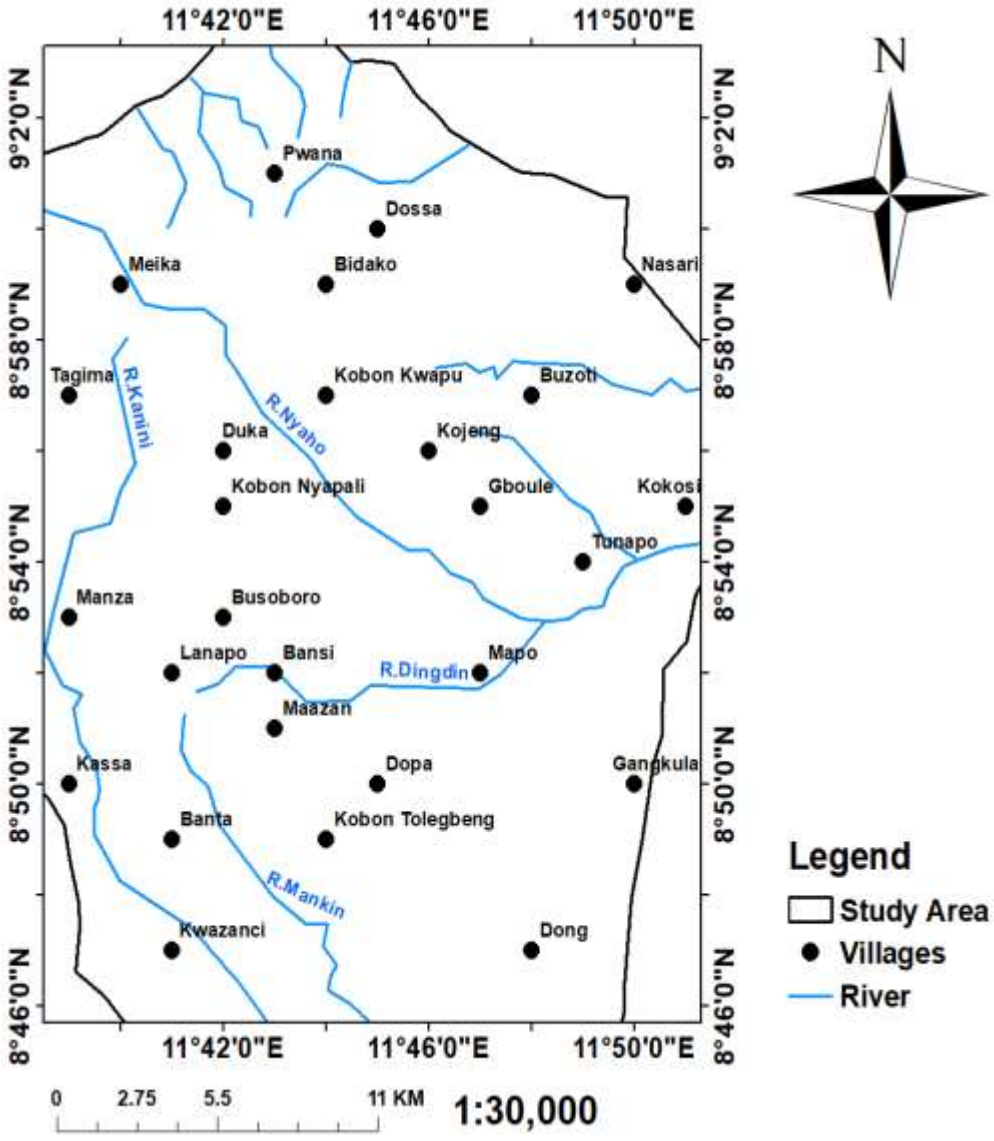

Figure 1.2: Drainage Map of Zing and Environs.

1.7 Vegetation and Climate

The study area lies within the transitional belt of savanna grassland belt particularly in the Guinea savanna. It has two distinct seasons namely-the rainy and dry seasons. The mean annual precipitation ranges from 819 to 1,761 mm. The onset of the rains is in April; with low amount but increases gradually reaching a maximum in August and drops gradually with cessation in October. The temperature is between 25^0C and 33^0C in both

the dry and rainy season with good climatic conditions for agricultural activities (Andy and Silas, 2020)

1.8 Land Use

The dominant tribe in the area is the Mumuye who account for 98% of the population. Other tribes are the Hausas and Zandis. The majority of the residents are farmers, few engage in petty trading while others are in the civil and public service of the Taraba State Government (Andy and Silas, 2020)

CHAPTER TWO

2.0 LITERATURE REVIEW

2.1 Preamble

Groundwater is a major source of fresh water globally and is being utilized for domestic, agricultural, and industrial purposes. Approximately one third of the global population depends on groundwater for drinking (International Association of Hydrogeologists (IAH, 2020). More often than not, groundwater chemistry is usually influenced by geogenic processes as a result of dissolution of the natural mineral deposits within the earth's crust (Pandey *et al*., 2016; Subba Rao *et al*., 2020). However, due to rapid global population expansion, urbanization, industrialization, agricultural production, and the economy, the population is faced with the challenge of negative impacts of contaminants from anthropogenic origin caused by chemicals, road salt, bacteria, viruses, medications, fertilizers, and fuel.

Groundwater contamination differs from contamination of surface water in that it is invisible and recovery of the resource is difficult (MacDonald and Kavanaugh, 1994). Contaminants in groundwater are usually colorless and odorless. In addition, the negative impacts of contaminated groundwater on human health are chronic and are very difficult to detect (Chakraborti *et al*.,2015). Once contaminated, remediation is challenging and costly, because groundwater is located in the subsurface geological strata and residence time are lengthy (Wang *et al*., 2020; Su *et al*., 2020). The natural purification processes for contaminated groundwater can take decades or even hundreds of years, even if the source of contamination is cut off (Tatti *et al*.,2019).

2.1.1 Types and sources of groundwater contaminants

The number of contaminants species detected in groundwater are increasing rapidly, but can be broadly classified into three major types namely; the chemical contaminants, biological contaminants, and radioactive contaminants. These contaminants may come from either natural and anthropogenic source (Elumalai *et al*.,2020). The natural sources of groundwater contamination include seawater, brackish water, surface waters with poor quality, and mineral deposits. These natural sources may become serious sources of contamination if human activities upset the natural environmental balance, such as depletion of aquifers leading to saltwater intrusion, acid mine drainage as a result of exploitation of mineral resources, and leaching of hazardous chemicals as a result of excessive irrigation (Wu *et al*., 2015; Li *et al*., 2016, Su *et al*., 2020).

The contaminants of Nitrogen such as nitrate, nitrite and ammonia are prevalent inorganic contaminants. Nitrate is predominantly from anthropogenic sources, including agriculture (fertilizers, manure) and domestic wastewater (Hansen *et al*., 2017; Serio *et al*., 2018; Zhang *et al*., 2018; Karunanidhi *et al*., 2020). Groundwater nitrate contamination has been widely reported from regions all over the world. Other common inorganic contaminants found in groundwater include anions and oxyanions, such as F^{-}, SO_4^{2-}, and Cl^{-}, and major cations, such as Ca^{2+} and Mg^{2+}. The Total dissolved Solids (TDS), which refers to the total amount of dissolved chemical constituents in water may also be elevated in groundwater. These contaminants are usually of natural origin, but human activities also can elevate levels in groundwater (Adimalla and Li, 2019).

Toxic metals and metalloids are a risk factor for the health of both human populations and for the natural environment. Chemical elements widely detected in groundwater include metals, such as zinc (Zn), lead (Pb), mercury (Hg), chromium (Cr), and cadmium (Cd), and metalloids, such as selenium (Se) and arsenic (As). Exposures at high

concentrations can lead to severe poisoning, although some of these elements are essential micronutrients at lower doses (Hashim *et al*., 2011). Exposure to hexavalent chromium (Cr^{6+}) can increase the risk of cancer (He and Li, 2020). Arsenic is ranked as a Group 1, human carcinogen and can react with sulfhydryl (–SH) groups of proteins and enzymes to upset cellular functions and eventually cause cell death (Rebelo and Caldas 2016; Abbas *et al*., 2018;). Toxic metals in the environment are persistent and subject to moderate bioaccumulation when they enter the food chain (He and Li 2020; Hashim *et al*.,2011).

Radioactive contaminants in groundwater can originate from geological deposits of radionuclides but also can originate from anthropogenic sources, such as wastes from nuclear power plants, nuclear weapons testing, and improper disposal of medical radioisotopes (Dahlgaard *et al*., 2004; Huang *et al*., 2012; Lytle *et al*., 2014). Radioactive substances can enter the human body through a variety of routes, including drinking water. However, radioactive contaminants have been rarely detected in groundwater at levels that are a threat to human health.

2.1.2 Consequences of groundwater contamination

Groundwater contamination can impact human health, environmental quality and socioeconomic development. For example, studies have shown that high levels of fluoride, nitrate, metals, and persistent organic pollutants are a health risk for human populations (Wu *et al*., 2020). This is especially critical for infants and children who are more susceptible to the effects of these contaminants than adults (Wu and Sun, 2016; Karunanidhi *et al*., 2020; Mthembu et al., 2020; Ji *et al*., 2020; Subba Rao *et al*., 2020; Zhou *et al.*, 2020). For example, "blue baby syndrome," also known as infant methemoglobinemia is caused by excessive nitrate concentrations in drinking water used

to make baby formulas. Human health also can be affected by the groundwater contamination through effects on the food production system. Irrigation with groundwater contaminated by heavy metals and wastewater containing persistent contaminants can result in the accumulation of toxic elements in cereals and vegetables, causing health risks to humans (Jenifer and Jha, 2018; Yuan *et al*., 2019; Njuguna *et al*., 2019).

Groundwater contamination affects the quality of lands and forests as well as facilitates soil degradation. In many agricultural areas in the arid regions, high groundwater salinity is one of the major factors influencing soil salinization (Wu *et al*., 2014). The soluble salts and other contaminants, such as toxic metals accumulates in the root zone thereby affecting vegetation growth. The quality of surfacewater can negatively be affected when a contaminated groundwater interacts with it resuting to deterioration of surface water quality (Teng *et al*., 2018).

Sustainable economic development requires a balance between the rate of renewal of natural resources and human demand (Li *et al*., 2017a). Freshwater is probably the most valuable of the natural resources. However, chronic groundwater quality deterioration may reduce the availability of freshwater, breaking the balance between water supply and demand and leading to socioeconomic crises and even wars. Water shortages induced by contamination may become a factor causing conflicts among citizens in the future (Schillinger *et al*., 2020), possibly delaying the socioeconomic development of a nation. Groundwater contamination is not only an environmental issue but also a social issue, demanding collaboration between both natural scientists and social scientists.

2.2 Previous and Similar Works

The studies on groundwater quality have also been conducted in Nigeria following growing concern of water quality deterioration considering increased human activities and natural processes on the environment. Groundwater has become unsafe for utilization in some parts of the country due to high concentration of chemical constituents (Kana *et al*., 2014). Therefore, the health risks associated especially with the consumption of these type of groundwater is massive and are not limited to urinary tract diseases, blue baby syndrome or infantile methemoglobinemia, adverse effect on nervous and cardiovascular systems including fluorosis (Adelana and Olasehinde, 2003; NSDWQ 2007; WHO, 2011).

According to a study conducted around Beddegi, Central Bida Basin in Nigeria on the assessment of chemical quality of water from shallow aquifers, the concentration of chemical ions such as (Ca^{2+}, Mg^{2+}, Na^{+}, K^{+} , Cl^{-}, HCO_3 , CO_3, SO_4 ,NO_3, F^{-} and PO_4) from the shallow wells was attributed to atmospheric input from rainfall recharge and to a large extent from natural geological processes or agricultural activities within the area (Waziri *et al*., 2016). Hence, the health risks associated with some of these ions particularly those found beyond the prescribed permissible limits of the National and International regulating Agencies such as the Nigerian Standards for Drinking Water Quality (NSDWQ) and the World Health Organization (WHO) are massive.

In a realated development, statistical techniques employed to evaluate hydrogeochemical parameters towards establishing relationship between measured parameters and their sources at Kafin-Koro and its environs, north central, Nigeria suggested that the groundwater is suitable for drinking and livestock feeding considering concentration of cations (Ca^{2+}, Mg^{2+}, Na^{+}, K^{+}) and anions (Cl^{-}, HCO_3, CO_3, SO_4, F^{-}, NO_3, NO_2, PO_4)

within WHO permissible limits while heavy metals (Zn, Cu) except (Fe) and (Mn) were found higher than the acceptable limits in some locations (Waziri et al., 2019). The study at Kafin-Koro further confirmed the suitability of the water for irrigation purposes as indicated by irrigation indices such as sodium absorption ratio, percentage soluble sodium, magnesium ratio and permeability index. The geochemical processes such as weathering, ion exchange and carbonate weathering was said to the the major processes that influenced the chemistry of the groundwater in the area unmarsked through Gibb's Plot, Stoichiometric Ratio and Chloro-Alkaline Indices (CAI). The outcome of the study further revealed that the overall quality of groundwater of the area is being controlled by the lithology of the area.

The principal component analysis and ionic cross plots of data conducted by Olufemi *et al*. (2019) at the mining site in the Albian carbonaceous shale aquifers around Enyigba-Ameri, Southeastern Nigeria also revealed that water chemistry of both surface and groundwater of the area was shaped by anthropogenic activities. Likewise weathering of Lead (Pb) – Zinc (Zn) and Iron (Fe) rich minerals, dissolution of silicate and carbonate minerals and ion exchange processes was also identified as some of the major driving force influencing the chemistry of water in the area. The investigations further revealed that the potential contaminants of the water in the area include $Pb^{4+,}$ $Zn^{2+,}$ and Fe^{2+} and $^{3+}$ emanating from mining activities inspite of the generally high aquifer protective capacity of shale that underlies the entire area compared to NO_3^- and Cd^{2+}.

In North Western Nigeria, particularly in the Sokoto basin, mixing of water in certain proportions and other physio-chemical reactions with different aquifers were attributed to the lithological formation of the groups (Adelana *et al*., 2004). Moreover, the main sources of pollution are related to agricultural activities as well as indiscriminate disposal of human and animal wastes as indicated by relatively high nitrate and sulphate contents

in many wells sampled following physio-chemical analyses of water samples in the Basin(Adelana *et al*., 2004).

Similarly, in the Northeastern segment of the country, low fluoride concentration in Chad formation of the Chad Basin especially the Upper aquifer, is as a result of the shallow nature of the aquifer which is actively recharge compared to the Middle and Lower aquifers with minimal recharge and high fluoride due to dissolution of fluoride bearing minerals within the confining clay horizons of the aquifer systems (Bura *et al.,* 2018).

The high fluoride concentration in groundwater is facilitated by the long residence time of groundwater as well as increased temperature within the aquifers enabling water-rock interaction. In addition, the alkaline nature of water in these aquifers and their moderate electrical conductivity are favourable conditions for fluoride dissolution (Bura *et al.,* 2018). The impact of fluoride concentration above the WHO acceptable limit of 1.5mg/l in the Middle and Lower aquifers of the Chad formation and cases of dental fluorosis manifested by black staining on the teeth of the young and adult as well as cases of skeletal fluorosis in localities emanates where fluoride concentrations is 9 mg/l (Bura *et al.,* 2018).

In Nigeria, the distribution of fluoride in groundwater is more concentrated within the crystalline basement complex rocks rather than the sedimentary, younger granites and volcanic aquifers. The areas identified as high fluoride groundwater provinces showed symptoms of dental fluorosis among various age groups and positive correlation between consumption of groundwater rich fluoride amongst school children in Langtan, Plateau State (Dibal *et al*., 2012). The geology of an area has a strong influence on the chemistry of groundwater. The natural processes of weathering and dissolution may also be

responsible for the release of fluoride bearing minerals as well as heavy metals into groundwater system (Amadi *et al.*, 2016*)*

2.3 Geology of Nigeria

The geology of Nigeria is made up of three (3) major rock types (Adelana *et al*., 2008), namely, the Precambrian Basement Complex Rocks, Mesozoic to Tertiary Sediments, Granites and Volcanic and Quaternary Alluvial deposits as described in Kogbe (1989) and shown in Figure 2.1

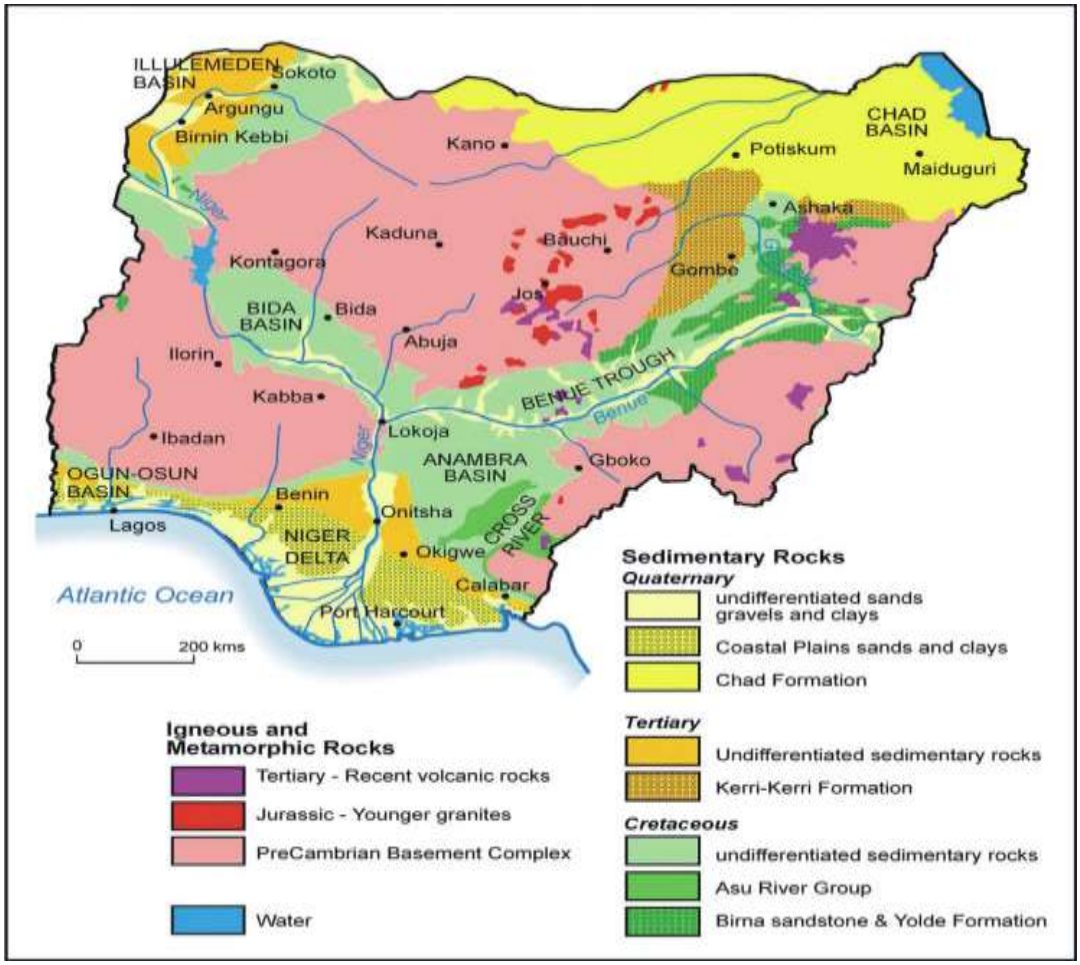

Figure 2.1: Geological Map of Nigeria (Adapted from Mac Donald *et al*., 2008; Olasehinde *et al*., 2010)

2.3.1 Precambrian basement complex rocks

The rocks underlain three area in Nigeria namely the North Centra Area including the Jos Plateau, South Eastern Area adjacent to Republic of Cameroon (Oyawoye, 1972 and Rahaman, 1989). The rocks of the North Central area are composed of gneisses, migmatites, granites, schists, phyllites and quartzites. The narrow, tightly folded north-south trending "schist belts" of Northwestern and Southwestern Nigeria include igneous rocks, pelitic schist, phyllites and banded ironstones. The migmatite gneiss complex of amphibolite, diorites, gabbros, marbles and pegmatites form a transition zone between the schist belt of Northwestern Nigeria and the granites of the Jos Plateau to the east. They have been intruded by Jurrasic age Younger Granites that are characteristic of ring complex structures (Oyawoye, 1972).

The Precambrian Basement Complex rocks of southwestern Nigeria as found in the Dahomey (Benin) Basin, consist of migmatites, banded gneisses and granite gneisses with low grade metasedimentary and meta-volcanic schists, intruded by Pan African age granites and charnockites (Oyawoye, 1972). The migmatite and gneissic metasediments are often intruded by pegmatite veins and dykes (Oluyide *et al.,* 1998). Older granites, granodiorites and syenites, with dolerite dykes, also form part of the Precambrian basement of the southwestern Nigeria. The Precambrian basement rocks of the south eastern Nigeria occur in three blocks along the border with Cameroon (Figure 2.1). The crystalline basement rocks include biotite-hornblende gneiss, kyanite gneiss, migmatite gneiss and granites that are well fractured (Ekwueme, 1987).

2.3.2 Tertiary volcanic rocks

These are rocks of the tertiary age consisting of olivine basalts, trachytes, rhyolites and tuffs overlying or interbedded with coarse grained alluvial sediments. They occur in Jos

Plateau and adjacent plateau areas. The surfaces of these volcanic lava flows have been weathered to form succession of laterites paleosols on the Jos Plateau related to the uplift of the plateau (Farnbauer and Tietz, 2000).

2.3.3 Mesozoic to tertiary sedimentary rocks

These includes rocks of sedimentary basins namely, the Iullemeden Basin, Chad Basin, Benin Basin, Niger Delta Basin, Benue Basin, Bida Basin and The Mesozoic and Tertiary strata of the Iullemeden Basin in Northwestern Nigeria comprise interbedded sandstones, clays and limestones that dip to the northwest. These formations are capped by laterites (Mac Donald *et al*., 2008). The sedimentary sequence includes the Cretaceous Illo and Gundumi Formations, The Maastrichtian Rima Group, the late Paleocene Sokoto Group and the Eocene-Miocene Gwandu Formation (Figure 2.1). These are deposited during the series of overlapping marine transgressions. Over 1250m of sediments occur in the down warped Sokoto Basin, unconformably overlaying Precambrian Basement rocks. Quaternary age alluvial deposits occur along the course of the river Sokoto (Mac Donald *et al*., 2008)

In the Chad Basin of Northeastern Nigeria, Cretaceous sediments include the Albian-Cenomanian Bima Sandstone Formation, continental, poorly sorted and thickly bedded feldspathic sandstones and conglomerates to fluviatile and deltaic sediments. The early Turonian age Gongila Formation, up to 500m thick, includes marine limestones, sandstones and shales. The Senonian-Maastrichtian ahe Fika Shale Formation, 100 to 500m thick, consist of gypsiferous shales and limestones of marine and continental origin. The Maastrichtian age Gombe Sandstone Formation consist of estuarine and deltaic sediments, deposited upon marine shales with sandstone/shale intercalations. The lower deposits of siltstones, mudstones and ironstone are overlain by well bedded sandstones

and siltstones. The upper formation contains coals and cross bedded sandstones. The Cretaceous ended with a period of uplift and erosion. The Paleocene age, the Keri- Keri Formation rest unconformably on the Gombe Sandstone Formation and thickens towards the basin center where it is overlain by the Chad formation (Figure 2.1). The Pleistocene age of Chad Formation (up to 840m thick) consist of poorly sorted, fine to coarse sand with sandy clay and diatomite (Mac Donald *et al*., 2008).

The Southern Nigeria Sedimentary Basin include the Lagos-Osse and the Niger Delta Basins that are separated by the Benin hinge Line (the Okitipupa ridge). These basins have a common basal of marine Albian age, arkosic, gravelly, poorly sorted, cross bedded sandstones and sandy limestones. The Lagos-Osse Basin, the eastern sector of the Benin Basin in Nigeria, underlies the western low-lying coastal zone where rock exposures are poor due to thick soil cover. The Tertiary geology of the area comprises the basal Araromi/Ewekoro Formation, consisting os shelly and sandy black shale with thin sandstones and limestones that are overlain by the Paleocene age Imo Shale Formation. These are overlain by the Oshosun Formation of shales, clays and sandstones. The succeeding Miocene age Benin Formation consists of up to 200m of sands with shales, clays and lignite (Okosun, 1998). The near surface quaternary geology comprises of recent littoral sandy alluvium and coastal plain sands **(**Jones and Hockey, 1964; Longe *et al.*, 1987). In the Niger Delta Basin, Quaternary age sediments underlying the Delta Plain consists of coarsed to medium grained unconsolidated sands and gravel with thin peat, silts, clays and shales, forming units of old deltas. The underlying Miocene age Benin Formation is composed of gravels and sands with shales and clays. This multi-aquifer system formation crops out to the northeast of the coastal belt (Mac Donald *et al*.,2008).

The Cretaceous sediments of the down faulted and failed rift that is the Benue Trough occur in a series of sedimentary basins that extend north east of the confluence of the Niger and Benue Rivers, bounded by the Basement Complex rocks to the north and south of the Benue River ***(***Reyment, 1965) (Figure 2.1)**.** The Lower Benue Basin consist of shales, silts and silty shales with subordinate sandstones and limestones intruded by dolerite dykes while the Upper Benue basin consist of a thick succession of continental sandstones overlain by marine and estuarine deposits. The basal formation is the Bima Sandstone (Carter *et al*., 1963).

The Bida Basin runs northwest from the confluence of Niger and Benue Rivers towards the Sokoto Basin (Figure 3). The basin contains Cretaceous age sandstones, siltstones, clay stones and conglomerates mainly of continental origin. The Middle Niger Basin at confluence of the Niger and Benue Rivers contains 500 to 100m of alluvial to deltaic coarse to medium-grained cross-bedded to massive sandstones with subordinate siltstones, kaolinitic clay stones and shales (Adelana *et al*., 2008).

2.3.4 Quaternary alluvial deposits

The Quaternary to recent age alluvial deposits occur along main river valleys. These deposits range from thin discontinuous sands to thick alluvial deposits up to 15km wide and 15 to 30m thick along the Niger and Benue rivers (Adelana *et al*., 2008). The alluvial deposits include gravel, coarse and fine sand, silt and clay. Thin beds of unconsolidated and mixed sands and gravels occur along the courses of ephemeral “fadama” in northern Nigeria.

2.3.5 Geological and hydrogeological setting of Taraba State

The geology and geological history of Taraba State is rather complex. Taraba State is underlain by the Crystalline Basement Complex and Sedimentary rocks of Nigeria, each occupying a very distinctive part of the State (Oruonye and Abbas, 2011). The Basement Complex rocks occupies the greatest part of the State (above 80%), while the sedimentary rocks are found along the valleys of River Benue and its major tributaries such as Rivers Donga and Taraba (Figure 2). The undifferentiated Basement Complex rocks comprising of gneisses, migmatites, phyllites, schists and pegmatites cover a greater part of the Basement Complex area. The migmatites of the undifferentiated Basement Complex rocks, generally vary from coarsely mixed gneisses to diffused textured rocks of variable grain size and are frequently porphyroclastic (Macleod *et al*., 1971). This rock unit constitutes principally the undifferentiated igneous and metamorphic rocks of Precambrian age (Grant, 1971).

The Pan African Older Granites are equally widespread in the area. They occur either as basic or intermediate intrusive (Turner, 1964). Different kinds of textures ranging from fine to medium to coarse grains can be noticed on the Older Granites (McCurry, 1976). Other localized occurrences of minor rock types include some dolerite and pegmatitic rocks mostly occurring as intrusive dykes and vein bodies (Oruonye and Abbas, 2011***)***. These are the Basement Complex and the Older Granite rocks (Carter *et al*., 1963; McCurry, 1976). The Tertiary basalts on the other hand are found in the Mambila Plateau mostly formed by trachytic lavas and extensive basalts which occur around Nguroje (Du Preez and Barber,1965). Between early Cretaceous and recent times, the Basement Complex area was subjected to repeated regressions and transgressions which led to the deposition of the sedimentary rocks (Ogezi, 2002). The earliest of this belongs to the Albian period. These rocks are partly terrestrial, marine, deltaic, estuarine, lagoonal and

fluvio-marine in origin and consists mainly of poorly bedded grits, conglomerate, sandstones, shale, clay, mudstone etc.

The sedimentary rocks of the state belong to the sub group of the Middle Benue Basin/trough or Makurdi and Wukari Basins, which is one of the rocks of the sedimentary series that covers about 50% of the surface area of Nigeria (Ogezi, 2002). Sedimentary materials filling the basins vary in thickness and often display complete single or multiple cycles of development characterized by basal continental facies overlain by marine facies and, in turn by continental sediments (Ogezi, 2002). This varied geologic rock types provide rich solid mineral resource potentials for the state as represented in Figure 2.2

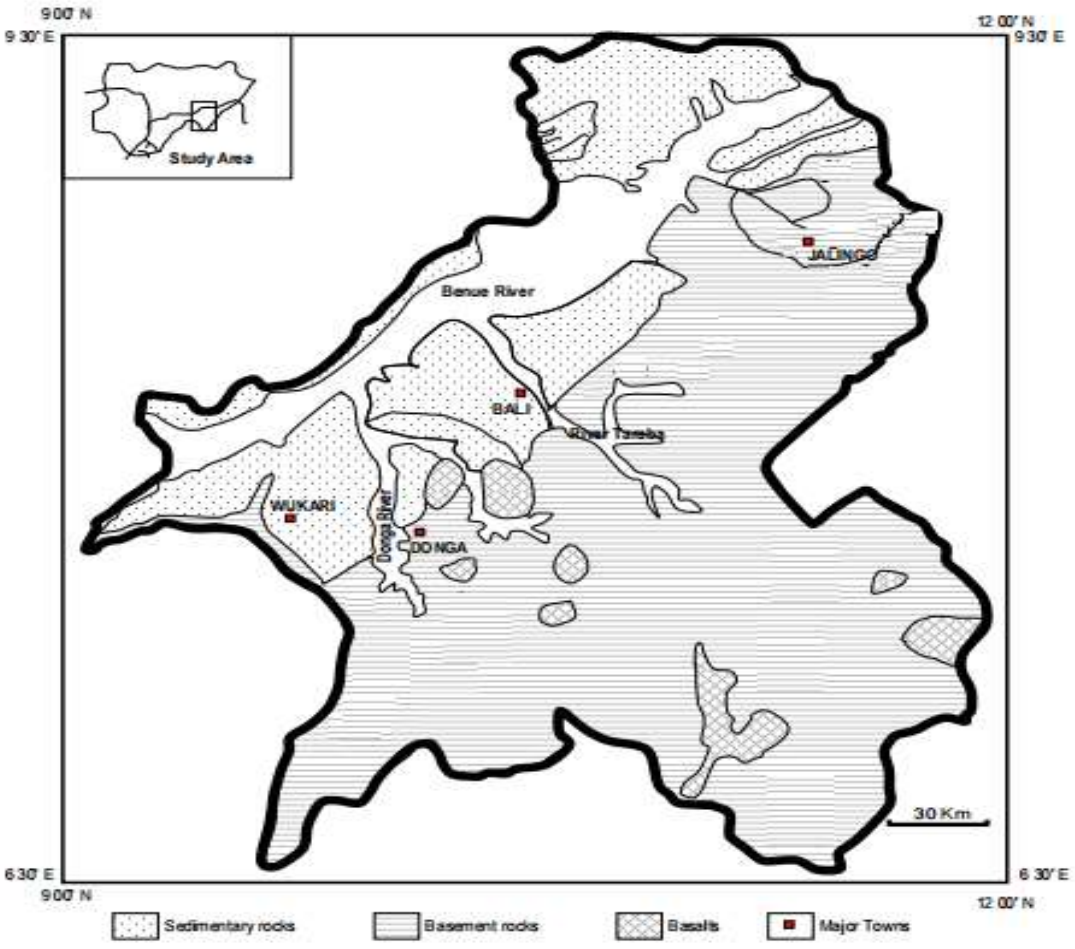

Figure 2.2: Geological Map of Taraba State (Adapted from Badafash Consulting Engineers,1991)

2.3.6 Regional geology of the study area

The study area (Zing) lies within Adamawa massif, situated in Eastern Nigeria and consisting largely of granitoids and migmatite gneiss. Adamawa massif lies in an extensive area between the Benue Trough to the West and the Cameroun Line to the East complex (Figure 2.3). To the North, it is bordered by Hawal Massif and to the south, by Oban Massif (Figure 2.4). The three massifs extend into the Republic of Cameroon and form the Eastern Nigerian Basement Complex which is one of the three major basement complexes in Nigeria.

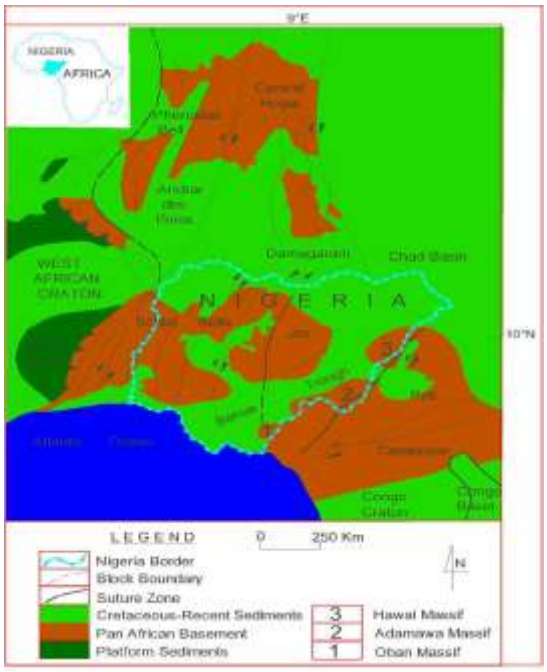

Figure 2.3: Regional Geological Setting of Nigeria (Ferre, 1996)

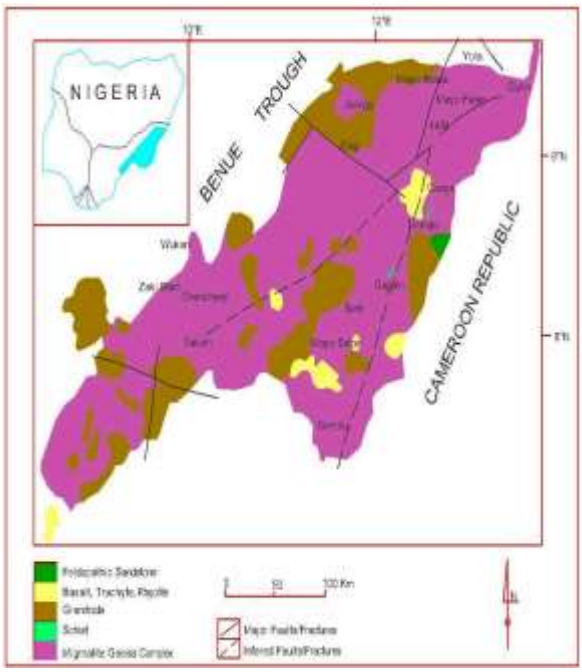

Figure 2.4: Geology of Adamawa massifs (NGSA, 1996)

2.3.7 Local geology of the study area

Zing Local Government Area is underlain by granitoids of Adamawa Massif according to Cox *et al*., (1969). Haruna *et al*., (2010), classified the granitoids as granites and granodiorites. The granites are similar in mineral composition but vary texturally and structurally. They include the granite-gneiss, coarse-grained granites, porphyritic granites

and fine-grained granites. The gneisses are of restricted occurrence in the area and consist of granitic materials alternating with biotite-enriched mafic materials. They are poorly foliated, mostly leucocratic, coarse-grained and show considerable variations in structure, texture and to a lesser extent, mineralogy. The granodiorite presents a wide range in composition and field distinction is difficult as they frequently grade into one another. They were therefore mapped as granodiorite. Granodiorite is distinguished from other rock units in the field by its fairly high mafic mineral content and its pronounced grayish colour. This greyish appearance strongly contrasts with the pink and pale reddish-brown of the granites.

2.3.8 Local hydrogeology

The study area is underlain by crystalline basement complex dominated by low rising hills and rock outcrops of the Adamawa massif of Northeastern. The area consists of both igneous and metamorphic rock units. Groundwater development in the area is met with difficulties due to lack of primary porosity in the bedrock. However, the secondary porosities such as fractures (joints and faults) and weathered zones are the sources of groundwater occurrence and movement (Chilton and Foster, 1995, Foster *et al.,* 2008, Srinivasa *et al*., 2000, Wright and Burgess, 1992). Hence, these features constitute the different aquifer systems and influences the storage, transmission and distribution of groundwater in the area.

However, the occurrence, distribution, movement, recharge-discharge and quality of groundwater in the aquifer materials vary largely from place to place and in some cases in boreholes located at some few metres apart in the same rock types (Banks *et al*., 1994). These differences are caused by a combination of both independent and inter-related factors on regional and local scales (Henrinksen and Braathen, 2006) which are

geomorphological, lithological, hydrogeological and hydrochemical (Chilton and Forester., 1995 and Dash, 2003).

The former occurred within the thick overburden derived from in situ chemical weathering of the underlying crystalline basement consisting of soil and highly decomposed rock materials while the later the fractured-rock zone is overlain by the weathered zone and acts as conduit pipe for groundwater movement. The fractured zone of the basement represents a productive aquifer system that is sustainable in the study area. The average depth of existing boreholes in the study area is between 23m and 40m with an average low yield of 0.5 l/sec considering the geological environment (JICA Report, 2011). The groundwater flow direction is controlled by the dominant joint direction, NNW-SSE.

According to Offodile (2002), a transmissivity range of 5 to 50m^2 /day could be regarded as high potential in crystalline rock situations. In view of the above standard, the basement aquifers of the area has transmissivity values of 0.3m^2/day to 19.7m^2/day indicating aquifers of negligible to high potentials. The hydraulic conductivity values vary from 3.0 x 10^{-2}m/day and 7.0 x 10^{-1}m/day with an average of 1.90 x 10^{-1}m/day (Ishaku *et al*., 2009). The range of values reveals moderate hydraulic conductivity (Todd, 1980). In view of the specific capacity values, most of the boreholes have moderate performance which corresponds to moderate hydraulic conductivity and negligible to high transmissivity values with yields ranging from 6.77m^3 /day to 21.6m^3 /day with an average of 14.41m^3 /day (Ishaku *et al*., 2009). The total yield of boreholes in the area is about 620.04m^3 /day which can sustain a population of 24,802 based on water supply standard of 25 litres per day for rural communities (Ishaku *et al*., 2009). The water supply situation is grossly inadequate in the area and water supply from boreholes mainly hand pumps are

supplemented by water from streams, ponds and hand dug wells. The existing hand pumps are over-stretched due to over population and frequent breakdown thereby creating acute water shortages. The average depth of hand dug wells in the area were confirmed with dip meter to be between 5m and 15m during the study. Where water cannot be obtained due to the seasonal nature of these sources, water is obtained through few metres below the stream beds and where streams does not exist, people in the area have to trek several kilometres in search of water

CHAPTER THREE

3.0 MATERIALS AND METHODS

3.1 Methodology

The research methodology includes reconnaissance and desk study, field work, laboratory analysis, data processing and interpretation of results.

3.1.1 Reconnaissance and desk work

This was undertaken to get acquainted with the environment under investigation, the people, land form and use towards planning a successful field activity. It was also planned to assemble and review information from various existing reports and academic papers on the subject under study as well as other related work conducted elsewhere.

3.1.2 Field work

3.1.2.1 *Rock samples collection and field observation*

This aspect of research methodology involves both geological and hydrogeological mapping to ascertain rock units and water sources and types. The activity consisted of field observations and measurements of parameters and collection of rock samples. The samples from rock exposures were collected at road cut, hilly areas, streams and river channels with the aid of a geological hammer and properly labeled using a permanent marker after a systematic description in hand specimen and the information at each location are recorded in a field note book. A total of nineteen (19) locations of rock exposure were sampled and represented on a topographic map (Figure 3.1). The elevation of rock exposures and attitudes of geological structures were also determined with the aid of a Global Positioning System (GPS) device and a compass-clinometer. Local sources of pollution such as latrines, burial grounds, cattle pence and market areas including waste dump sites were also observed. The images of geological features were also captured in

the field with a portable digital camera. Consequently, the results obtained from this exercise was finally utilized to update the existing geological map of the study area.

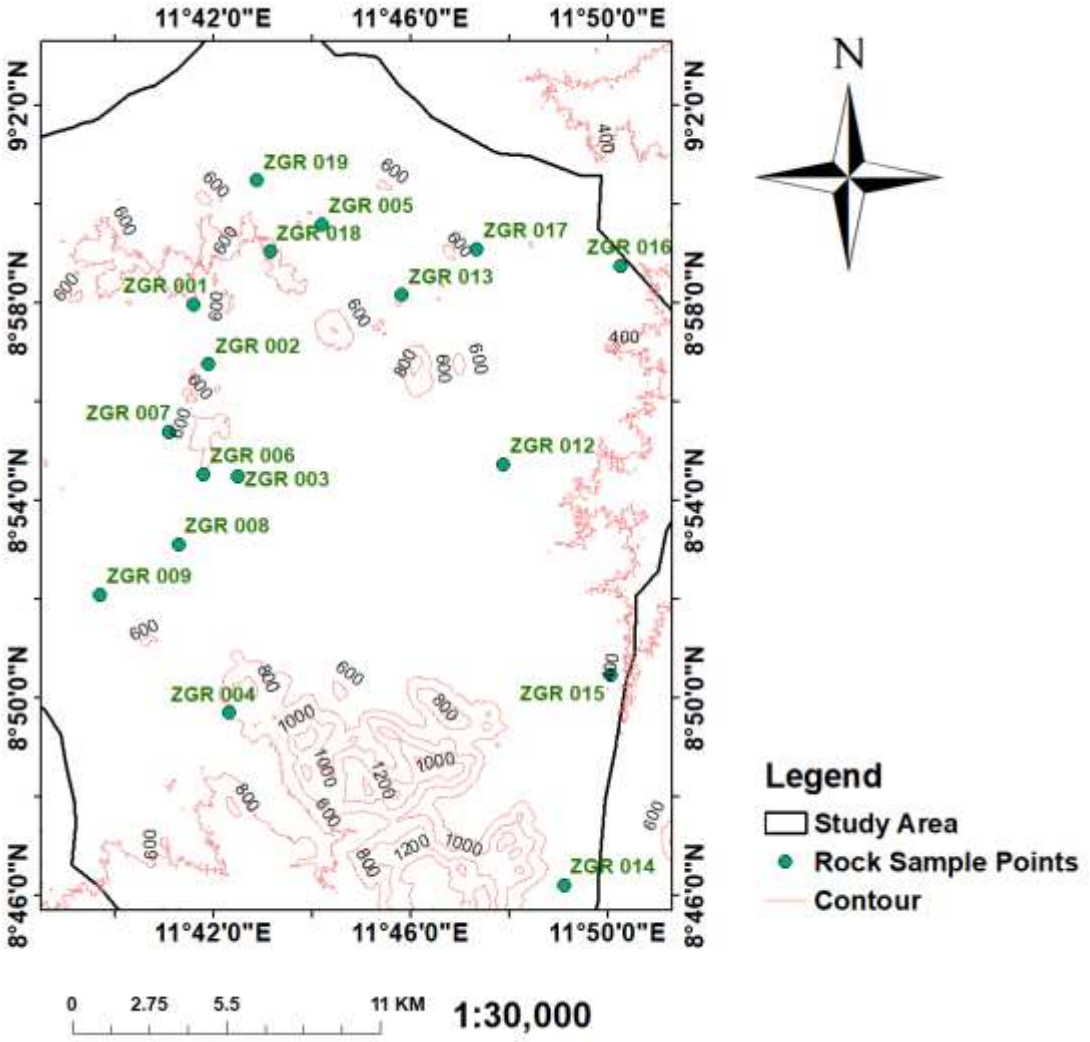

Figure 3.1. Rock sample location points

3.1.2.2 *Water sampling and field measurements*

The inventory of boreholes which are mainly hand pump types where groundwater samples were collected were recorded accurately on a field data sheet as shown in appendix A. The respective sample location coordinates such as latitudes and longitudes, altitude/elevation was also recorded with a handheld Global Positioning System (GPS). A total number of twenty-eight (28) water samples from boreholes were sampled as

represented in Figure 3.3. At each sampling location, two (2) water samples each were collected in a 250ml capacity high density polyethene plastic bottles. The samples earmarked for Cations analyses is acidified with concentrated Tri-oxo-nitrate V Acid also known as Nitric Acid (HNO_3) to homogenize, preserve and prevent absorption/adsorption of cations on the walls of the plastic bottles while the other sample scheduled for Anion's determination is collected as non-acidified in a separate container.

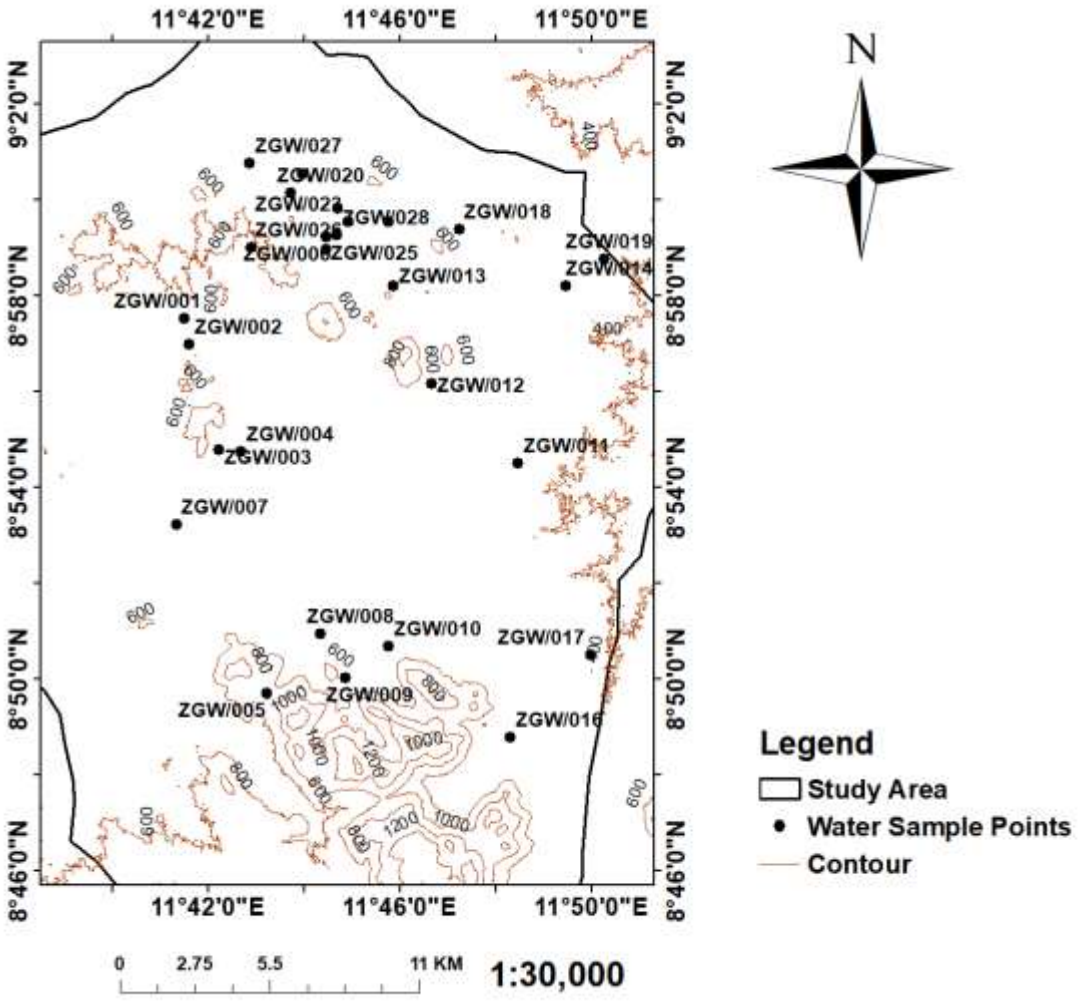

Figure 3.3 Water sample location points

3.1.2.3 *Measured physical parameters of water sample*

The Physical parameters of water samples such as pH, Temperature ($^{O}_{C}$), Total Dissolve Solids (TDS) and Electrical Conductivity (EC) were measured *in-situ* in the field using **HANNA**198191- multi-parameter equipment for pH and Temperature determination while **HANNA**198192 for determination of Electrical Conductivity and Total Dissolve Solids. The pH meter was operated in accordance with the aid of an manufacturer's instruction manual (Hanna,2019) and was calibrated prior to field sampling activity. Two standard pH buffer solutions point of 4.01 and 7.01 were used for calibration of the equipment. The pH of water samples was determined in the field by inserting the electrode into the water sample collected in a container. The value of the pH is taken when the value on the monitor of the equipment stabilizes and the electrode rinsed with deionized water after measurement is completed. Plates, II, III IV, V, VI VII, VIII and IX are field equipment, consumables utilized during sampling of water from various water points in the field.

Plate II. HANNA Test kits for measuring pH, TDS and EC

Plate III: Buffer Solutions for pH Calibration

Plate IV: High Density Pressurized Polyethene bottles of 250ml capacity

3.1.2.4 *Static water level and temperature (SWL/^{o} C)*

The SEBA KLL T meter is an electric contact and temperature measuring meter. The equipment is capable of measuring static water level (SWL), temperature of water and total drilled depth of accessible wells which are often, the hand dug wells. The values of SLW, Temperature and Total Drilled Depth (TDD) of wells were recorded using the equipment when the probe is in contact with the water and bottom of well respectively.

Plate V: Static water level and temperature measuring dip metre

3.1.2.5 *Electrical conductivity (µS/cm)*

The Electrical Conductivity (EC) of water samples was measured with the aid of an electrical conductivity meter which was first calibrated in the laboratory before deployed to the field for use. A calibration standard of 1413 µS/cm at 25^{o}C was used. The electrical conductivity values for water samples were recorded when the probe is inserted in water samples.

Plate VI: Reagent for calibration of electrical conductivity meter

Plate VII: Measurement of physical parameters of water samples in the field

Plate VIII: Cooler for storage of samples

Plate IX: Group photograph with locals in the field at Zing

3.2 Laboratory Analyses

3.2.1 Rock sample analyses

The geochemistry and mineralogy of rocks are studied for ascertaining the spatial distribution of the concentration of chemical elements, compounds, and other physicochemical parameters across a defined area**.** This method of investigation is the best to document the spatial variation of chemical elements, and other physicochemical properties including mineral species in materials occurring at or immediately below the earth's surface, such as rock, soil, stream, overbank and floodplain sediment, stream water, groundwater, vegetation, and even human tissues.

In view of the present study, the techniques were employed to determine the spatial occurrence, chemical compositions and their respective mineral species to further authenticate their origin and sources in groundwater of the study area.

The rock samples numbering twelve (12) were meticulously selected out of the nineteen collected on the field. The samples were analyzed using the Thermo Fisher Scientific Energy Dispersive X-ray Fluorescence (EDXRF) Analyser (Plate X) and the X-Ray Diffraction Empyrean diffractometer (Plate XI) for determination of elemental and mineralogical composition of rock samples respectively. The analyses were conducted at the Umaru Musa Yar'adua University Katsina, Katsina State, Nigeria.

The analyses of rock samples designated for elemental composition was done using the standard method which is 80% accuracy compared to standard less method of 50% accuracy. The standard method utilized to achieve accuracy of measurement were formed by standard Reference material obtained from International Atomic Energy Agency (IAEA) for geological materials. The instrument has three mediums of operation namely

the helium gas for liquid sample, vacuum pump for light elements and air for heavy element and light element excluding sodium can only be gotten in vacuum.

The laboratory procedure for XRF analyses of rock samples entails that the sample be first pulverised into a fine powder with the aid of mortar and pistol. Thereafter, 2g of each of the samples were weighed and then poured into a sample holder and covered with cotton wool to prevent it from spraying. The bottom of the sample's holder is made of polypropylene which is a thermoplastic. The sample holders containing the sample were run in a vacuum or air for 10 minutes and they were subsequently inserted into the XRF Spectrometer for the elemental analysis. The samples were further allowed to run in the EDXRF spectrometer for another 10 minutes each after which the results will be obtained in elemental and their respective peak forms.

The rock samples were finely pulverized, homogenized and the average bulk composition was determined with XRD machine. The powdered sample was prepared using sample preparation block and compressed in a flat sample holder (Plate XII) to create a flat surface. Smooth surface was mounted on the sample stage in the XRD cabinet. The sample was analyzed using the reflection transmission spinner stage employing the Theta-Theta setting. The results were presented as peak position at 2θ and X-ray counts(intensity) in the form of X-Y plot or table through a system linked to the equipment (Plate XIII). The peaks obtained from the analyses were matched with the minerals from Powdered Diffraction File (PDF) of International Centre for Diffraction Data (ICDD) database.

Plate X: EDXRF Analyzer

Plate XI: XRD Analyzer

Plate XII: Sample holder for XRD Analyses

Plate XIII: Computer System Linked to XRD and EDXRF for Result Processing

3.2.2 Water sample analyses

The twenty-eight (28) water samples collected during field activity were analyzed at the Regional Reference Laboratory of the Federal Ministry of Water Resources in Gombe, Gombe State, Nigeria. The analytical methods adopted were based on international acceptable methods and analytical application principles. Even though various caliber of instrument by different manufacturers were utilized (Table 3.1), the principles employed were based on accepted standard methods of the American Public Health Association APHA, 2000).

The chemical constituents in water samples such as Sodium (Na), Potassium (K), Calcium (Ca), Magnesium (Mg) Chloride (Cl), Carbonate (CO_3), Bicarbonate (HCO_3), Sulphate ($SO_{4,)}$, Nitrate (NO_3), Fluoride (F) Manganese (Mn), Zinc (Zn), Chromium (Cr), Lead (Pb), Cupper (Cu), Cadmium (Cd) and Cupper (Cu) were analyzed at the stated laboratory. The Ethaline Diamine Tetra Acetic (EDTA) titrimetric method was used to analyze calcium, magnesium and total hardness concentrations, sodium and potassium

was determined by Flame Photometer while carbonates and bicarbonates ions were determined by potentiometric method using HACH DR-890 Photometer. The CHROMA Colorimetric (252) method was utilized for determination of Sulphate, Nitrates and Nitrites were both determined by Nitraver-5 (HACH DR-900) equipment while Fluoride was analyzed with Palintest Photometer and SPADNS Reagent. Heavy and Trace elements such as Lead, Copper, Zinc and Manganese were analyzed by Trace O Metalyzer through Anodic stripping while Chromium and Iron by HACH DR-900 Photometer (Carbazide Method) and Phenanthroline Method (HACH DR-900 Photometer) respectively.

Table 3.1 is the summary of parameters, equipment and methodology utilised for the various laboratory analyses. The results of analyses of water samples of the study area will be compared with the World Health Organization(WHO) and the Nigerian Standard for Drinking Water Quality(NSDWQ) and other similar published results elsewhere.

Table 3.1 Summary of parameters and equipment for laboratory measurement

MEASURED PARAMETERS	EQUIPMENT AND METHODOLOGY
Total Hardness as ($CaCO_3$)	EDTA Titrimetric Method
Ca^{2+}	Flame Photometer
Mg^{2+}	Flame Photometer
Na^{+}	Flame Photometer
K^{+}	Flame Photometer
Carbonate and Bicarbonate (CO_3 & HCO_3	Potentiometric method
Sulphate	HACH DR-890 Photometer
Chloride	Argentometric method
Nitrate as (NO_3)	Nitraver-5 (HACH DR-900)
Nitrite as (NO_2)	Nitraver-5 (HACH DR-900)
Fluoride	Palintest Photometer (SPADNS Reagent)
Lead	Trace O Metalyzer (Anodic stripping)
Copper	Trace O Metalyzer (Anodic stripping)
Cadmium	Trace O Metalyzer (Anodic stripping)
Zinc	Trace O Metalyzer (Anodic stripping)
Mn	Trace O Metalyzer (Anodic stripping)
Chromium	HACH DR-900 Photometer (Carbazide Method)
Iron (II)	Phenanthroline Method (HACH DR-900 Photometer)
Elemental composition of rock samples (light and heavy elements)	Thermo Fisher Scientific Energy Dispersive X-ray Fluorescence (EDXRF) Analyzer: Model- ARL QUANT'X. EDXRF Analyzer
Mineralogical composition of rock samples	X-Ray Diffraction (XRD) diffractometer

3.2.3 Data processing and interpretation.

The chemical composition of groundwater usually begins as soon as water percolates/infiltrates into the subsurface of the earth. In order to evaluate the characteristics of rocks and the role played by weathering, the criterion by Chappell and White (1978) and the chemical index of alteration established by Nexbit and Young (1982) was employed. The concentration of chemical constituents in water, hydrochemical facies, hydrogeochemical processes and sources of measured chemical parameters in groundwater of the study area were determined through plots of various diagrams such as Schoeller, Stiff, Piper, Durov and Gibbs.

Sofware packages such as microsoft word, Geographic Information System (GIS) Version 10.3, Geochemical Data (GCD) Kit version 6.0 (Janousek et al., 2006), and Aqauchem Version 5.1 were all utilized for data handling, interpretation of results and reporting. The microsoft word was used to input all the data from the field and laboratory results of rocks and water samples in an excel spreed sheet data format while the GIS software package version 10.3 was employed for the production of geological and chemical concentration maps at appropriate scales. The Geochemical Data (GCD) Kit version 6.0 was utilized for handling and recalculation of geochemical data of rocks especially Total Akaline Silica (TAS) of the rocks while the aquachem software version 5.1 was deployed to produce the graphysical display and presentation of water types and hydrochemical facies of groundwater of the study area.

3.2.3.1 *Schoeller plot*

The Scholler diagram after Schoeller, (1955), represents a semi -logarithmic diagram of the concentration of groundwater samples of the study area, it is employed to illustrate the relative concentration of both cations and anions expressed in milliequivalent per litre.

It is also used for visual comparison of ionic concentration in water. It is beneficial because it allows multiple comparisons of water analyses and finding the degree of saturation in water.

3.2.3.2 *Stiff plot*

The Stiff diagram by Stiff (1951) was used to display major composition of water samples. The diagram is essentially a graphical display in the form of polygons of the major ion composition of a given water sample. It is useful in making visual comparison between water of different sources which could serve as a means to determine flow path and how ionic composition of groundwater changes over time. It is also essential in determining the composition individual water sample at a given point or group of samples as may be required. The Stiff patterns can be a relatively distinctive method of showing water composition, differences and similarities (Hem, 1985)

3.2.3.3 *Piper plot*

The piper diagram is an effective graphic procedure by Piper, (1944) for presenting water quality data to understand the sources of dissolved constituents in water. It is a graphical representation of the chemistry of a water sample or samples. This procedure is based on the premise that cations and anions in water are generally in chemical equilibrium. The cations and anions are shown by separate ternary plots. The apexes of the cations plot are calcium, magnesium, sodium and potassium whereas the apex of the anions are the sulphate, chloride, carbonate and bicarbonate. The two ternary plots are projected into a diamond which is a matrix transformation of a graph of the Anions $(\frac{SO_4 + Cl^-}{Total\ Anions})$ and Cations $(\frac{Na^+ + K^+}{Total\ Cations})$.

The Gibbs, Durov Diagrams including the Source Rock Deduction and Reasoning table by Hounslaw(1995) was also employed to establish the geochemical processes influencing water chemistry as well as the sources or origin of measured chemical parameters in groundwater samples of the study area.

The Gibbs diagram prposed by Gibbs (1970) represents the ratios of sodium and potassium ions to sodium, potassium and calcium ions $(Na^{+}+K^{+})/(Na^{+}+K^{+}+Ca^{2+})$ for cations and chloride to chloride and bicarbonate ions $Cl^{-}/Cl^{-}+HCO_3^{-}$) for anions as a function of Total Dissolved Solid (TDS). It is widely used to determine the sources and processes such as weathering and rock dorminance, rock water interactions , evaporation, precipitation resulting to concentration of chemical constituents in groundwater system.

3.2.3.4 *Durov plot*

In a related development, the hydrogeochemical processes occurring in groundwater system of the study area revealed by Durov Diagram developed by Lloyd and Heathcoat (1985). The source rock deduction assessment is aimed at determining the possible origin and sources chemical ions in groundwater of the study area. The following equations presents a summarized source rock deduction process on the basis of ratio of chemical constituents as proposed by Hounslaw, 1995. The composition and groundwater quality of the study area was used to deduce source rock .

$$\frac{Na^{+}+K^{+}-Cl^{-}}{\mathrm{Na}^{+}+K^{+}-Cl^{-}+Ca^{2+}} \qquad (3.1)$$

$$\frac{Na^{+}}{\mathrm{Na}^{+}+Cl^{-}} \qquad (3.2)$$

$$\frac{Mg^{2+}}{\mathrm{Ca}^{2+} + Mg^{2+}} \tag{3.3}$$

$$\frac{Ca^{2+}}{\mathrm{Ca}^{+} + SO_4^{2-}} \tag{3.4}$$

$$\frac{\mathrm{Ca}^{2+}+Mg^{2+}}{SO_4^{2-}} \tag{3.5}$$

$$\frac{Cl^{-}}{\text{Sum of Anions}} \tag{3.6}$$

$$\frac{\mathrm{HCO_3}}{\text{Sum of Anions}} \tag{3.7}$$

CHAPTER FOUR

4.0 RESULTS AND DISCUSSION

The geological mapping, geochemistry, mineralogical and physiochemical results of analyses of rocks and water samples within the framework of this research work were interpreted using relevant data processing software, figures, tables and graphical representations.

4.1 Geological Mapping and Field Observations

The geology of the area has been studied and based on field observations, the major rock units in order of increasing abundance are; the porphyritic granites, granodiorites, coarse-grained granite, fine-grained granite, granite-gneiss and pegmatites. Figure 4.1 is the geological map of the study area.

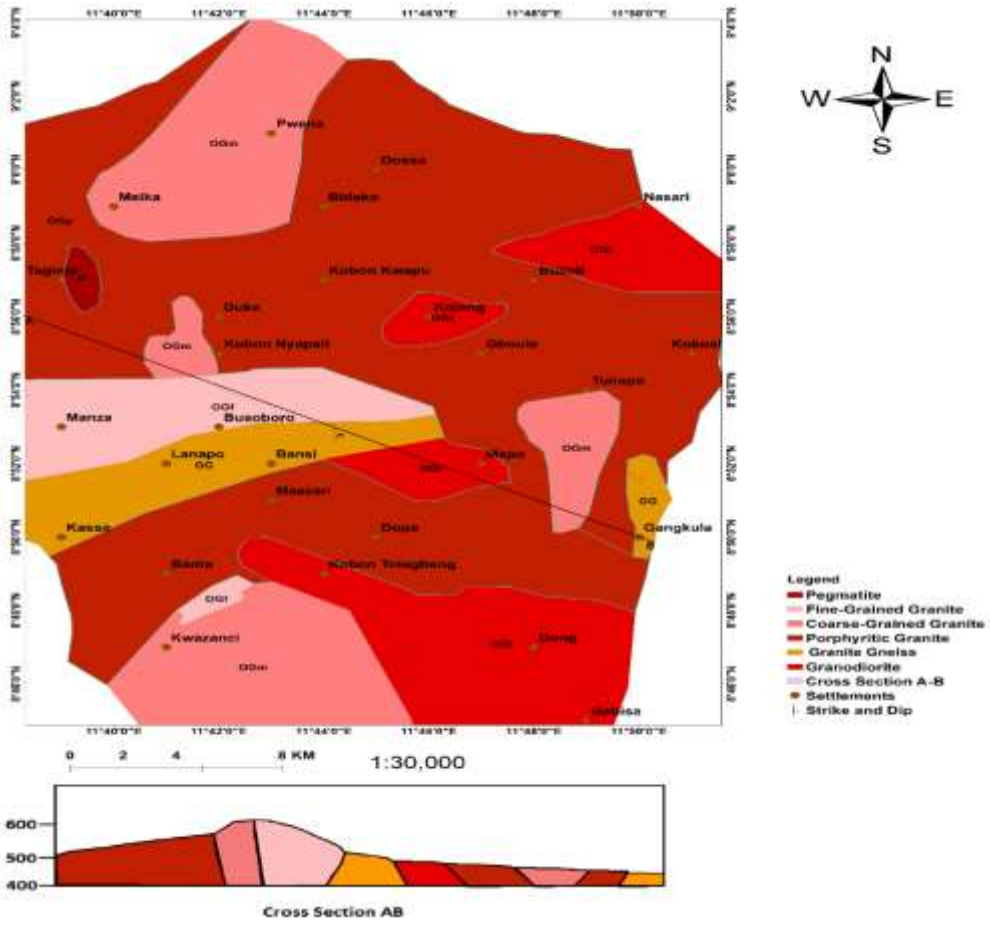

Figure 4.1: Geological map of the study Area.

4.1.1 Porphyritic granite

This is the most abundant rock type in the area, especially at the northern section of Zing (Plate XIV). The most striking characteristic of porphyritic granites is their porphyritic texture consisting phenocrysts of feldspars (mineral grains in the size range 15mm × 20mm to 25mm × 30mm) set in a medium to coarse-grained mineral matrix ranging in size from 2mm×3mm to 4mm×5mm. They are relatively homogeneous, having predominantly gradational (transitional) and restricted sharp contacts with coarse and fine grained granites. The composition and texture of the porphyritic granites changes as one traverse the intrusions from the center to the borders (margins). At the center, feldspar phenocrysts are crowded and the rock appears to be homogeneous biotite granite.

Plate XIV: Gradational contact between porphyritic granite and coarse-grained granite boulder at Yakoko village ($8^0$54′29.3″N, 11^0 42′30.8″E)

4.1.2 Coarse-grained granites

They have mineral grains of the order 3mm × 3mm, and in some instances medium-coarse-grained and equigranular in sizes. They include a diverse series of granites varying slightly in texture, structure and mineralogy. The contacts between the various types are mostly gradational. The coarse-grained granites are massive in some places and weakly foliated in others. The foliation is expressed by elongate biotite and to a lesser extent feldspar and quartz crystals. (Figure 4.1 and Plate XIV).

Plate XV: Xenolith in a coarse-grained granite outcrop close to Bansi village ($8^0 46' 12.5''$N, $11^0 49' 06.5''$E)

4.1.3 Granodiorites

This rock belongs to a group of feldspathoid, intermediate and basic rocks. It is distinguished from other rock units in the field by its high mafic mineral content, giving it a dark greyish colour. This greyish appearance strongly contrasts with the pink and pale red of the granites. Two varieties of granodiorites are texturally distinguishable in the

field. These are the medium-coarse-grained (measuring 2mm x 3mm to 3mm x 4mm in size) and porphyritic (30mm x 30mm) varieties. The medium-grained variety occurs as inselbergs north of Wuro Alkali and occasionally as marginal mass of larger fairly porphyritic granodiorite bodies around Kobon Tolegbeng in the southern part of the area. The coarse-grained to porphyritic variety occupies most of the eastern part of the area occurring as sub circular to large elongate plutonic bodies spanning some tens of kilometers. Though widely distributed in the eastern part of the area, individual occurrences are small except in the northeastern and southeastern parts where they occur as large elongated bodies. The outcrops are mostly massive and almost restricted to the eastern part of Zing-Monkin area (Figure 4.1 and Plate XV)

Plate XVI: Jointed and fractured granodiorite outcrop at Dinding ($8^0 50' 38.5'' N$, $11^0 46' 10.2'' E$)

4.1.4 Fine-grained granites

The fine-grained granites are pale grey to dark grey, fine-grained and show little variation in appearance (Plate XVI). The rock consists of predominantly quartz, microcline and feldspar. Similar rock forms enclaves as irregular bodies and as vein-like lenses within the fine-grained granites. In some places, veins of fine-grained granite interfinger and penetrate the porphyritic granites. Fine-grained granite, like the granite genies, is of subordinate occurrence in the study area and well exposed along Yakoko-Monkin road (Plate XVI).

Plate XVII: Fine grained granitie intrusion into Porphyritic granite at Yakoko Monkin area of Zing

4.1.5 Granite Gneiss

The gneisses are of restricted occurrence in the area with a good outcrop around Koju, Bitako Nyali and Kobanko areas, South of Zing (Plates XVII and XVIII). They consist of granitic materials alternating with biotite-enriched mafic materials.

They are moderately to poorly foliated, coarse-grained and show considerable variations in structure, texture and to a lesser extent in mineralogy. Pegmatitic segregations, patches of granites and xenoliths of mafic rocks are very conspicuous in the gneisses around the area.

Plate XVIII: Gneissic foliation on granite gneiss outcrop exposed between Bitako-nyali and Kobanko villages ($8^0$50′20.2″ N,$11^0$47′38.3″E)

Plate XIX: Gneiss outcrop in Koju village ($8^0$50′27.8″N, 11^0 50′02.5″E)

4.1.6 Pegmatite

Pegmatite does not form an independent or mappable rock unit in the study area except at a Dokwobo where it occurs as a small hill consisting of graphic intergrowth of quartz and potash feldspars (Plate XVIX). At this locality, the rock takes the form of quartz-feldspar body a few tens of meters in length. In other rock units, especially the coarse-grained granites at Kwana village, pegmatite takes the form of irregular cross cutting vein-like bodies (Plate XVIX).

Plate XX: Pegmatitic veins (striking E-W) having pink orthoclase feldspars on weathered and jointed dark grey coarse-grained granite at Kwana village (9^0 00′ 28.9″N, 11^0 42′ 54.2″E).

4.1.7 Structural Geology

Secondary igneous structures such as foliation, xenolith and fractures/joints were observed within the study area.

4.1.8 Foliation: This is the preferred orientation of mafic and felsic minerals (formed under differential stress in the direction perpendicular to the direction of compressive stress (Nelson, 2015). Gneissic foliation was observed in the granite gneiss outcrops between Bitako-Nyali and Kobanko villages as explained in paragraphs 4.1.5.

4.1.9 Xenolith: A xenolith is an inclusion (rock fragment) in igneous rocks entrained during magma ascent, emplacement and eruption (Plate XX). Consequently, it is older than the rock where it is found.

Plate XXI: Xenolith of basic rock on grey coarse-grained granite outcrop close to Bansi village ($8^0$46′12.5”, $11^0$49′06.5″)

4.1.10 Fractures

The granites in Zing and its environs are highly fractured, jointed and weathered (Plate XXI). This provides pathways for movement of ground water and its accompanying ions. The major joints observed on the granodiorite, porphyritic granite and the coarse-grained granites, have a dominantly NW-SE and N-S direction. A sinistral strike-slip fault was observed displacing a 0.2m thick fine-grained granite vein on porphyritic granite off Yakoko-Monkin road (Plate XXII). The general and subordinate joint direction of the rock types are displayed on the rose diagram displayed on Figure 4.2.

Plate XXII: Cross-cutting Joints on porphyritic granite at Lakwanti Yakoko ($8^0$57′57.5”N, $11^0$41′36.9”E)

Plate XXIII: A fault line (in yellow colour), striking N206 displaced a 0.2m thick caorsed-grained graniten (8^0 50′ 38.5″N; 11^0 46′ 10.2″E)

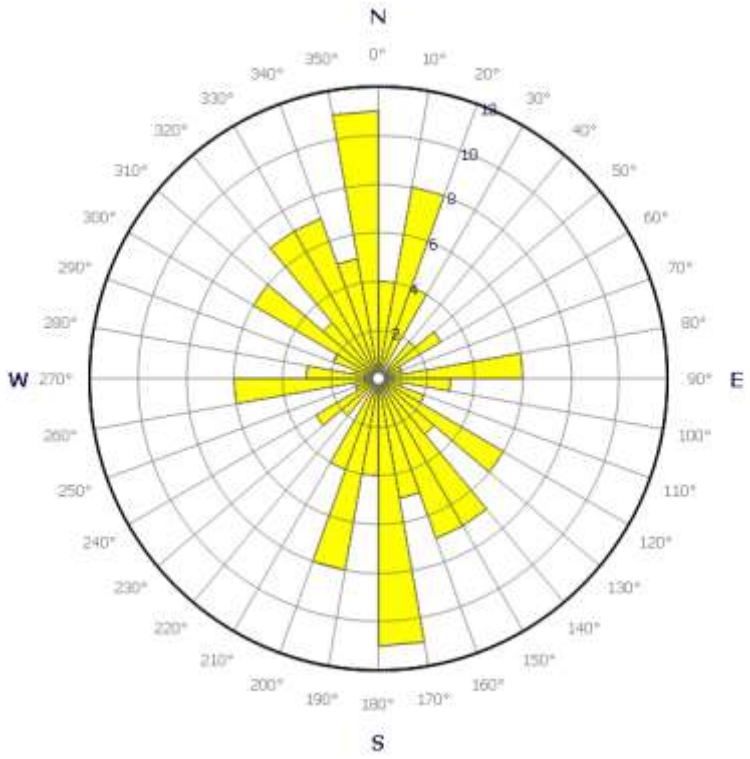

Figure 4.2: Rose Diagram of the Study Area The dominant joint direction of major rocks in Zing and its Encirons is NNW-SSE, with subordinate NE-SW, NW-SE and some E-W joint directions.

4.1.11 Other geological features

Other geologic features are the sharp and gradational contacts, aplite dyke as revealed in the following plates.

Plate XXIV: Sharp contact between porphyritic granite and fine-grained granite intrusion at Yakoko (8^0 54′ 29.3″N, 11^0 42′ 30.8″E)

Plate XXV: Gradational contact between porphyritic granite and coarse-grained granite boulder at Yakoko village (8^0 54′ 29.3″N, 11^0 42′ 30.8″ E)

Plate XXVI: Aplite dyke vein (30cm thick) on porphyritic granite at Bubong (8^0 59′05.1″N, $11^0$47′20.0″E).

4.1.12 Age relationship

Field observation and relationships were used to suggest the relative age of the various rock types in the study area. The granodiorite is the oldest rock type in the study area. The xenolith of granodiorite observed on the coarse-grained granite at Bansi suggested the granodiorites are older. The subordinate occurrence and patches of granite gneiss sporadically found within the coarse-grained granite, suggested that the later was emplaced after the earlier

In addition to this, blocks of coarse-grained granite are frequently found within the porphyritic granites. This implies that the coarse-grained granites were emplaced earlier. The porphyritic granites contain less inclusion of other rock material but around Yakoko and some other areas, fine-grained granite interfinger and penetrate the porphyritic

granite, indicating that the fine-grained granites are younger. Late acid segregation seems to be responsible for the formation of pegmatites, aplite and quartz veins in the area and they are more exposed in the coarse-grained granites than the porphyritic granites. Therefore, the rocks of the study area, on order of decreasing relative age, are granodiorites, granite gneiss, fine grained granites, coarse-grained granite, porphyritic granite and the pegmatites.

4.2 Petrogenesis, Geochemistry and Mineralogical Composition of Rocks in the Study Area

The mantle and the crust are two major sources of granitic rocks and they are not mutually exclusive. Chappell and White, (1978) recognised two types of granites (each, related to a particular orogenic belt) – the I-type granite (which is compositionally expanded) and the S-type granite (which is compositionally restricted). Both granites have calc alkaline characters and distinctive petrochemical characteristics which reflect the differences in the sources of the magmas. The I-type granites are derived from a basic igneous source by remelting of deep seated igneous material or the mantle, while the S-type granites are derived from melting of metesedimentary source materials. The fundamental distinguishing mineralogical and field characteristics of the different sources, as recognised by Chappell and White (1978) are compared with those of Zing and its environs in Table 4.1. Such comparison shows that the rocks in Zing and its environs have I-type characteristics and support the model of its derivation by partial melting of basic source rock of mantle origin. The paucity of foliation, the mafic enclaves and the gradational contact relation between the rock units have led to a conclusion that the rock types are probably I-type, genetically related to a common source by fractional crystallisation quartz, biotite, albites, microcline and accessory minerals such as actinolites, annites, magnetite, sanidine and zircon. The rock types which are granitic in

nature are probably formed by partial melting of basic rocks (most likely derived from igneous source) in the uppermost mantle and/or lower crust.

Table 4.1. I- and S-type Granite Characteristics compared with those of Zing and its Environs.

Criteria	I-Type	S-Type	Zing and Environs
Field	Massive with little or no foliation, contains mafic hornblende-bearing Xenoliths	Usually foliated, contains metasedimentary Xenoliths. May be associated with regional metamorphism, more likely to be found near their source and show evidence(migmatite,regional metamorphism).	Little foliation, contains zenolith enclaves in the granodiorite
Mineralogical	Hornblende and Biotite+ accessory magnetite	Muscovite + accessory ilmenite	Biotite, albites + accessory magnetite
Chemical	High oxygen fugacity, high Na_2O, >3.5% in felsic rocks decreasing to >2.2% in more mafic types.	Low oxygen fugacity, low Na_2O; normally <3.5% in rocks with approximately 5% K_2O decreasing to >2.2% in rocks with approximately 2% K_2O.	Not determined
Isotope	Isotope $\delta^{18}0$ <10% SMOW $^{87}Sr/^{86}Sr$ = 0.704 - 0.706 $\delta\ ^{34}S$ = 3.6 – 5.0%	$\delta\ ^{18}0$ >10% SMOW $^{87}Sr/^{86}Sr$ = >0.7061 $\delta\ ^{34}S$ < - 5.00%	Not determined, but there is Sr chemical enrichment in the rocks, an indication of isotopes of Sr.
Ore Association	Porphyry copper, Mo	Tin	Porphyry copper and Mo not determined.

(after Chappell and White, 1978)

The major elemental composition of the rocks in the study area revealed that Silicon (Si) and Aluminum (Al) are the most enriched elements in the rocks compared to other elements (Table 4.2). The concentration of Silicon ranges from 30.18% to 39.18% with a mean value of 35.14% while aluminum ranged from 7.14% to 12.09 with an average 8.19%. Other chemical elements have mean values in order of decreasing abundance as Potassium (3.44%) ; Iron (1.72%); Sodium (1.67%) ; Calcium (0.78%) and Magnesium (0.72%). The least elemental composition in the rocks are Titanium (0.23%) ; Phosphorous (0.19%) as well as Manganese (0.00%)(Table 4.2 , Figure 4.3). The plot of the Oxides of Silicon (SiO_2) versus that of Sodium (NaO) and Potassium (K_2O) on Total Alkali Silica(TAS) diagram after Middlemost (1994) infers that the rocks are granitic in nature (Table 4.3, Figures 4.4 and 4.5) as confirmed by the geology of the present study.

The bulk chemical composition of all the rock samples shows that the percentage weight (wt%) of SiO_2, Al_2O_3, K_2O and MgO suggests enrichment of both felsic and mafic minerals (Table 4.3, Figure 4.5) . The SiO_2 ranges from 64.54% to 75.81% with a mean value of 70.75%; Al_2O_2 ranges between 12.56% and 18.83% with a mean value of 14.88%, K_2O between 2.62% and 5.89% and a mean of 4.40%; Na_2O between 2.04% and 4.45% and a mean of 3.5%. The low mean concentration of Fe_2O_3 (2.45%), CaO(1.94%), MgO (1.19%) , P_2O_5 (0.45%) and MnO (0.05) in order of decreasing aboundance reflects the felsic nature of the rocks as well as granitic origin .

The trace elements in the rocks measured in ppm showed significant concentration of Strontium (Sr) and Barium (B) compared to other elements. The Sr concentration in the rocks ranged from 1.27ppm to 6760ppm with a mean value of 3343.40ppm while B is between 525 ppm to 4300ppm with a mean value of 1641.63ppm. others are Lead with a mean value of 239.10ppm, Chloride with 390.43ppm, Rubidium with 188.21ppm, Zinc with 177ppm, Cupper with 53.10ppm, Thorium with 33.85ppm, Vanadium with

28.69ppm and Gallium with 24.61ppm, Nickel with 6.45ppm while the least is Arsenic with 0.00ppm concentration in order of decreasing abundance. Table 4.4 and Figure 4.6 is the result of X-RF analyses for trace element concentration (ppm) and their respective mean bar chart plots. The presence of the respective chemical elements in rock sample therefore indicates that the elements are intergral part of the rock composition during when they are formed and subsequently emplaced.

Table: 4.2. Results of XRF Analyses showing concentrations of major elements (Wt.%) of the Study Area

Sample Code	Al	Ca	Cr	Fe	K	Mg	Mn	Na	P	Si	Ti
ZGR001	7.74	0.79	ND	0.85	3.99	0.82	0.03	2.17	0.20	35.11	0.12
ZGR003	7.21	1.57	ND	3.20	3.84	0.74	0.06	1.52	0.27	35.73	0.29
ZGR005A	7.30	0.40	ND	1.03	3.96	0.44	0.01	1.86	0.02	39.18	0.06
ZGR005B	7.15	0.41	ND	1.39	3.64	0.45	0.03	1.68	0.21	36.62	0.10
ZGR006	12.09	0.05	0.04	0.38	0.11	0.28	0.01	0.1	0.23	36.82	0.82
ZGR008	10.05	0.03	ND	1.39	2.99	0.31	0.04	0.23	0.18	36.21	0.12
ZGR010	7.14	2.16	ND	4.72	3.04	0.95	0.09	1.64	0.37	30.18	0.51
ZGR011	7.70	1.01	ND	0.70	3.65	0.32	0.02	2.12	0.15	35.74	0.03
ZGR012	8.88	0.38	ND	2.25	5.86	2.05	0.09	2.14	0.16	31.24	0.31
ZGR017	7.18	0.96	ND	1.98	4.06	0.59	0.04	1.81	0.18	35.08	0.14
ZGR018	8.16	0.73	ND	1.99	3.81	1.27	0.06	2.19	0.21	33.55	0.23
ZGR019	7.65	0.83	ND	0.74	2.38	0.42	0.02	2.56	0.16	36.23	0.04
MAX	12.09	2.16	0.04	4.72	5.86	2.05	0.09	2.56	0.37	39.18	0.82
MIN	7.14	0.03	0.04	0.38	0.11	0.28	0.01	0.10	0.02	30.18	0.03
MEAN	8.19	0.78	0.00	1.72	3.44	0.72	0.00	1.67	0.19	35.14	0.23
SD	1.50	0.61	0.01	1.24	1.34	0.52	0.03	0.76	0.08	2.46	0.23

***Note:** Max= Maximum; Min= Minimum; SD=Standard Deviation

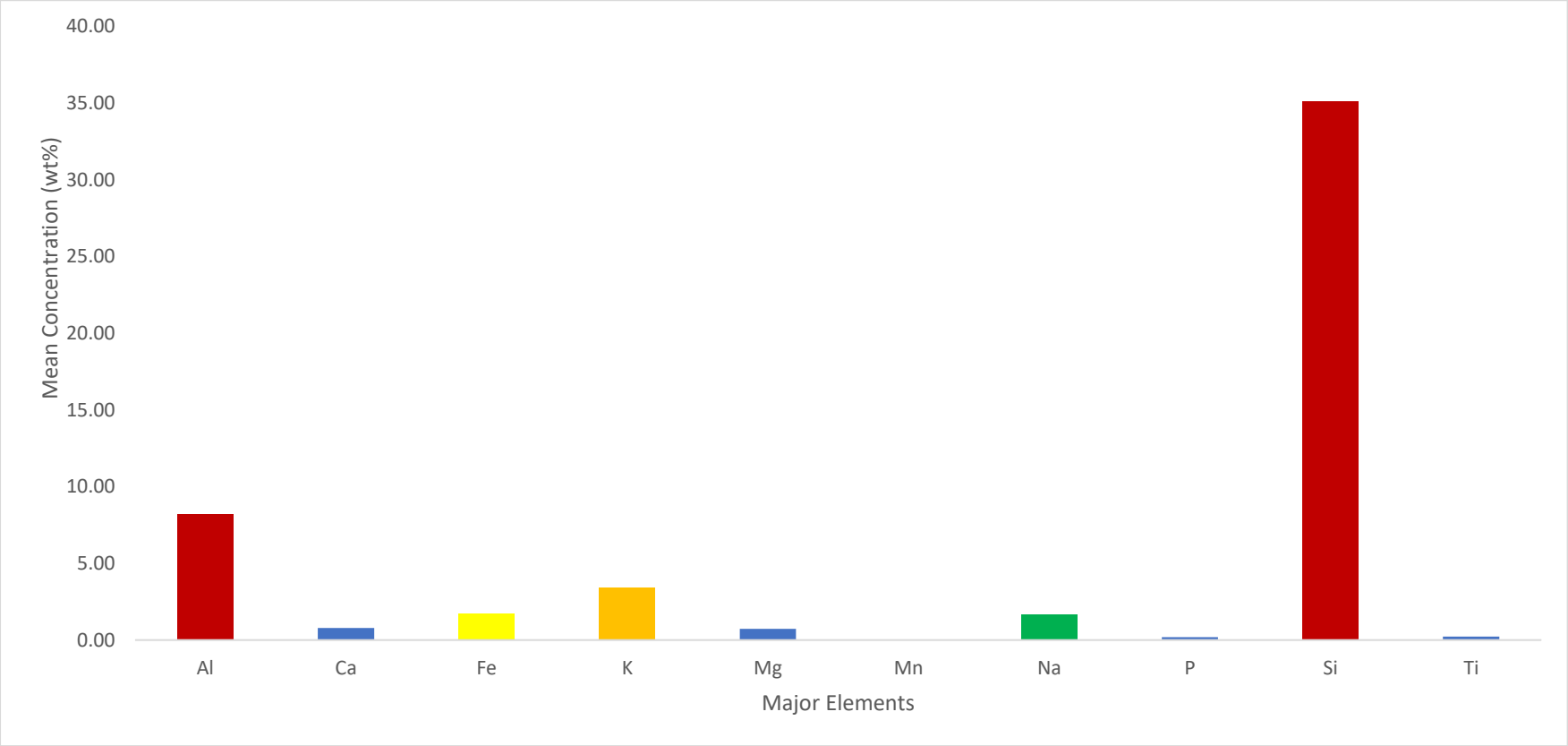

Figure: 4.3. Bar Chart of X-RF mean concentrations major elements of the study Area

Table 4.3: XRF Results of Major Oxides of Elements in %

Sample Code	Fe_2O_3	Na_2O	MgO_2	Al_2O_3	SiO_2	P_2O_5	K_2O	CaO	TiO_2	MnO	Total
ZGR001	1.12	3.93	1.36	13.62	73.09	0.45	4.81	1.98	0.2	0.03	**100.59**
ZGR003	3.58	2.04	1.23	12.63	73.42	0.61	2.62	3.91	0.49	0.07	**100.6**
ZGR005A	1.47	2.51	0.73	13.78	75.81	0.04	4.77	1.01	0.11	0.02	**100.25**
ZGR005B	1.98	4.26	0.74	13.51	72.32	0.48	5.39	1.03	0.16	0.04	**99.91**
ZGR006	0.54	4.13	0.47	18.83	70.76	0.54	4.13	0.13	1.38	0.01	**100.92**
ZGR008	1.99	4.3	0.51	17.98	70.46	0.41	4.6	0.09	0.21	0.05	**100.6**
ZGR010	6.75	2.21	1.58	13.49	64.54	0.84	3.67	5.39	0.86	0.12	**99.45**
ZGR011	2.03	2.86	0.53	16.54	70.44	0.34	4.39	2.51	0.06	0.03	**99.73**
ZGR012	3.22	3.89	3.4	15.77	67.82	0.38	3.06	0.95	0.52	0.12	**99.13**
ZGR017	2.83	4.43	0.97	12.56	70.03	0.42	5.89	2.4	0.24	0.05	**99.82**
ZGR018	2.85	2.96	2.11	15.41	69.76	0.48	4.59	1.82	0.38	0.07	**100.43**
ZGR019	1.06	4.45	0.7	14.45	70.5	0.36	4.87	2.06	0.07	0.03	**98.55**
MIN	0.54	2.04	0.47	12.56	64.54	0.04	2.62	0.09	0.06	0.01	
MAX	6.75	4.45	3.4	18.83	75.81	0.84	5.89	5.39	1.38	0.12	
MEAN	2.45	3.5	1.19	14.88	70.75	0.45	4.40	1.94	0.39	0.05	
SD	1.64	0.91	0.85	2.05	2.85	0.19	0.92	1.53	0.39	0.04	

*Note: Min= Mimimum; Max= Maximum;SD= Standard Deviation

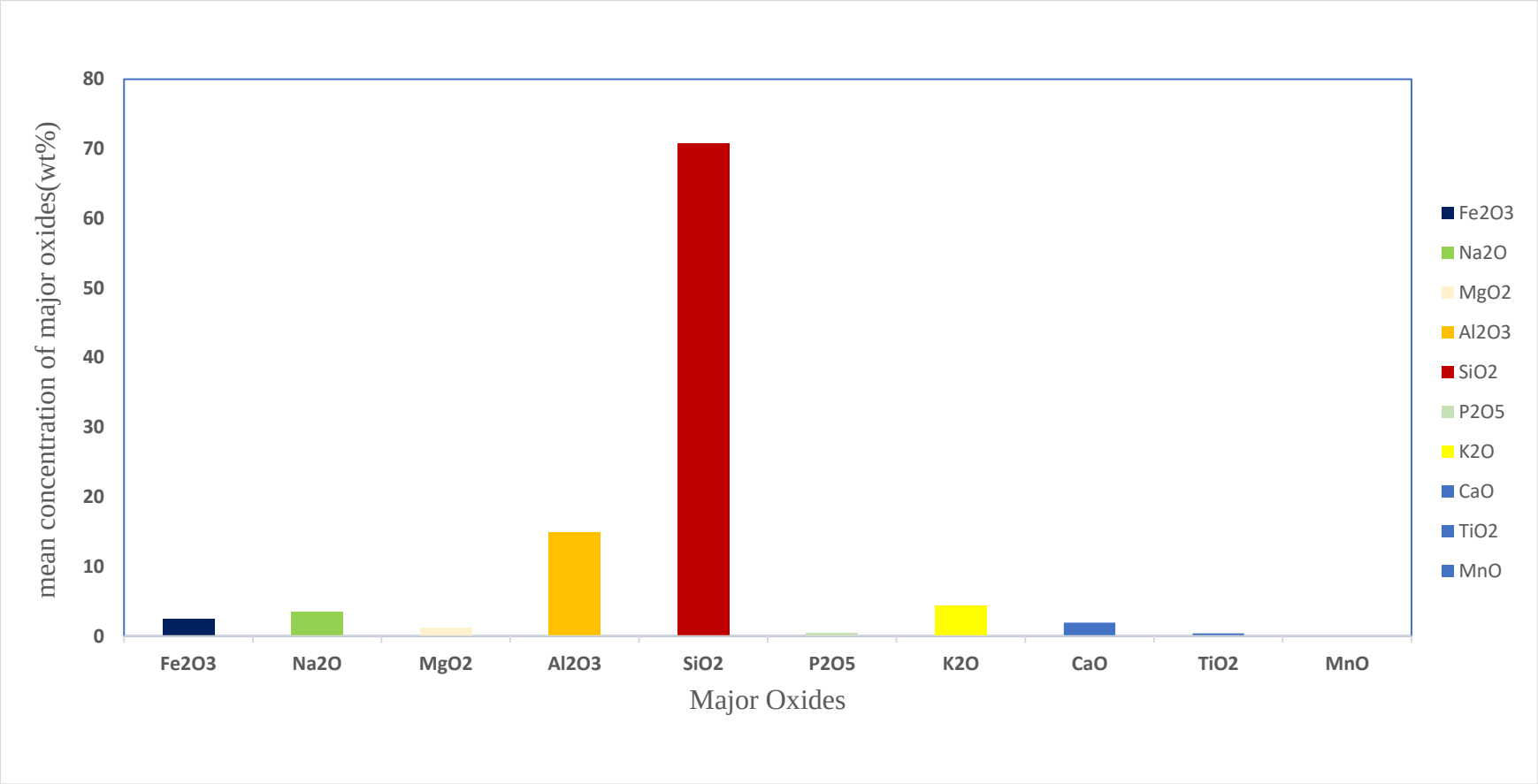

Figure: 4.4: Bar Chart of X-RF mean concentrations of major oxides of the study Area

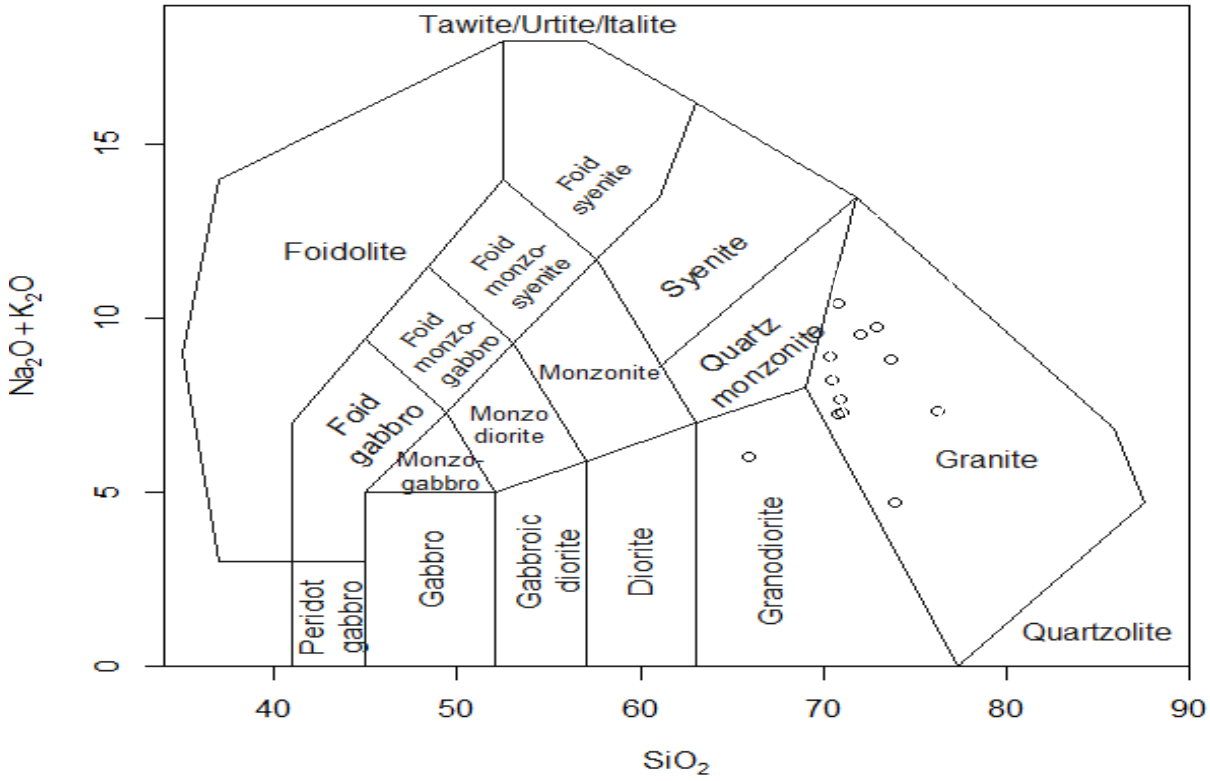

Figure 4.5. Total Alkali Silica(TAS) diagram of the study Area

Table 4.4: Result of XRF showing concentration of Trace elements(ppm) of the study area

S/N	As	Ba	Cu	Ga	Ni	Pb	Rb	Sr	Th	V	Zn	Cl	Cr
ZGR001	ND	1101	24.6	21.7	6.1	208.2	214.6	1271	26.5	17	107.4	196	ND
ZGR003	ND	966	45.6	19.8	3.1	115.5	144.6	4594	9.4	14.6	202	510	ND
ZGR005A	ND	ND	27.9	24.9	ND	141.1	254.2	1014	13.05	5.4	119.5	ND	ND
ZGR005B	ND	ND	59.9	17.1	17.7	389	271.3	1778	93.2	9	208.9	ND	ND
ZGR006	ND	3151	60.2	48.8	6.08	272.2	7.3	1436	ND	100.4	129.4	ND	0.04
ZGR008	ND	570	30.3	17.6	6.84	164.9	117.7	3256	21.2	13.5	99.1	ND	ND
ZGR010	ND	1003	47.1	18.3	4.8	60.8	112.6	6170	17.6	58.9	191	520	ND
ZGR011	ND	ND	51.3	29.9	3.76	184.9	327.1	1005	42.7	4.9	102.3	117	ND
ZGR012	ND	1517	69.2	20.5	9.6	160	245.2	5050	14.5	47.8	309.8	810	ND
ZGR017	ND	4300	54	23.3	4.13	122.8	245.2	3277	78.4	ND	185.1	421	ND
ZGR018	ND	525	55.5	28.2	3.84	120.8	199.5	6760	46.5	30.8	227	159	ND
ZGR019	ND	ND	111.6	25.23	4.98	929	119.2	5780	9.3	6.8	170.5	ND	ND
MAX	0	4300	111.60	48.80	17.70	929	327.1	6760	93.20	100.40	309.8	810	0.04
MIN	0	525	24.60	17.10	3.10	60.8	7.30	1.27	9.30	4.90	99.10	117	0.04
MEAN	0.00	1641.63	53.10	24.61	6.45	239.10	188.2	3343.44	33.85	28.10	171	390.43	0.04
SD	0	1358.18	23.06	8.64	4.15	233.43	89.42	2301.01	28.69	29.94	63.04	249.73	0.01

***Note:** ND means Not Detected; Min = Mimimum; Max = Maximum;SD = Standard deviation

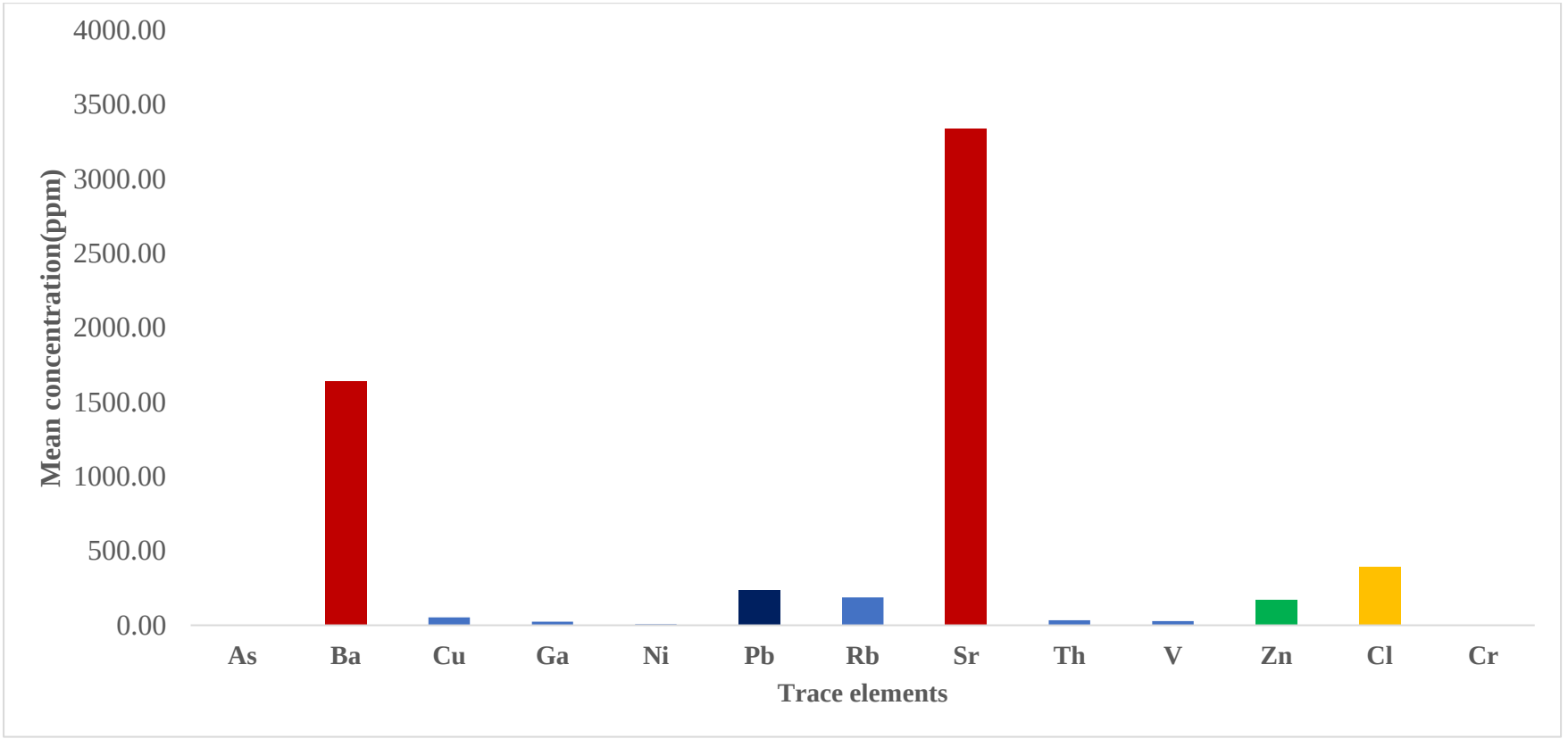

Figure: 4.6. Bar Chart of X-RF mean concentrations of trace elements of the study Area

The Chemical Index of Alteration (CIA) proposed by Nesbit and Young (1982) as a measure to determine the role played by chemical weathering in the production of clastic sediments is the most accepted of available weathering indices. Its provides crucial insights into the changes in the relative contributions of chemical and physical weathering in the production of sedimentary detritus and defined as :

$$\text{CIA} = \left(\frac{Al_2O_3}{Al_2O_3 + Na_2O + K_2O + CaO^*}\right) \text{x } 100. \qquad (4.1)$$

According to Nesbitt and Young (1984), when CIA values ranges from 30% to 55%, it is an indication of weathering at incipient zone, while CIA values ranging from 51% to 85% could be considered as intermediate zone of weathering. The weathering that is at the advanced stage will have CIA values greater than 85% while fresh and unaltered granitic rocks will have CIA values around 50%. A residual soil rich in clay minerals such as kaolinite would have a CIA value close to 100%. The CIA value of weathered products of rocks is a good indicator of the extent of chemical weathering experienced by the rock (Nesbitt and Young, 1984, Anuspam and Rajamani, 2000). Table 4.5 shows the summary of the calculated Chemical Index of Alterations (CIA) for the rock types in the study area. According to the CIA values obtained from the twelve (12) representative samples of the rocks collected in the study area, its indicated that chemical weathering on the rocks is between intermediate to advanced stage. The CIAs value of pegmatite is 68.47, granite gneiss is 71.20, coarse graine granites are between 65.47 and 76.50, porphyrictic granite has a value between 59.75 and 90.28 and granodiorite with 91.03. Therefore, the CIA values of the rock types as enunciated in Table 4.5 suggests that the rock samples are not fresh but have experienced progressive chemical weathering of intermediate to a matured stage capable of mobilizing clemical consitients into groundwater systems of the study area. The evidences of the chemical weathering of feldspathic minerals in the granitic

rocks into clay minerals (kaolinite) is a vivid example (Table 4.5 and samples 6 and 8 respectively).

Table 4.5: Summary of Calculated Chemical Index of Alteration of Rocks in the Study Area

Sample Code	Rock type	Na_2O	Al_2O_3	P_2O_5	K_2O	CaO	CaO*	CIA
ZGR001	PG	3.93	13.62	0.45	4.81	1.98	**-1.53**	**65.39**
ZGR003	PG	2.04	12.63	0.61	2.62	3.91	**-3.3**	**90.28**
ZGR005A	PG	2.51	13.78	0.04	4.77	1.01	**-0.97**	**68.59**
ZGR005B	PG	4.26	13.51	0.48	5.39	1.03	**-0.55**	**59.75**
ZGR006	PEG	4.13	18.83	0.54	4.13	0.13	**0.41**	**68.47**
ZGR008	CGG	4.3	17.98	0.41	4.6	0.09	**0.32**	**66.10**
ZGR010	GD	2.21	13.49	0.84	3.67	5.39	**-4.55**	**91.03**
ZGR011	CGG	2.86	16.54	0.34	4.39	2.51	**-2.17**	**76.50**
ZGR012	GG	3.89	15.77	0.38	3.06	0.95	**-0.57**	**71.20**
ZGR017	PG	4.43	12.56	0.42	5.89	2.4	**-1.98**	**60.10**
ZGR018	PG	2.96	15.41	0.48	4.59	1.82	**-1.34**	**71.28**
ZGR019	CGR	4.45	14.45	0.36	4.87	2.06	**-1.7**	**65.47**

PG = porphyrictic Granite; PEG = Pegmatite; CGG = Coarse Grained Granite; GD=Granodiorite;

The overall mineralogy of the rocks indicates that Quartz, Albite, Microcline and Biotite are the major mineral composition. The mineral assemblage in the rocks such as quartz occurs in all the 12 rock samples representing 100% while albite in 10 samples indicating 83% occurrence. Microcline occur in 9 samples representing 75% occurrence in the rocks analyzed and biotite shows 50% in 6 of the rock samples. Additional minerals such as kaolinite indicated 16.7% occurrence in 2 samples each while Sinidine, Annites, Actinolite, magnetite and Phlogopite representing 8.3% in 1 sample each (Table 4.6 and appendices **B-M)**. The elemental (Tables 4.2, 4.4) and mineralogical (Table 4.6 and apendices(B-M) composition of the rocks therefore suggests that they are integral part of the rock at formation and emplacement stage.

Table: 4.6: XRD Results of Rock Samples of the Study Area

Sample Code	Rock Type	Min. Composition	Chemical Formular
ZGR/001	Porphyritic Granite	Biotite (26.7%)	$\mathbf{K_6Mg_{18}Si_{18}Al_6O_{66}F_6}$
		Microcline (26.7%)	$K_{1.9}NaAl_2Si6O_{16}$
		Albite (26.7%)	$Na_2Al_2Si_6O_{16}$
		Quartz (19.6%)	Si_3O6
ZGR/003	Porphyritic Granite	Albite (62%)	$Na_2Al_2Si_6O_{16}$
		Sinidine(19%)	$K_4Ga_4Si_{12}O_{32}$
		Quartz (13%)	Si_3O_6
		Biotite(6%)	$K_4Fe_{5.57}Mg_{4.64}Ti_{1.10}Si_{11.17}Al_{4.83}O_{48}$
GR/005A	Porphyritic Granite	Microcline(70%)	$K_{1.9}NaAl_2Si_6O_{16}$
		Albite(22%)	$Na_2Al_2Si_6O_{16}$
		Quartz (8%)	Si_3O
ZGR/005B	Prophyritic Granite	Microcline (50.5%)	$K_{1.9}NaAl_2Si_6O_{16}$
		Albite (33.3%)	$Na_2Al_2Si_6O_{16}$
		Quartz (10.1%)	SiO_2
		Annite (6.1%)	$K_{1.84}NaMg_2Fe_2TiAl_2Si_5O_2$
ZGR/006	Pegmatite	Quartz (46%)	Si_3O_6
		Kaolinite(41%)	$Al_2Si_2O_9H_4$
		Zircon (9%)	$Zr_4Si_4O_{16}$
		Magnetite(4%)	$Fe_{24}O_{32}$
ZGR/008	Coarsed Grain Granite	Quartz (48.5%)	$S_{i3}O_6$
		Microcline(41.4%)	$K_{1.9}NaAl_2Si_6O_{16}$
		Kaolinite(10.1%)	$Al_2Si_2O_9H_4$

Table: 4.6 Continued.

Sample Code	Rock Type	Min. Composition	Chemical Formular
ZGR/010	Granodiorite	Biotite (18%)	$K_6Mg_{18}Si_{18}Al_6O_{66}F_6$
		Actinolite(22%)	$Fe_{5.51}Mn_{0.63}Mg_{4.10}Al_{0.59}Ti_{0.01}Ca_{3.54}Na_{0.38}Si1_{5.51}KH_{3.67}O_{47}\mathbf{F_{0.10}}$
		Albite (36.%)	$Na_{1.96}Ca_{0.04}Si_{5.96}Al_{2.04}O_{16}$
		Quartz(24%)	Si_3O_6
ZGR/011	Coarsed Grain	Microcline (38%)	$K_{1.9}NaA_{l2}Si_6O_{16}$
	Granite	Albite (33%)	$Na_{1.96}Ca_{0.04}Si_{5.96}Al_{2.04}O_{16}$
		Quartz (18%)	Si_6O_6
		Biotite (11%)	$K_6Mg_{18}Si_{18}Al_6O_{66}\mathbf{F_6}$
ZGR/012	Granite Gneiss	Microcline (32%)	$K_{1.9}NaA_{l2}Si_6O_{16}$
		Albite(17%)	$Na_2Al_2Si_6O_{16}$
		Quartz (33%)	Si_3O_6
		Biotite (18%)	$Si_{5.36}Al_{3.80}Fe_{2.76}Mg_{1.46}Ti_{0.28}Na_{0.0}4K_{1.92}Ca_{0.06}Ba_{0.02}O_{23.36}\mathbf{F_{0.64}}$
ZGR/017	Porphyritic Granite	Microcline (40%)	$Si_{5.44}Al_{4.96}Fe_{5.60}Mg_{2.84}Ti_{0.64}Na_{0.08}K_{3.92}O_{48}$
		Albite(38%)	$Na_2Al_2Si_6O_{16}$
		Quartz (17%)	Si_3O6
		Biotite (6%)	$K_{1.9}NaAl_2Si_6O_{16}$
ZGR/018	Porphyritic Granite	Albite (42%)	$Na_2Al_2Si_6O_{16}$
		Phlogopite (29%)	$K_{1.86}Na_{0.14}Mg_{3.00}Fe_{2.22}Ti_{0.78}Si_{5.76}O_{24}$
		Microcline (15%)	$K_{1.9}NaAl_2Si_6O_{16}$
		Quartz (14%)	Si_3O_6
ZGR/019	Coarse Grain	Albite (36%)	$Na_2Al_2Si_6O_{16}$
	Granite	Microcline (46%)	$K_{1.9}NaAl_2Si_6O_{16}$
		Quartz (19%)	Si_3O_6

4.3 Results of Physiochemical Analyses of Water Samples

4.3.1 Physical parameters

4.3.1.1 *Electrical conductivity (EC)*

Electrical Conductivity of water is its ability to conduct electric current due to the presence of salts and other chemical constituents of positively and negatively charged ions. The Electrical Conductivity (EC) of the groundwater water samples of the study area varied from 97.1 and 1138 µS/cm with an average of 562.11 µS/cm. However, a total of two (2) groundwater samples representing 7.18% of the total sample have EC above 1000 µS/cm which is high compared to WHO (2017) and NSDWQ (2015) permissible limit as presented in Table 4.7. High EC in water is an indication of its capacity to conduct electric current due to mineralization resulting from dissolve salts and other aquifer materials in the groundwater. The groundwater in the two locations (Koko and Yelwa) may have been enriched with chemicals ions from the host rock through water rock interaction and other geochemical processes cor depth of the well because the deeper the well, the more groundwater is mineralized.

4.3.1.2 *Total dissolved solids (TDS)*

The Total Dissolve Solids (TDS) indicates the physical characteristics and general nature of water quality. TDS concentration in groundwater of the study area ranged from 63.1 to 740mg/l with a mean value of 365.43mg/l as displayed in Table 4.7. The concentration of TDS in four (4) locations found to be higher than the permissible limit of 500.00mg/l by NSDWQ (2015) but were within the permissible limit of WHO (2017) (Table 4.7). Total Dissolved Solids are valuable indicators of the amount of rock materials dissolved in water. The wide range of EC and TDS values observed particularly in two (2) of the groundwater samples of the study area at Koko and Yelwa could be due to mineralization at depth as a result of the interaction of water with the minerals in the aquifer matrix over

time as well as the confining beds and soil zones as the water flows through a distance by infiltration or percolation. These processes influences mineralization expecially when the medium through which water flows is weathered and contains mineral species. However, the groundwater of the study area based on EC and TDS composition could best be described as generally fresh except in few locations where EC is greater than 1000µS/cm and TDS greater than 500mg/l and 600mg/l respectively due to mineralization . The plot of electrical conductivity (EC) µS/cm versus total dissolved solids (TDS) mg/l of groundwater samples (Figure 4.7) gives a high correlation coefficient of 1.0 confirming linear relationship of the parameters and efficacy of field measurements.

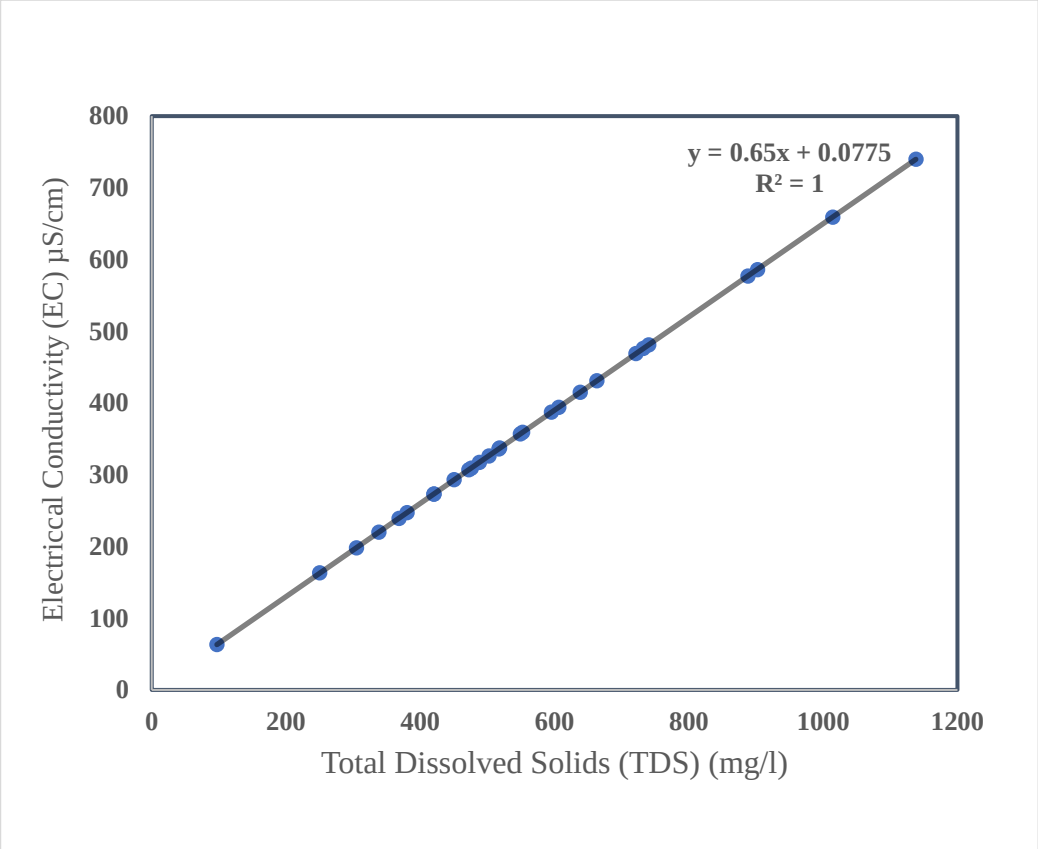

Figure 4.7. EC Versus TDS of groundwater of the study area

The result of measured physical parameters of groundwater water samples of the study area are summarized in Table 4.7.

Table 4.7: Results from In-situ Measurements of Water Samples

Sample Code	Locality	EC (µS/cm	TDS (ppm)	pH	Temp(°C)
ZGW/001	Lakwanti	552	359	7.03	28.9
ZGW/002	Benbon-Yakoko	740	481	7.03	28.2
ZGW/003	Yakoko A	638	415	6.62	29.1
ZGW/004	Yakoko B	902	586	6.69	28.2
ZGW/005	Monkin	250	163	6.63	28.7
ZGW/006	Mission House	595	387	7.13	29.9
ZGW/007	Lajah	450	293	7.24	29.1
ZGW/008	Yukwa	606	394	7.04	30.1
ZGW/009	Dango	368	239	7.41	28.6
ZGW/010	Dindin	420	273	7.18	29.8
ZGW/011	Kobanko	517	336	7.35	28.7
ZGW/012	Jen	380	247	7.2	30.3
ZGW/013	Tuyebuboung	97.1	63.1	6.8	29.8
ZGW/014	Bansi	338	220	6.85	30.4
ZGW/015	Dandi	518	337	7.2	29.4
ZGW/016	Lamma	305	198	7.19	30.4
ZGW/017	Koyu	721	469	7.49	31.3
ZGW/018	Bubong	502	326	7.34	30.8
ZGW/019	Zensi	732	476	7.38	29.8
ZGW/020	Low Cost	472	307	6.9	30.2
ZGW/021	Zandi	549	357	7.14	29.4
ZGW/022	Koko	1014	659	7.05	29.2
ZGW/023	Yelwa	1138	740	7.07	29.3
ZGW/024	Didonko	476	309	7.5	30.1
ZGW/025	Kangon	488	317	7.48	29.1
ZGW/026	Kakulu	663	431	7.21	29.5
ZGW/027	Kwana	420	273	7.21	29.1
ZGW/028	Taraba One	888	577	7.47	28.4
	Min	97.1	63.1	6.62	28.2
	Max	1138	740	7.5	31.3
	Mean	562.11	365.43	7.14	29.49
	Stand. Deviation.	231.34	150.36	0.26	0.79
	WHO, 2017	1000	600	6.5-8.5	Ambient
	NSDWQ, 2015	1000	500	6.5-8.5	Ambient

***Note:** Min= Minimum; Max= Maximum

4.3.1.3 pH

The pH also known as 'potential hydrogen' is a measure of how acidic or basic water is. The pH scales ranges from 0-14, with 7 being neutral. A pH of less than 7 indicates acidity, whereas a pH of greater than 7 indicates a base. The pH of a substance is a

measure of the relative amount of free hydrogen (H^+) and hydroxyl ions (OH^-). The pH values of groundwater samples in the study area ranged between 6.62 and 7.5 with a mean value of 7.14 as represented in Table 4.7. These values of pH in groundwater of the area compared with the prescribed permissible limits by the World Health Organization (WHO, 2017) and the Nigerian Standard for Drinking Water Quality (NSDWQ, 2015) in Table 4.7 are within the permissible range of 6.5 to 8.5 by the two stated national and international regulary bodies. The range of values obtained is responsible for the slightly acidic to alkaline water of the area. The pH is an indication of water quality and extent of water quality deterioration and its values could affect mobility of most metal elements (Tirumelesh *et al*.,2007 and Offodile, 2014) . Many biochemical processes in groundwater are facilitated by changes in pH. Although, other processes, such as absorption may be more effective in controlling pH distribution in groundwater (Offodile, 2014).

4.3.1.4 Temperature

The Temperature of groundwater samples of the area are between 28.2^0C and 31.3^0C with a mean of 29.4^0C (Table 4.7). The temperature values are evenly distributed with slight variations in some locations particularly in the north eastern and south eastern part of the study area. The groundwater samples at Yukwa, Jen, Lamma, Bubong, Lowcost and Didonko showed temperatures between 30.1^0C and 31.3^0C. The ambient temperature of water in the tropics is between 22^0C - 29^0C and cooler waters are generally more palatable than warm water (Waziri *et al*., 2016). Temperature of water has an impact on the acceptability of a number of other inorganic constituents and chemical contaminants that may affect taste of water. Higher temperature conditions for groundwater could encourage the growth of microbials resulting to altering the physical characteristics of water such as odour, taste, colour and corrosion (Bakari, 2014). The temperatures of

30.1^0C and 31.3^0C recorded in few of the wells as stated above could be attributed for the slight potassic and alkaline tastes of the water from the stated wells.

4.4.2 Chemical parameter

4.4.2.1 *Total hardness*

Total Hardness of water samples ranges between 66.0mg/l and 2520mg/l with a mean value of 303.43mg/l (Table 4.9). Total Hardness of water depends solely on quantity of divalent metallic cations where Ca^{2+} and Mg^{2+} are more abundant in groundwater. Groundwater exceeding permissible limit of 300 mg/l $CaCO_3$ are said to be very hard (Sawyer and McCarthy, 1967)(Table 4.8). The results of the study area as indicated in Table 4.8 show that 2(7%) the groundwater samples have total hardness concentration <75mg/l hence term as soft water, 14 (50%) samples have between the range of 75mg/l to 150mg/l hardness concentration described therefore as modereately soft water, a toal of 9 (32%) samples are have handness concentration between 150mg/l to 300mg/l while 3(10.7%) samples were above 300mg/l. These results indicates generally that the groundwater could best be described as 'soft to very hard water' and 'moderately to hard water: in particular. However, the maximum permissible limit of Total Hardness in water is 500mg/l while the most desirable limit is 150mg/l for both World Health Organisation (2017) and Nigerian Standard for Drinking Water Quality(2015) respectively (Table 4.9). A total of 12 (34%) samples were above NSDWQ (2015) permissible limit while 16(57%) samples are within the prescribed limit. Conversely, 2(7.14%) of the total samples were above WHO (2017) acceptable limit while 26(92.86%) are within the limit (Table 4.9).

The total hardness of groundwater in the study area could have resulted from the weathering and leaching of rock forming minerals rich in calcium, magnesium and bicarbonate minerals with hard to very hard groundwater restricted to the extreme

northern section of the area as the source of hardness and moderate to soft groundwater within the central and southern portion of the study area (Figure 4.8). Drinking hard water could results to incidences of heart disease, degenerative theart desease, hypertension or sudden death of cardio-vascular origin (WHO, 2009).

Table 4.8: Classification of Groundwater Based on Total Hardness

Total Hardness as $CaCO_3$ (mg/l)	**Water Class**	**No. of samples**
<75	Soft	2
75–150	Moderately hard	14
150–300	Hard	9
>300	Very hard	3

(Sawyer and Mc Carthy, 1967)

The hardness of water is usually indicated by precipitation of soap scum and the need for excess use of soap to achieve cleaning. Depending on the interaction of other factors, such as pH and alkalinity, water with a hardness above approximately 200 mg/l may cause scale deposition in the treatment works, distribution system and pipework and tanks within buildings(WHO, 2017). Figure 4.8 is the Total Hardness concentration map of groundwater in the study area based on Sawyer and McCarthy,1967 classification.

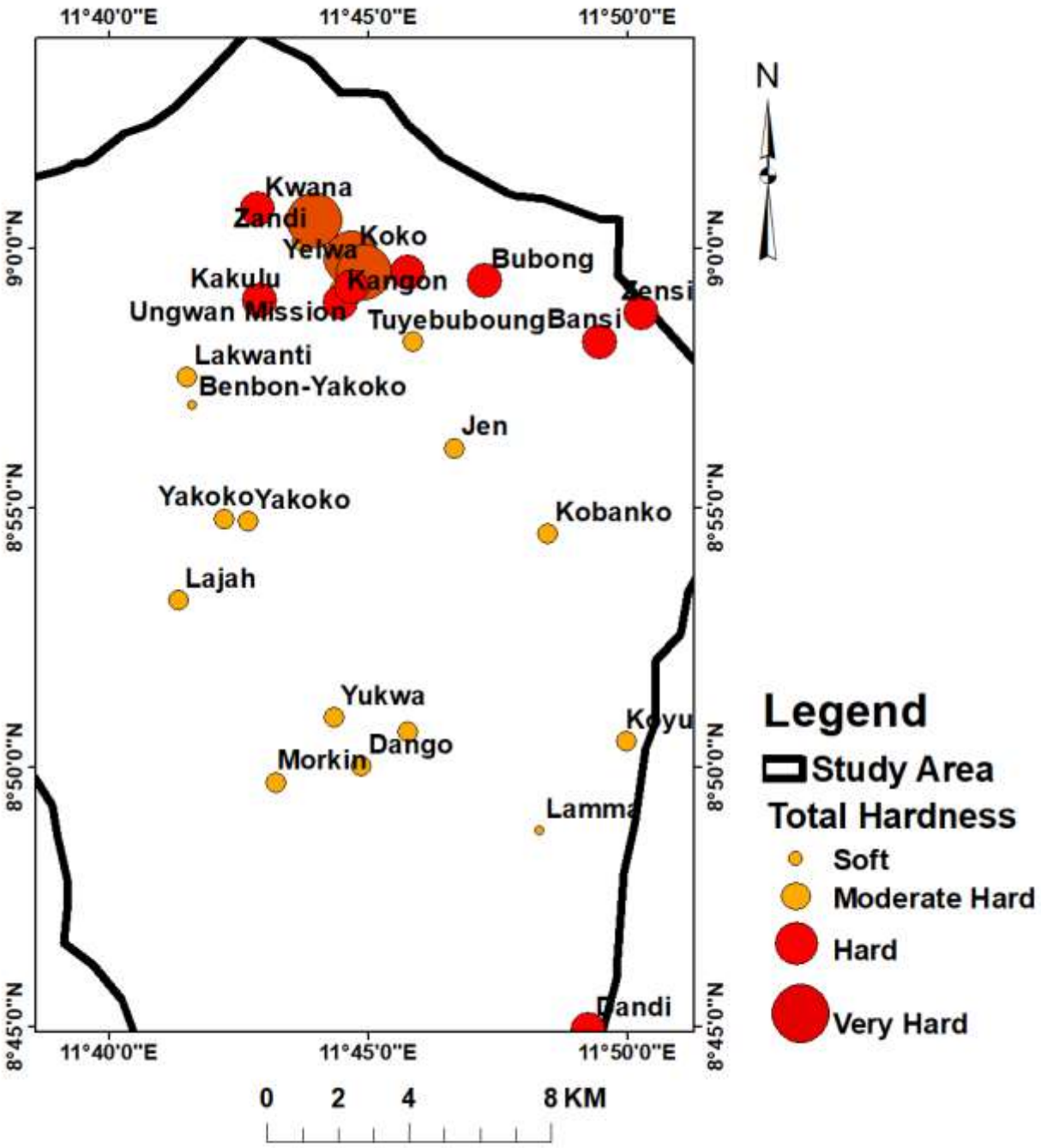

Figure 4.8 Total Hardness concentration of groundwater in the study.

Table 4.9: Results of Measured Chemical Parameters of Water Samples Compared with WHO(2017) and NSDWQ(2015)

Sample Code	Locality	Total Hardness	Ca^{2+}	Mg^{2+}	Na^{+}	K^{+}	CO_3	HCO_3	SO_4	Cl	NO_3	NO_2	F
ZGW/001	Lakwanti	82	21.2	8.12	25.1	41.6	18.6	25	15.6	28.85	4.48	0.03	3.18
ZGW/002	Benbon-Yakoko	74	18.8	7.56	18.4	42.7	38.6	73.2	18.5	57.08	5.84	0.08	2.51
ZGW/003	Yakoko A	104	28.4	9.24	21.6	39	21.6	115	10.7	38.85	8.79	0.02	2.96
ZGW/004	Yakoko B	118	34	9.24	23.2	29.3	33.4	98.4	23.1	68.85	7.23	0.01	3.83
ZGW/005	Morkin	126	30.8	13.7	16.1	25.2	29.4	115	21.3	17.08	10.4	0.07	0.92
ZGW/006	Anguwan Mission	110	32.4	8.12	12.3	40.6	ND	15.0	10.7	356	3.09	0.05	3.49
ZGW/007	Lajah	96	26,0	8.68	15.3	54.3	ND	12.5	14.2	8.85	4.32	0.018	4.18
ZGW/008	Yukwa	78	23.2	5.6	23.1	36.9	17.4	124	12.7	14.2	5.38	0.012	5.33
ZGW/009	Dango	94	25.2	8.68	22.5	38.6	21.4	136	17.3	8.85	6.02	0.057	2.27
ZGW/010	Dindin	92	24.4	8.68	31.3	33.4	30.0	125	15.8	27.08	8.8	0.013	3.58
ZGW/011	Kobanko	142	38.8	12.6	22.1	35.8	19.8	75.0	28.2	15.9	16.4	0.01	5.84
ZGW/012	Jen	136	42.0	8.68	32.3	41.4	11.2	110	25.4	10.6	8.15	0.06	0.97
ZGW/013	Tuyebuboung	78	20.4	7.56	14.2	39.7	13.7	123	16.8	54.9	7.59	0.015	1.83
ZGW/014	Bansi	166	47.2	13.4	15.8	34.3	41.3	182	10.4	17.08	6.85	0.014	2.26
ZGW/015	Dandi	200	52.4	19.3	24.4	38.7	32.1	198	26.3	18.85	11.1	0.009	0.66
ZGW/016	Lamma	66	16.4	7.0	33.5	42.3	33.6	85.6	15.7	40.6	7.04	0.057	0.47
ZGW/017	Koyu	130	32.8	13.4	22.1	29	27.3	82.8	9.3	56.6	9.83	0.01	0.91
ZGW/018	Bubong	194	57.2	14.3	16.1	38.1	23.4	115	7.43	14.2	19.7	0.013	0.69
ZGW/019	Zensi	280	87.2	17.4	19.2	31.3	21.7	75.0	13.5	47.08	13.5	0.236	1.48
ZGW/020	Low-Cost Quarter	106	29.2	9.24	18.0	47.0	38.1	112	8.79	19.5	21.3	0.012	2.14
ZGW/021	Zandi	340	100	25.2	12.3	53.2	40.3	125	14.2	17.7	5.82	0.018	3.38
ZGW/022	Koko	2300	720	140	30.9	73.4	27.6	116	35.9	78.85	6.32	0.059	5.12
ZGW/023	Yelwa	2520	840	118	38.4	85.6	23.9	136	38.2	12.4	15.3	0.033	1.56
ZGW/024	Didonko	168	48.4	13.2	29.7	50.2	16.7	54.6	11.5	15.9	16.2	0.045	1.83

Table 4.9: Continued

ZGW/025	Kangon	158	45.2	12.6	26.7	43.1	28.3	68.2	16.3	22.4	8.82	0.044	1.96
ZGW/026	Kakulu	168	38.8	19.9	19.4	39.6	32.6	75	14.4	36.2	5.76	0.059	1.65
ZGW/027	Kwana	164	46.8	13.2	33.2	40.2	33.9	84	12.3	18.1	6.09	0.015	3.38
ZGW/028	Taraba One	206	64.4	12.6	14.2	36.8	ND.2	78.2	17.2	29.7	13.7	0.012	2.14
	Min Values	66.0	16.4	5.6	12.3	25.2	BDL	12.5	7.43	8.85	3.09	0.009	0.47
	Max Values	2520	840	140	38.4	85.6	41.3	198	38.2	356	21.3	0.236	5.84
	Mean Values	303.43	92.56	20.19	22.55	42.19	25.18	97.66	17.20	29.71	9.42	0.04	2.52
	Standard Deviation	599	195.8	31.2	7.2	12.6	10.7	42.91	7.7	19.2	4.78	0.04	1.46
	WHO, 2017	500	250	150	200	75	**-**	**-**	**250**	**250**	**50**	**3.0**	**1.5**
	NSDWQ,2015	150	100	20	200	-	**-**	**-**	**100**	**250**	**50**	**0.2**	**1.5**

***Note:** Min= Minimum; Max = Maximum and ND = Not Detected.

4.3.2.2 *Calcium (Ca^{+2})*

Calcium concentration in groundwater samples of the study area varied from 16.4mg/l to 840mg/l with a mean value of 92.56mg/l (Table 4.9). Twenty-six (26) samples representing 92.85% of the total samples have calcium ions within the permissible limit of 100mg/l prescribed by NSDWQ, 2015 (Table 4.9). Although, two (2) samples (Koko and Yelwa) representing 7.14% recorded higher values of 720 mg/l and 840mg/l (Table 4.9) respectively which is very high compared to the the taste threshold for calcium ion which is in the range of 250mg/l, depending on the associated anion (WHO, 2017).

The sources of the calcium in groundwater could have been from actinolites, albites, biotites from the underlyind host rocks (Table 4.6).Calcium in the form of calcium sulphate ($CaSO_4.2H_20$) is relatively less soluble in water whereas calcium in the form of calcium chloride and calcium nitrate are very soluble (Offodile, 2014). High concentration of calcium in water provides a certain taste depending on the type of salt present in water and its presence is significant in bone formation and also on nerve integrity and transformation (Adedapo and Fakolade, 2014). Figure 4.9 is a Calcium ion concentration in groundwater of the study area.

4.3.2.3 *Magnesium (Mg^{+2})*

Magnesium concentration in groundwater samples of the area ranges between 5.6mg/l to 140mg/l with a mean value of 20.18mg/l. All the samples (92.85%) except two (7.14%)) falls within the prescribed limits by NSDWQ (2015) and WHO (2017) (Table 4.9). Magnesium occurs as carbonates, hydroxides, oxide, phosphate and silicates. As carbonate, hydroxides, oxides and phosphates, the mineral is hardly soluble in water but other compounds of Magnesium are readily soluble. Magnesium has the same effect on water as Calcium, producing hard water when the concentration is very high. The sources

of magnesium in the area could be from mineral such as biotite, phlogopite and annite (Table 4.6). Figure 4.10 is magnesium ion concentration map of the study area.

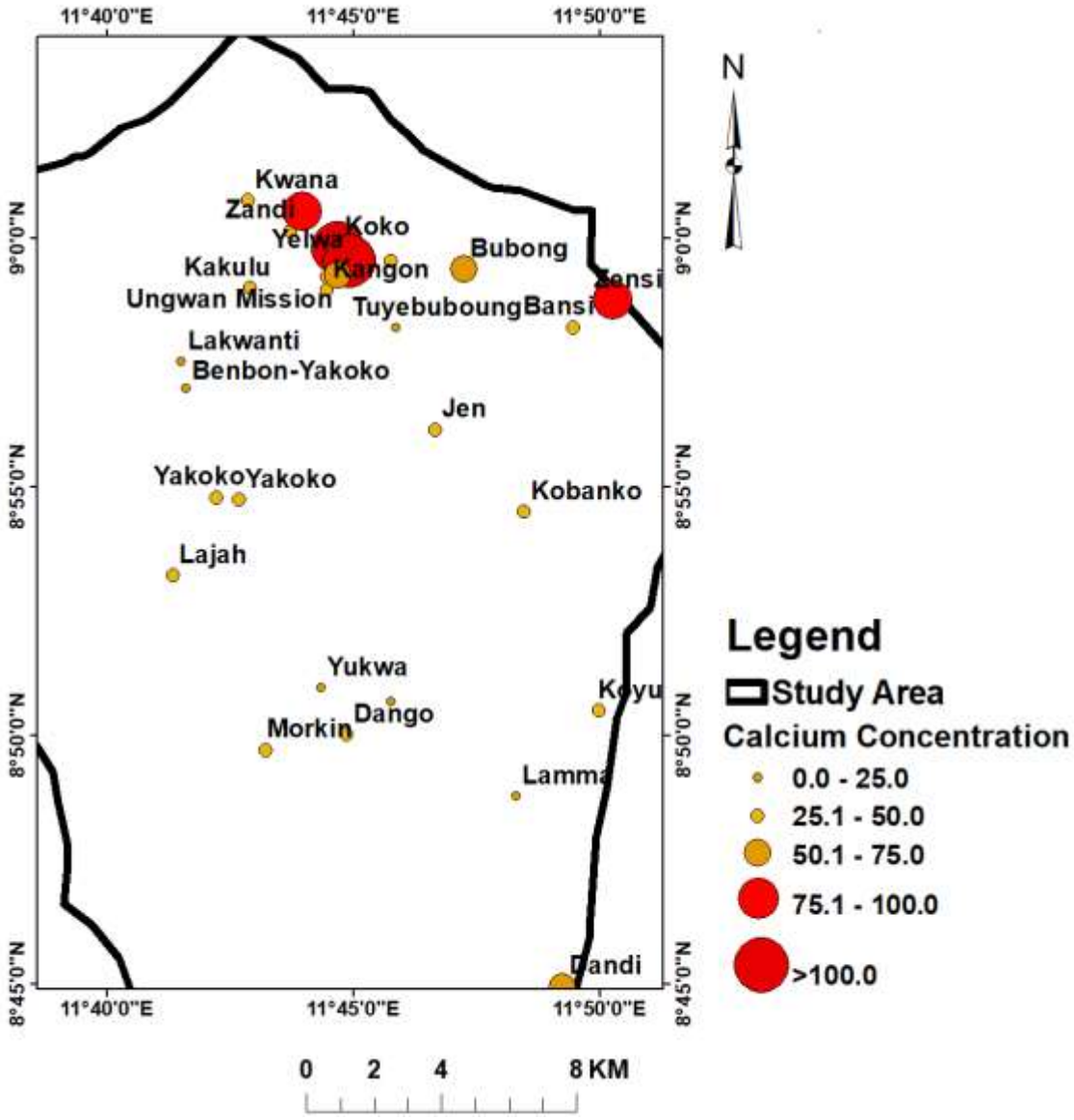

Figure 4.9. Calcium concentration map of the study area

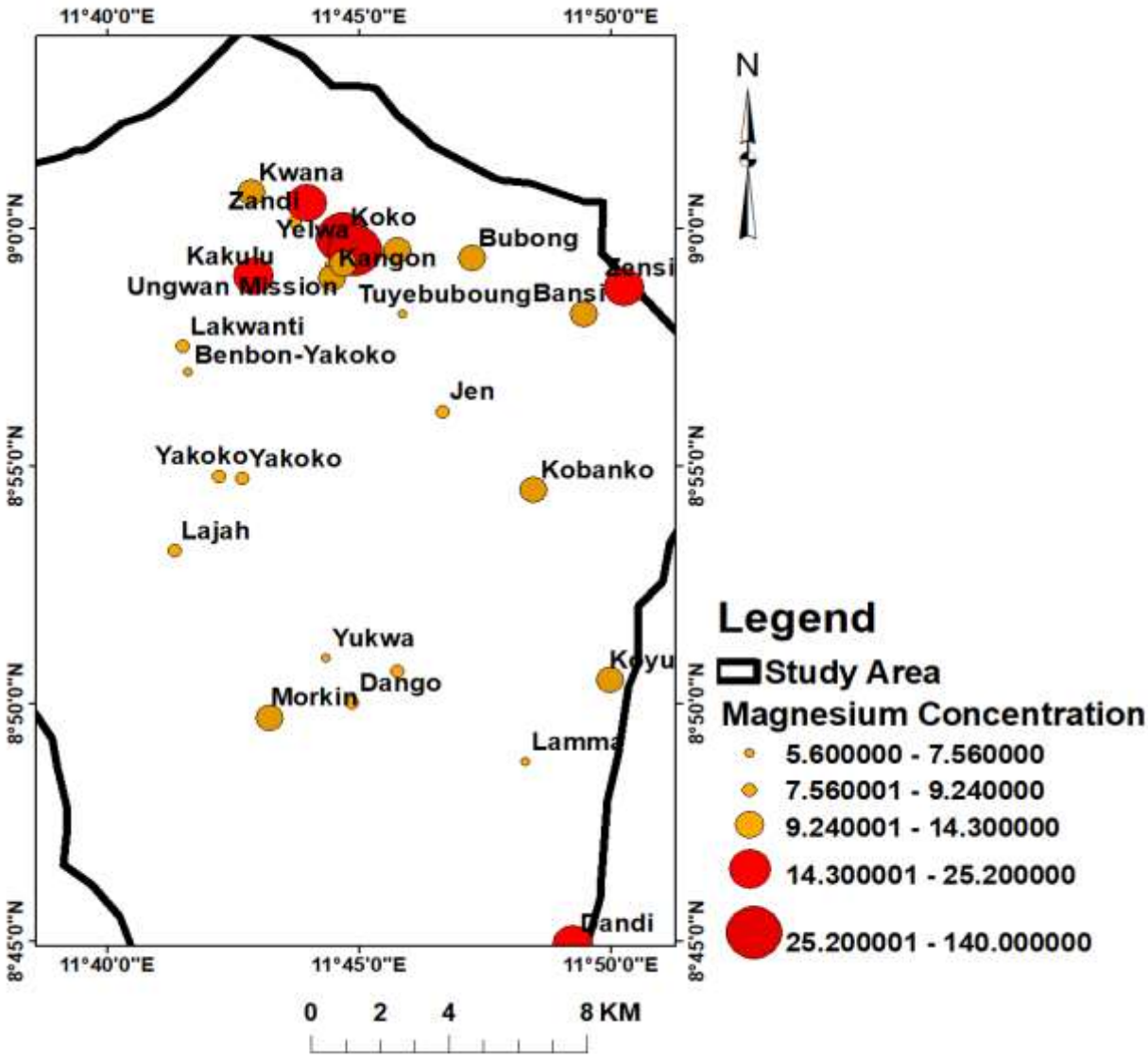

Figure 4.10. Magnesium concentration map of the study area.

4.3.2.4 *Potassium (K^+)*

Potassium concentration in groundwater samples of the area varied from 25.2mg/l to 85.6mg/l with a mean value of 42.19mg/l (Table 4.9). Drinking water of concentration greater than 75mg/l is harmful to heath (WHO, 2017). Only one (1) sample at Yelwa with 86.5mg/l shows K^+ ion greater than 75mg/l in the area Potassium compounds, except the silicates, are readily soluble in water. It is a common constituent of most igneous rocks and because of its high solubility, it is less common in sedimentary rocks. Potassium,

when leeched from rocks, easily recombines with other minerals. As a result, Potassium is found only in small concentration in ground water (Offodile, 2014). The concentration of potassium in the water samples therefore could have been derived from weathering of rock bearing minerals such as microcline, phlogopites,biotite, actinolite, annite and sanidine (Table 4.6). Figure 4.11 is Potassium ion concentration map of the study area.

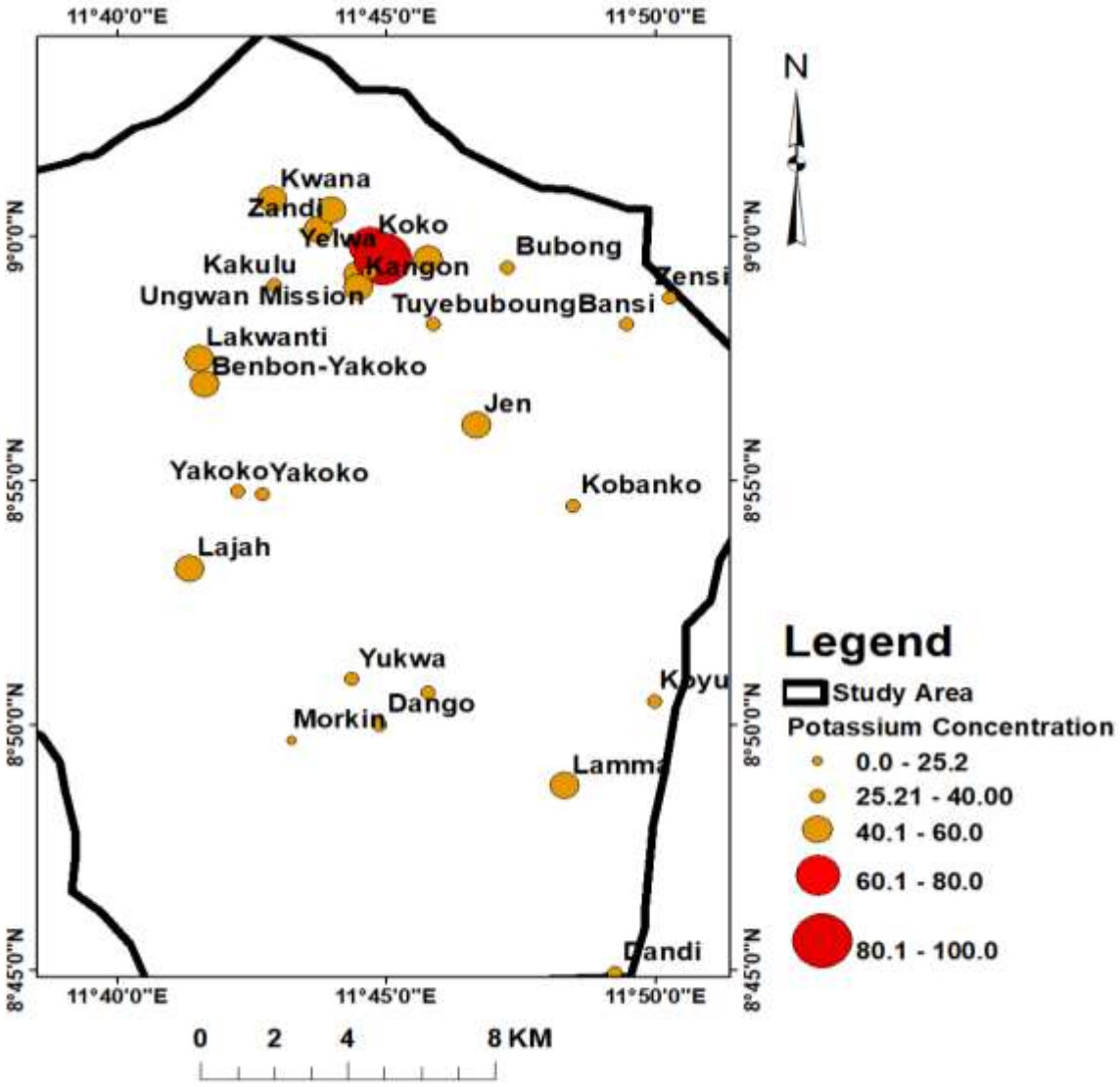

Figure 4.11. Potassium ion concentration map of the study area

4.3.2.5 *Sodium (Na^+)*

The concentration of sodium in groundwater samples of the area ranges between 12.3mg/l and 38.4mg/l with a mean value of 22.55mg/l. The concentration of sodium in individual sample are below the permissible limits of 200mg/l by WHO, 2017 and NSDWQ, 2015 (Table 4.9). Sodium occurs widely in water and in many igneous rocks. It is an essential component of most groundwater but more abundant in saline waters (Offodile, 2014).

Sodium in a compound form is readily soluble in water. A correlation between hypertension and sodium level in drinking water has been observed while the effect of sodium on blood vessels have been known for years (Pascual *et al*., 2004). The sources of sodium in the groundwater samples could have been as a result of weathering of rock bearing minerals such as albites, microcline, annites, biotite ad phlogopite(Table 4.6)

4.3.2.6 *Carbonate (CO_3^2)*

Groundwater samples range between 0.00mg/l and 41.3mg/l and a mean of 25.18mg/l as displayed in Table 4.9. The carbonates occur mainly as carbonates of sodium, magnesium, and potassium. The carbonates of sodium and potassium are water soluble while those of calcium and magnesium are insoluble. The presence of the ions in groundwater of the area signifies that the carbonates are of sodium and potassium source (Offodile,2014).

4.3.2.7 *Bicarbonate (HCO_3)*

Bicarbonates in the study area occur in varied concentration between 12.5mg/l and 198mg/l with a mean value of 97.66mg/l as represented in Table 4.9. Bicarbonate is a dominant ion in groundwater of of Zing and its environs. Bicarbonate forms as carbon dioxide dissolved in water as its presence in water is highly dependent on pH of the water because when a pH is 8.2 and above, bicarbonate loses its hydrogen to become carbonate.

Although calcium and bicarbonate are the dominant cation and anion in the groundwater system from the study area, their concentrations are well below their respective maximum permissible limits. The implication is that the groundwater in the area is calcium-bicarbonate type. This confirms that the groundwater in the study area is shallow (Olasehinde and Amadi, 2009; Okunlola *et al*., 2014). The weathering of rocks also contributes bicarbonate salts in groundwater. In areas of noncarbonated rocks, the HCO_3 and CO_3 originates entirely from the atmosphere and soil CO_2, which is peculiar to the study area whereas in areas of carbonated rocks, the rock itself contributes approximately 50% of carbonate and bicarbonate presence (Chapman and Kimstach, 1996).

4.3.2.8 *Sulphate (SO_4)*

The sulphate concentration in the water samples ranged between 7.43mg/l and 38.2mg/l with a mean value of 17.2mg/l. The values of sulphate in individual samples is very low when compared to the permissible limits of 250mg/l prescribed by WHO (2017) and 100mg/l by NSDWQ(2015) (Table 4.9). Sodium and magnesium Sulphate are readily soluble in water while calcium sulphate is less so. Sulphate concentration in groundwater occur due to leaching of gypsum, sodium sulphate, and some shales (Offordile, 2014). As a result of oxidation of pyrites, mine drainage may contain high concentration of sulphate. However, the highest concentration of sulphate is usually from groundwater and are from natural sources. Sulphate exerts a cathartic action in the presence of magnesium or sodium ions and at a concentration of 1000-2000mg/l, laxative effect may occur but with no increase in diarrhoea, dehydration or loss of weight (Olasumbo and Olufemi, 2020).

4.3.2.9 *Chloride (Cl^-)*

Chloride concentration in water samples of the area ranged between 8.85mg/l and 356mg/l with a mean value of 41.15mg/l (Table 4.9). All the values of chloride except

one falls within the permissible limits of 250mg/l by WHO, 2017 and NSDWQ, 2015. Chloride anion is generally present in natural waters. High concentration occurs in water from chloride containing geological formations otherwise, high chloride content may indicate pollution by sewage or some industrial waste or an intrusion of sea water or saline water. A salty taste produced by chloride depends on the chemical composition of the water. Chloride concentrations in excess of 250 mg/l are increasingly likely to be detected by taste, but some consumers may become accustomed to low levels of chloride-induced taste (Olasumbo and Olufemi, 2020). The sources of chloride in the groundwater samples of the area could have been as a result of weathering of rocks containing chloride (Table and Figure 4.6) . Figure 4.12 is a chloride concentration map of the study area.

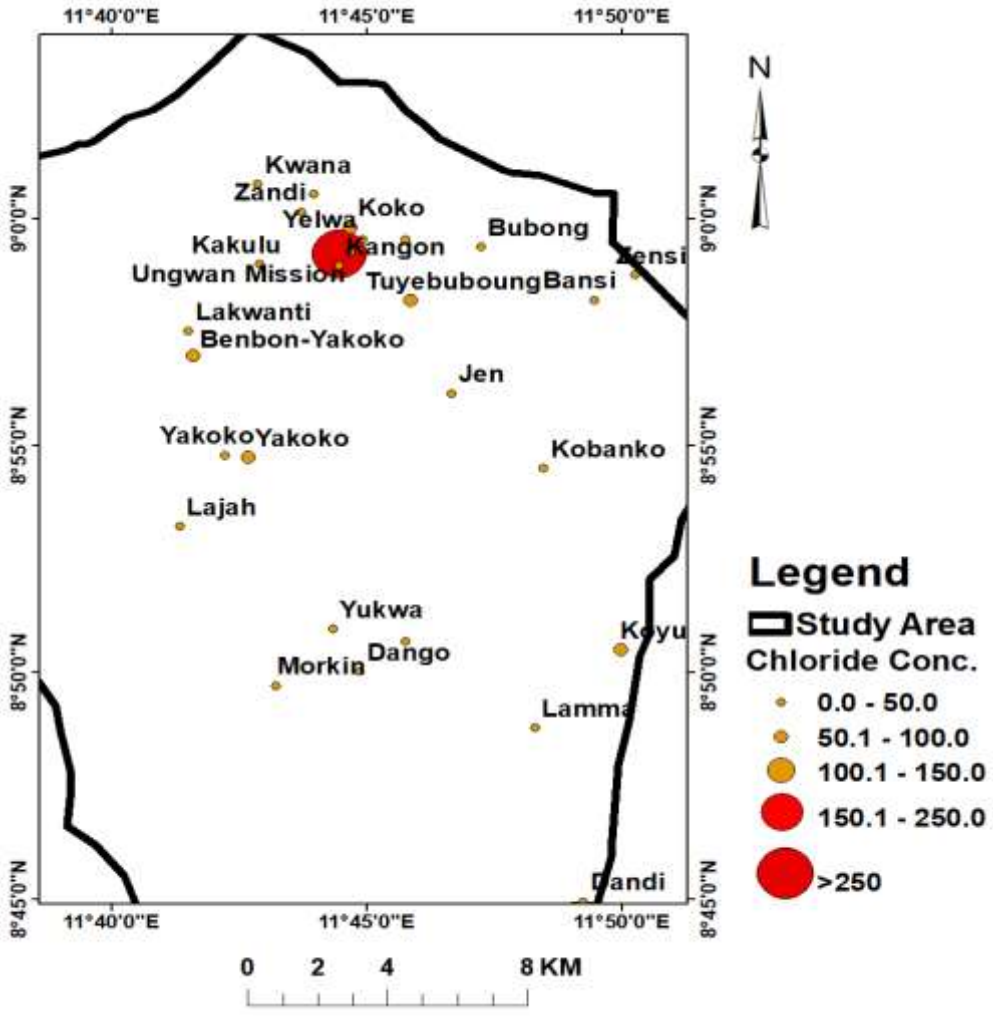

Figure 4.12. Chloride Concentration map of the study area

4.3.3.0 *Nitrate (NO_3) and Nitrites (NO_2)*

Nitrate concentration in groundwater of Zing and its environs ranged between 3.09mg/l and 21.3mg/l with a mean value of 9.42mg/l . The nitrate concentration of individual samples were observed to be very low compared to the 50mg/l prescribed by WHO, 2017 and NSDWQ 2015 as permissible limit (Table 4.9). Nitrate, the most highly oxidized form of Nitrogen compounds, is commonly present in rural waters and areas of agricultural activities because it is the end product of the aerobic decomposition of organic nitrogenous matter. Nitrate can reach both surface and groundwater as a consequence of agricultural activity, waste water disposal and from the oxidation of nitrogenous waste products in human and other animal excreta including septic tank. Nitrate can also reach the groundwater as a consequence of natural vegetation. Excessive concentration of nitrate in drinking water are considered hazardous to infants. In their intestinal tracts, Nitrate are converted to Nitrites which causes methaemoglobinaemia (Olasumbo and Olufemi, 2020).

Nitrite concentration in the study ranges from 0.009mg/l to 0.236mg/l with a mean value of 0.04mg/l. The values were observed to be below the permissible limit of 3.0mg/l and 0.2mg/ l of WHO, 2017 and NSDWQ, 2015 (Table 4.9). Nitrite (NO_2) is not usually present in significant concentration in groundwater except in a reducing environment. Nitrite concentration in the area could also be as a consequence of leaching from natural vegetation or nitic oxides produced by lightening (Olasumbo and Olufemi, 2020).

4.3.3.1 *Fluoride*

Fluoride concentration in groundwater samples of the area ranged between 0.47mg/l and 5.84mg/l with a mean value of 2.52mg/l (Table 4.9). A total of 21 locations representing 75% of the total samples has fluoride concentration above 1.5mg/l while 7 locations

representing 25% of the total area contains fluoride concentration less than 1.5mg/l in groundwater samples (Table 4.9, Figure 4.13).

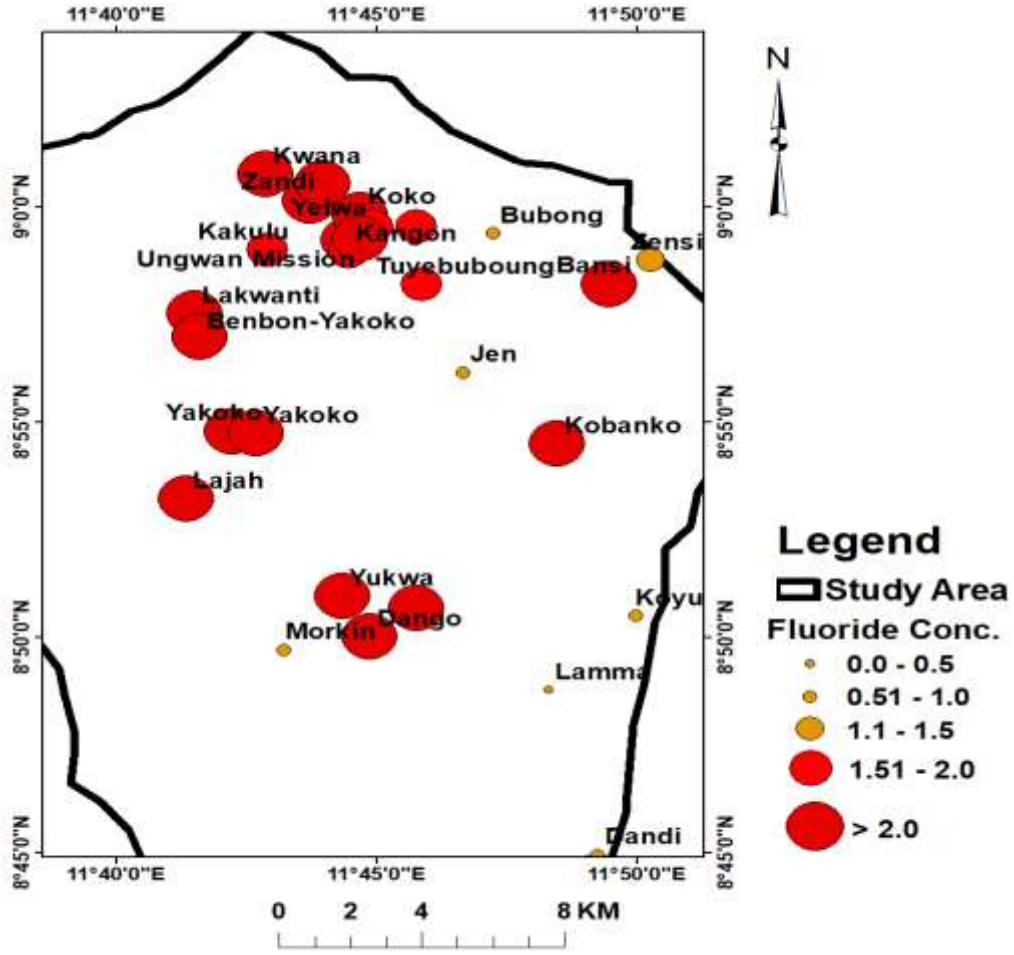

Figure 4.13. Fluoride concentration map of the study area

These values implies that the fluoride concentration in most of locations exceeds the permissible limit of 1.5mg/l by WHO (2017) and NSDWQ (2015) which demands for an urgent attention from concerned authorities and relevant stakeholders in terms of remediation before the situation becomes critical (Table 4.9). Fluoride is the most electronegative and reactive element among known elements in the periodic table. It is always present in a combine state because of its high chemical reactivity (Tirumelesh *et al*., 2007). In general, fluoride concentration in groundwater is less than 1.0mg/l and its

mainly due to natural contamination (Hems, 1985). Fluoride is associated with soluble rock bearing minerals such as fluorite, fluorapatite, cryolite, villiaumite, nacaphite (Aminu and Amadi, 2014, Maspalma *et al*., 2016).

The natural concentration of fluoride in groundwater generally depends on the geology, chemical and physical characteristics of the aquifer, the porosity and acidity of the soil and rocks, the surrounding temperature, the action of chemical elements, depth of aquifer and intensity of weathering (Feenstra *et al*., 2007). Higher fluoride concentration in groundwater has caused health problems in humans estimated at over 260 million residing in more than 25 nations around the world. Fluoride concentration of at least <0.5mg/l in groundwater result to dental carries, mottled enamel while fluoride content between the range of 0.5 to 1.5mg/l is beneficial for teeth and bone development (Okunola *et al*., 2016). Fluoride concentration between 1.5 and 4.0 mg/l leads to dental fluorosis, skeletal and crippling fluorosis (Msonda *et al*., 2007 and Ndolo, 2002) while other studies revealed that the effects of fluoride could also lead to mental retardation in children (Andy and Silas., 2020). Other conditions and health challenges associated with excess fluoride intake include, abdominal pain, excessive saliva, nausea and vomiting, seizures and muscle spasm (Chae *et al*., 2007; Aminu and Amadi, 2014).

The result of X-Ray Diffraction analyses of rock samples contained in Table 4.6 revealed that Biotite and Actinolite could have been responsible for fluoride concentration in groundwater system of the area. Plates XXVI to XXXII are evidences of fluorosis in the study area.

PLATE XXVII Evidence of fluorosis at Yakoko village.

PLATE XXVIII – Evidence of fluorosis at Dingdin village.

PLATE XXIX – Evidence of fluorosis at Kobanka village.

PLATE XXX – Evidence of fluorosis at Koko.

PLATE XXXI – Fluorosis at Zandi village.

PLATE XXXII – Fluorosis and Mottled enamel at Zing Town

4.4 Heavy Metal and Trace Element

The heavy and trace elements are referred to as solutes in natural water that are always or closely occur in concentration of less than 1.0mg/l (Hem, 1985). The speciation and bioavailability of trace metals in water are controlled by physical and chemical interactions affected by many factors including pH, temperature, hardness, carbon dioxide concentration and concentration of metal ions. The toxicity and bioavailability of trace elements in groundwater are potential for bioaccumulation and hazards to human health (Olasumbo and Olufemi, 2020). The following heavy metals and trace element concentration in groundwater of the study area are hereby summarized as follows:

4.4.1 Lead (Pb)

Lead concentration in the groundwater sample of the area ranged between 0.00mg/l and 0.068mg/l with a mean value of 0.011mg/l. A total of 8 (28.6%) samples have lead concentration greater than 0.01mg/l above the prescribed permissible limit for drinking water by WHO, 2017 and NSDWQ, 2015 (Table 4.10). The remaining 20 (71.4%) samples are withing the prescribed limits of the stated national and international water regulating bodies. Lead concentration above 0.01mg/l is restricted the extreme North, Northeast, Northwest and South east sections of the study area resulting from mineralization of lead in rocks of the area (Table 4.4 and Figure 4.6).

Table: 4.10. Results of Heavy and Trace Elements of Water Samples Compared with WHO, 2017 and NSDWQ, 2015 Guidelines

Sample Code	Locality	Pb	Cu	Cd	Cr	Zn	Mn	Fe
ZGW/001	Lakwanti	**0.017**	0.021	0	**0.07**	0.083	0.002	**0.44**
ZGW/002	Benbon-Yakoko	0.014	0.009	0	0.04	0.089	0.016	**0.58**
ZGW/003	Yakoko A	0.005	0.01	0	**0.08**	0.077	0.002	**0.61**
ZGW/004	Yakoko B	0.004	0.008	0	**0.06**	0.091	0.017	0.33
ZGW/005	Morkin	0.01	0.003	0	0.01	0.055	0.014	**0.46**
ZGW/006	Anguwan Mission	0.011	0	0	**0.09**	0.024	0.009	0.26
ZGW/007	Lajah	0.01	0.005	0	0.04	0.044	0.016	**0.38**
ZGW/008	Yukwa	0.001	0.001	0	**0.07**	0.069	0.013	**0.82**
ZGW/009	Dango	0.002	0	0	0.05	0.085	0.018	**0.47**
ZGW/010	Dindin	0.014	0	0	0.04	0.017	0.019	0.28
ZGW/011	Kobanko	0.006	0.001	0	0.03	0.068	0.014	**0.84**
ZGW/012	Jen	0.003	0.023	0	0	0.018	0.017	**0.63**
ZGW/013	Tuyebuboung	0.001	0.045	0	0.02	0.014	0.019	0.21
ZGW/014	Bansi	0	0	0	0.01	0.058	0.016	**0.62**
ZGW/015	Dandi	0.012	0.004	0	0	0.019	0.011	**0.46**
ZGW/016	Lamma	**0.031**	0.002	0	0.02	0.073	0.014	0.16
ZGW/017	Koyu	0.007	0	0	0	0.045	0.006	0.22
ZGW/018	Bubong	0.003	0	0	0.01	0.063	0.026	0.33
ZGW/019	Zensi	**0.022**	0.018	0	0	0.022	0.009	**0.52**
ZGW/020	Lowcost Qtrs	**0.015**	0	0	**0.06**	0.034	0.102	**0.63**
ZGW/021	Zandi	**0.023**	0.037	0	0.1	0.013	0.012	0.27
ZGW/022	Koko	**0.017**	0.081	0.003	**0.15**	**0.361**	0.111	**0.61**
ZGW/023	Yelwa	**0.068**	0.073	0.012	**0.34**	**0.472**	0.127	0.23
ZGW/024	Didonko	0	0	0	0	0.017	0.004	0.32
ZGW/025	Kangon	0.002	0	0	0.01	0.021	0.006	**0.37**
ZGW/026	Kakulu	0	0	0	0.02	0.012	0.012	0.25
ZGW/027	Kwana	0	0	0	0	0.011	0.003	**0.41**
ZGW/028	Taraba One	**0.019**	0.022	0	0	0.032	0.004	**0.36**
	Min	0.00	0.00	0.00	0.00	0.011	0.002	0.16
	Max	0.068	0.081	0.012	0.34	0.472	0.127	0.84
	Mean	0.011	0.013	0.001	0.047	0.071	0.023	0.431
	Standard Deviation	0.014	0.022	0.002	0.069	0.102	0.033	0.182
	WHO, 2017	**0.01**	**2.0**	**0.003**	**0.05**	**0.1**	**0.1**	**0.3**
	NSDWQ, 2015	**0.01**	**1.0**	**0.003**	**0.05**	**3.0**	**0.2**	**0.3**

The concentration of lead in drinking water are generally low but much higher concentration have been measured where lead services connections of fittings are present (WHO, 2017). Lead exposures is associated with a wide range of effects including various neurodevelopmental effects, mortality mainly due to

cardiovascular diseases, impaired renal function, hypertension, impaired fertility and adverse pregnancy outcomes (Olasumbo and Olufemi, 2020). Figure 4.14 is a lead concentration map of the study area.

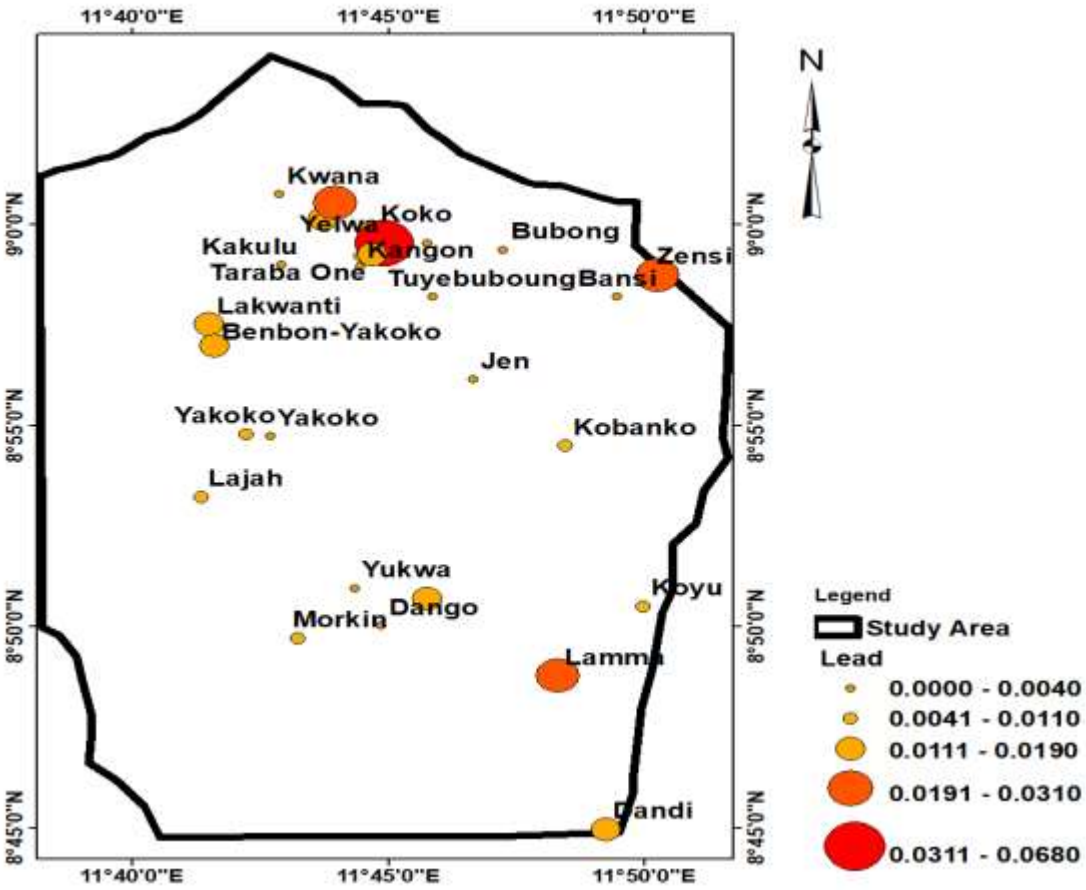

Figure 4.14. Lead concentration map of study Area

4.4.2 Copper

Copper concentration of water samples ranged between 0.00mg/l and 0.081mg/l with a mean value of 0.013mg/l. All the 28 samples representing 100% have copper concentration less than the permissible limits of 2.0mg/l and 1.0mgl/l prescribed by WHO(2017) and NSDWQ (2015) respectivel (Table 4.10). Copper is a widely distributed trace element but because most of its minerals are relatively insoluble and because copper is absorbed to solid phase, only low concentrations are normally

present in natural waters. Higher concentration of copper is usually attributed to corrosion of copper pipes, industrial wastes, or particularly in reservoirs to use the copper sulphate as an algicide. Higher concentration of copper in groundwater above the permissible limit of 0.003mg/l could result to gastrointestinal disorder is one of the major health effects to man (WHO, 2017).

4.4.3 Cadmium (Cd)

Cadmium constituent in the water samples of the study area ranged from 0.00mg/l to 0.012mg/l with a mean value of 0.001mg/l. These statistics indicated that all the 28 water samples representing 100% recorded cadmium concentration less than the permissible limits of 0.003mg/l prescribed by WHO (2017) and NSDWQ (2015). Table 4.10.

Cadmium is found in nature largely in the form of sulphide and as an impurity of zinc-lead ores. Cadmium may be present in water as a consequence of mining and smelting just like the lead. Cadmium may be present in wastes from electroplating plants, pigment works, textile and chemical industries. Metal and plastic pipes constitute an additional possible source of cadmium in waters. In the absence of anthropogenic inputs, cadmium concentration is below 1µg/l (Olasumbo and Olufemi, 2020). Cadmium is toxic to man and the kidney is the main target organ for cadmium toxicity. It accumulates primarily in the kidneys and has a long biological half-life in humans of 10-35 years (WHO, 2017). However, in the study area, considering the values recorded, it shows that the groundwater has no health risks when consumed.

4.4.4 Chromium (Cr^{+3})

The groundwater samples of area ranged between 0.00mg/l to 0.34mg/l with a mean value of 0.47mg/l. The permissible limit of chromium in groundwater is 0.05mg/l (WHO,2017 and NSDWQ, 2015) and the values obtained from chromium samples particularly in eight (8) sample locations representing 28.6% were above the permissible limits of 0.05mg/l. This could result to serious health challenge such as cancer to humans when consumed (WHO, 2017 and NSDWQ, 2015). Chromium concentration in natural water is usually in very low and elevated chromium concentration can result from mining and industrial purposes. The ultra-mafic igneous rocks are higher in chromium composition than other rock types, chromite ($FeCr_2O_4$) may be concentrated in lateritic residue overlying ultramafic rocks.

Chromium is also found naturally in most rocks, plants, soil and volcanic dust as well as sea animals. Adverse health effects associated with prolonged exposure to Chromium includes, kidney damage, liver damage, cancer and a whole lot of health issues WHO (2017). Chromium concentration map of the study area (Figure 4.15) shows that there is elevated chromium concentration from the extreme Northern section, North west and southwestern section of the area. Figure 4.15 is chromium concentration in groundwater of the area.

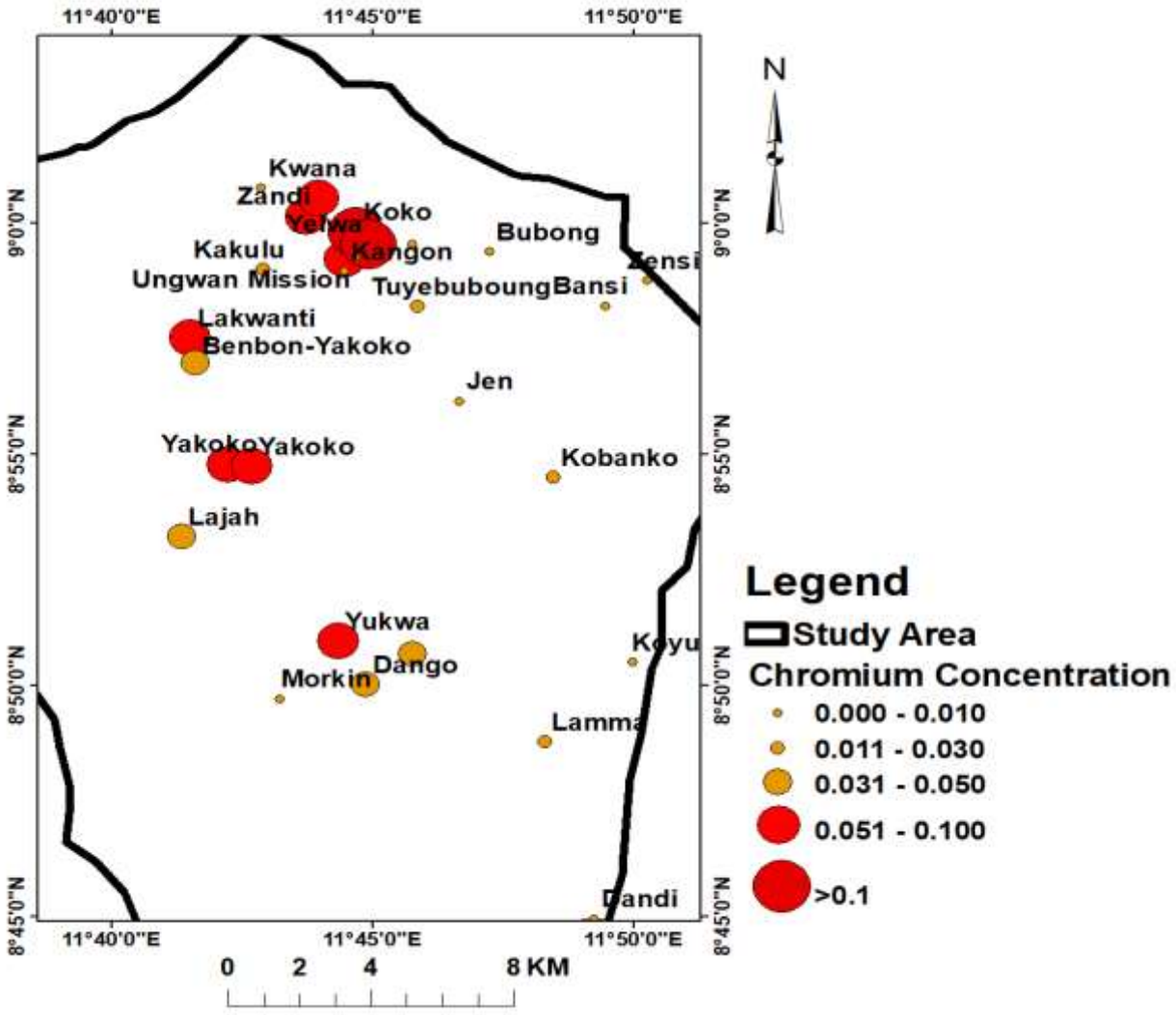

Figure: 4.15. Chromium concentration map of the study area.

4.4.5 Zinc (Zn)

Zinc concentration levels in groundwater samples of the area varied from 0.011mg/l to 0.472mg/l with a mean value of 0.071mg/l. A total of 2 (7.14%) samples shows Zinc concentration greater than 0.1mg/l(Table 4.4). The values are higher compared to the permissible limit of 0.1mg/l by NSDWQ (2015). However, the values are within the acceptable limit of 3.0mg/l for drinking water by WHO (2017). Table 4. 10.

Zinc is an abundant element in rock and ores but present in water as a minor constituent because of its insolubility of free metals and its oxides. It is an essential trace element found in virtually all food and portable water in the form of salts or organic complexes. It is also present in minor quantities in most alkaline surface and groundwater but more in acid waters. Therefore, the solubility of zinc in water is a function of pH and total inorganic carbon concentrations of carbonate species. A pH of 8.5 is sufficient to control the dissolution of Zinc in groundwater system (Olasumbo and Olufemi, 2020). The occurrence of Zinc in water samples of the area particularly the extreme north of the area was derived from weathering of the rocks undelying the area as confimed by the geochemistry of the rocks of the area. Zinc Concentration is elevated in the extreme north and northwestern and southern segment of the area. The concentration of Zinc element in groundwater sample is represented in Figure 4.16.

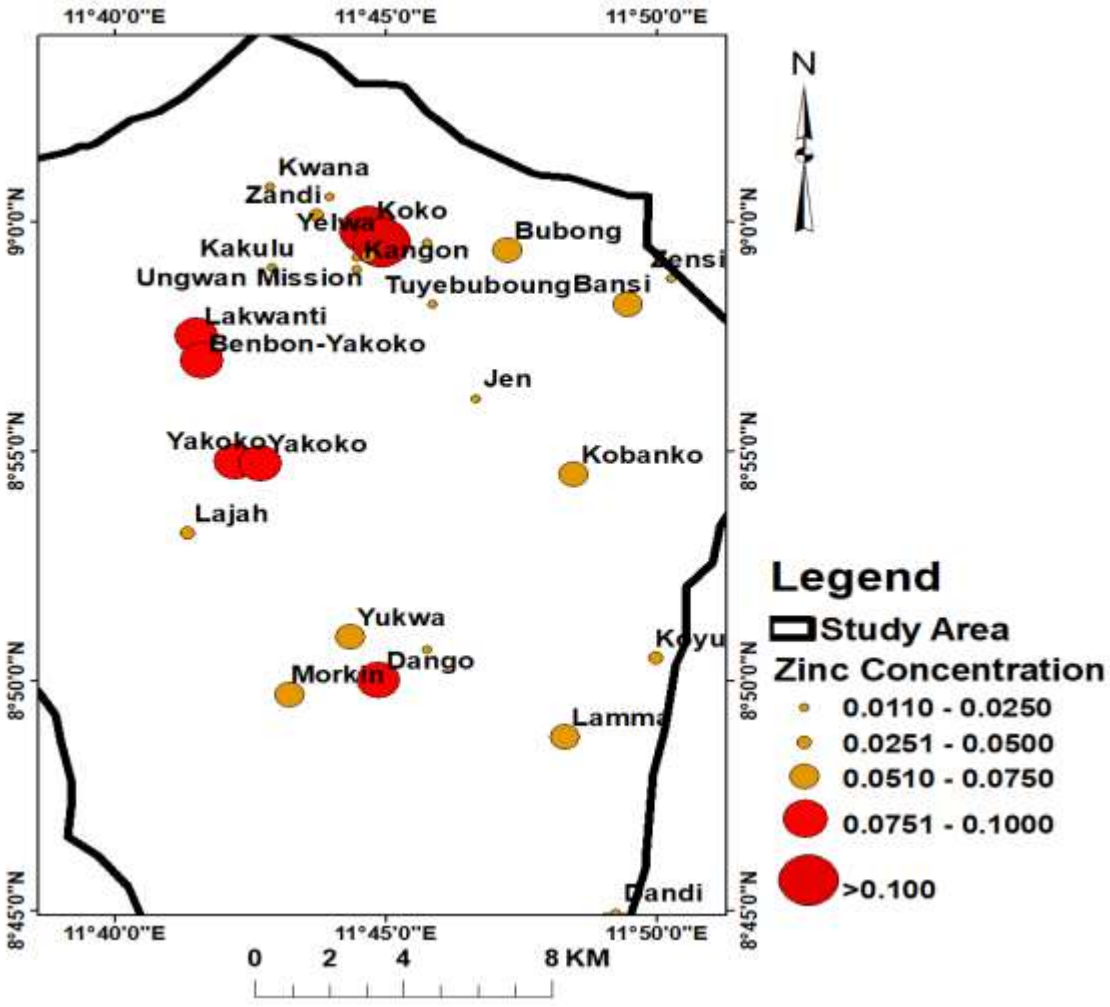

Figure: 4.16. Zinc concentration map of the study area

4.4.6 Manganese (Mn)

Manganese in the water samples of the area ranged from 0.002mg/l to 0.127mg/l with a mean value of 0.023mg/l. All the 28 samples representing 100% of the total groundwater samples analyzed have manganese concentration less than the prescribed permissible limits of 0.1mg/l and 0.2mg/l by WHO, 2017 and NSDWQ, 2015 respectively (Table 4.10). Manganese is a relatively common element in rock and soils where it exists as oxides or hydroxides in Mn II, III and IV oxidation states. Many igneous and metamorphic minerals contain manganese as a minor constituent. The oxides and hydroxides of manganese are capable of absorbing other metallic ions and in close

association with iron oxides. They are of great importance in controlling the concentration of various trace elements in natural water systems. The solubility of manganese in natural water is largely a function of pH and oxidation -reduction potentials. The presence of manganese in drinking water, like that of ion may lead to accumulation of deposit in the distribution system.

Manganese is needed by the human body to aid in the normal functioning of the health of man but increased level can be harmful to the body especially neurological disorder (NSDWQ, 2015). Manganese concentration although within permissible limit is found to be restricted within the extreme northern section of the study area. Figure 4.16 is a manganese concentration map of the study area.

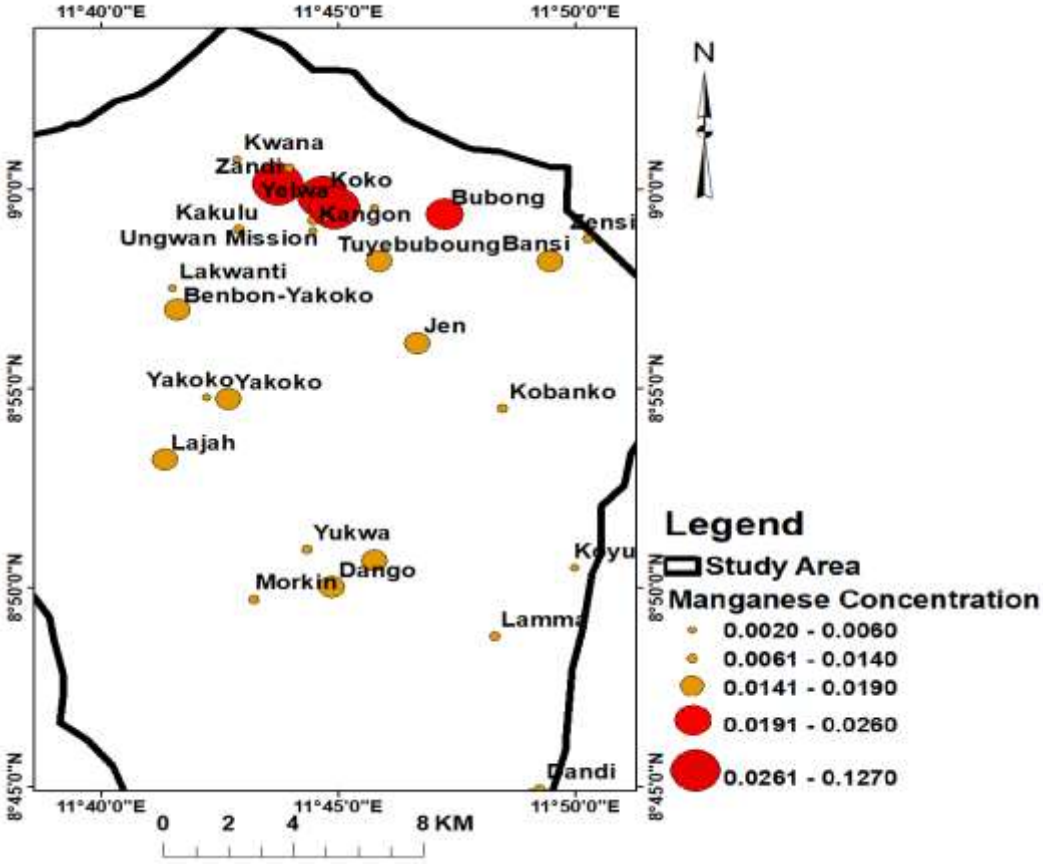

Figure 4.17. Manganese concentration map of the study area

4.5.7 Iron (Fe^{+2})

Iron II concentration of water samples varied from 0.16mg/l to 0.84mg/l with a mean value of 0.43mg/l. A total of 17 water samples representing 60.7% of the total sample have Iron II, concentration greater than 0.3mg/l prescribed as permissible limit for consumption by WHO, 2017 and NSDWQ, 2015 while the remaining 11(39.3%) samples are within the limits (Table 4.10). Iron is an abundant element in the earth crust but exists generally in minor concentrations in natural waters). Iron is an essential element in human nutrition which are taken as supplements for pregnant and lactation women or prescribed on specific clinical requirement. Iron also promotes the growth of "iron bacteria", which derive their energy from the oxidation of ferrous iron to ferric iron and in the process deposit a slimy coating on the piping. At levels above 0.3 mg/l, iron stains laundry and plumbing fixtures. No health-based guideline for Iron has been proposed by either WHO (2017) or NSDWQ (2015).

Igneous rock minerals whose iron content is relatively high include the biotites, magnetite, amphiboles, pyroxenes and particularly the nesosilicates olivine (Olasumbo and Olufemi, 2020*).* Iron may also be present in drinking water as a result of the use of iron coagulants or the corrosion of steel and iron pipes during water distribution. The form of solubility of iron in natural waters are strongly dependent on pH and oxidation-reduction of the water. (Olasumbo and Olufemi, 2020). The Iron concentration map displayed in Figure 4.13 is an overview of iron distribution in the study area.

The distribution of Iron in the area could best be described as regional controlled by geological structures and weathering of rocks rich in Iron minerals such as magnetite,annite,biotite and phlogopite (Table 4.6). Figure 4.18 is Iron concentration map of the study area.

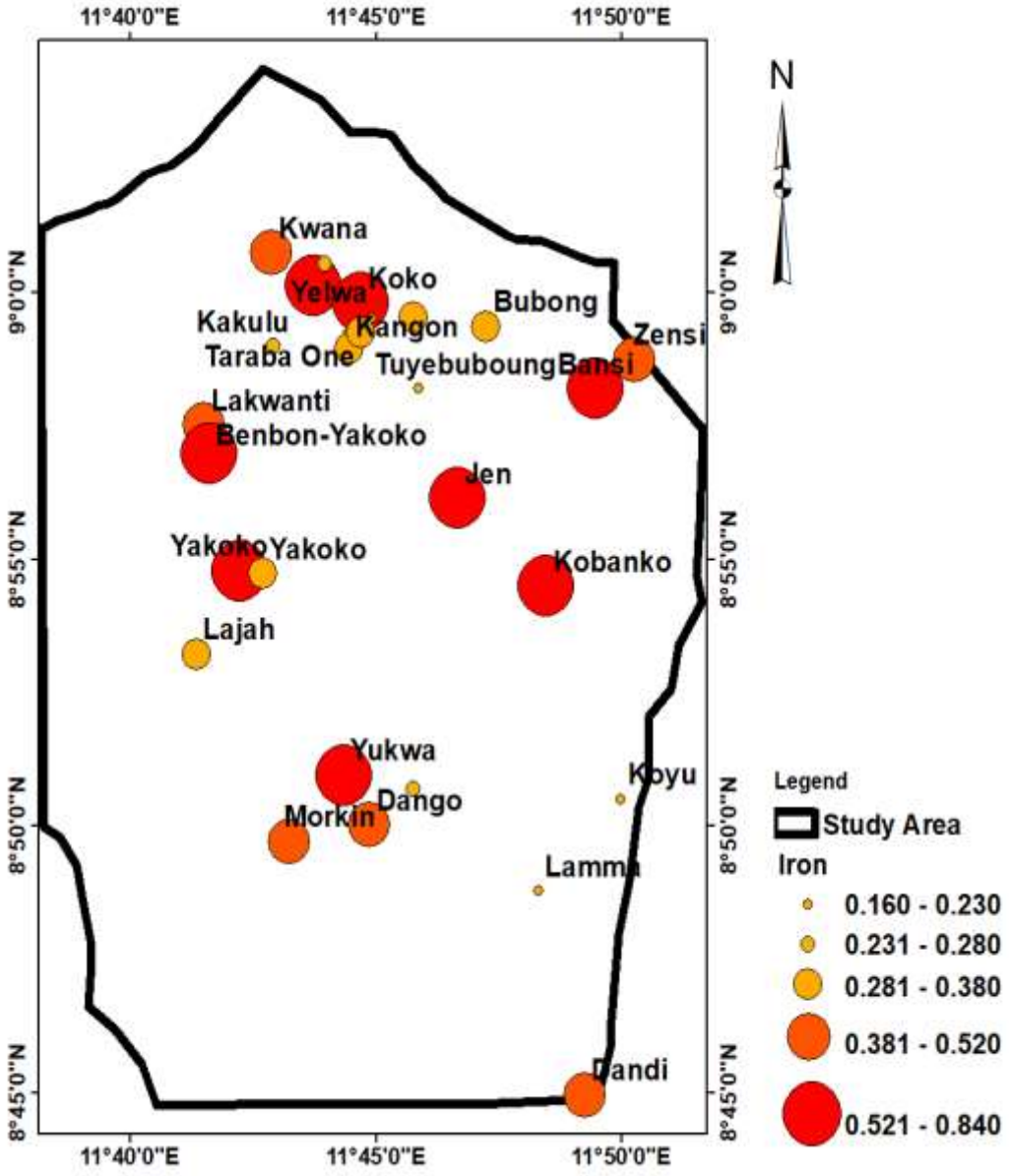

Figure 4.18. Iron concentration map of the study area

4.5 Hydrochemistry and Hydrogeochemical Assessment

In order to determine the groundwater characteristics with regards to relative concentration of chemical constituents, hydrochemical facies, hydrogeochemical processes and sources of measured chemical parameters in groundwater of the study area, the Schoeller, Stiff, Piper, Durov and Gibbs diagrams were employed. The Schoeller diagram of the study area as displayed in Figure 4.19 indicates that the dominant ions in

groundwater samples in order of abundance is **Ca^{+2} >K >Na^{+} >Mg^{+2}** or **Mg^{+2}<Na^{+}<K^{+}<Ca^{+2}** for major cations while **HCO_3 > Cl > CO_3 > SO_4> NO_3 >NO_2** or **NO_2<NO_3<SO_4<CO_3<Cl<HCO_3** for major anions with possible $CaMgHCO_3$ water type as the most dominant water type in the area.

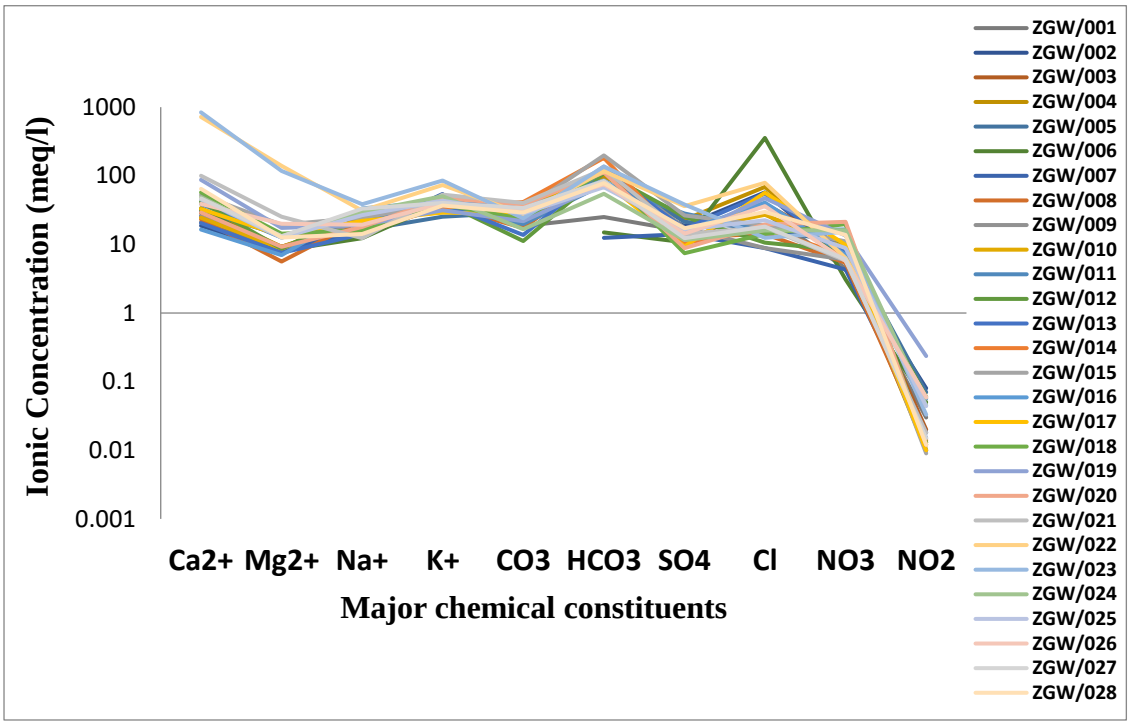

Figure 4.19. Scholler Plot of water samples in the study area

In a similar development, the Stiff plot of groundwater samples of the area presented in Figure 4.15 showed that 27 (96%) samples are HCO_3 + CO_3 with Cl^- as the dominant anion in only 1 (4%) sample. The dominant cation is Ca^{2+} in 20 (71.4%) samples while Na^+ is dominant in the remaining 8 (28.6) samples. The ionic abundance for the cations indicates that Ca^{2+} > Na^+ +K^+ > Mg^{2+} in 15 samples and Na^++ K^+ > Ca^{2+} >Mg in the remaining 13 samples while the ionic abundance for the anions shows HCO_3- > Cl^- >SO_4^{2-} in 23 samples and HCO_3-> SO_4^{2-} >Cl^- in 5 samples. The Stiff pattern in Figure 4.15 indicates similarities in almost all the samples except in four samples where the pattern appears to be distinctive. At Koko and Yelwa Yelwa where the pattern showed a

very high concentration of Ca^{2+} ion, at Mission House where it showed an indiscriminate concentration of Cl^- and at Lajah, all anions are almost of the same concentration. The variations in chemical constituents connotes groundwater evolution as its flows along its path over a period of time. Furthermore, a similarity in pattern can be used to identify ionically related water; based on this the following samples of water as grouped in Table 4.11 can be said to be ionically related.

Table: 4.11: Ionically related waters based on dissolved chemical constituents

Sample Code	Locality	Group	Peculiar Characteristics
ZGW/008	Yukwa	**A**	
ZGW/009	Dango		
ZGW/010	Dindin		
ZGW/003	Yakoko A		
ZGW/004	Yakoko B		
ZGW/016	Lamma		$Na^+ + K^+ > Ca^{2+} > Mg^{2+}$
ZGW/013	Tuyebuboung		
ZGW/001	Lakwanti		
ZGW/002	Benbon		
Yakoko			
ZGW/003	Bubong		
ZGW/014	Bansi		
ZGW/017	Koyu		
ZGW/019	Zensi		
ZGW/020	Lowcost		
Quarter			
ZGW/022	Koko	**B**	High Ca^{2+} concentration compared to
ZGW/023	Yelwa		other cations
ZGW/025	Kangon	**C**	Ca>Na+K>Mg
ZGW/027	Kwana		
ZGW/024	Didonko		
ZGW/026	Kakulu		
ZGW/021	Zandi		
ZGW/028	Taraba one		
ZGW/015	Dandi	**D**	$HCO_3^- + CO_3^{2-} > SO_4^{2-} > Cl^-$
ZGW/005	Morkin		
ZWG/011	Kobanko		
ZWG/012	Jen		
ZWG/006	Mission	**E**	Cl^- is extremely high
House			
ZGW/007	Lajah	**F**	All anions are almost of the same concentration

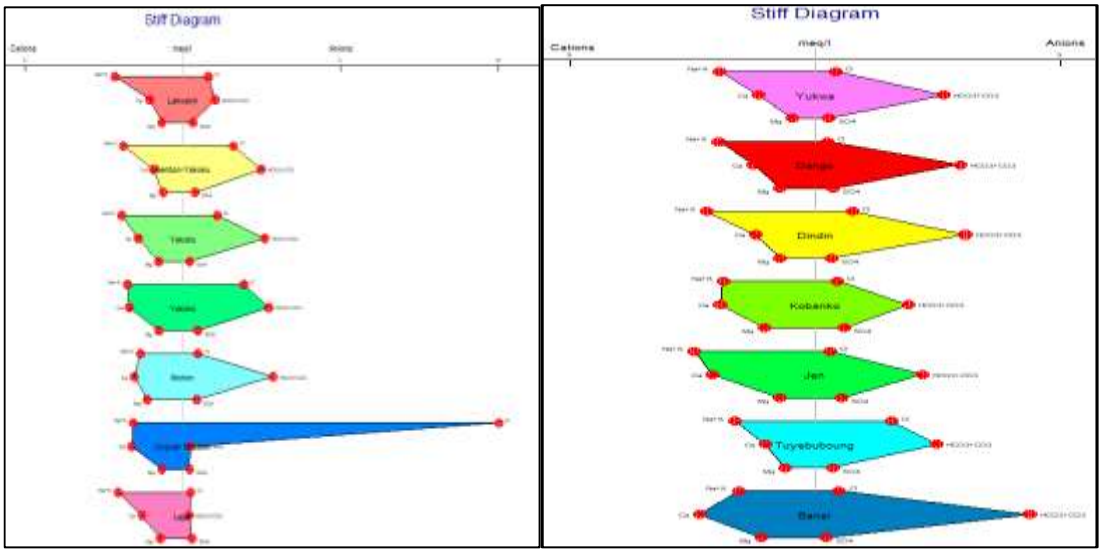

Sample No. ZGW/001-007 **Sample No. ZGW/008-014**

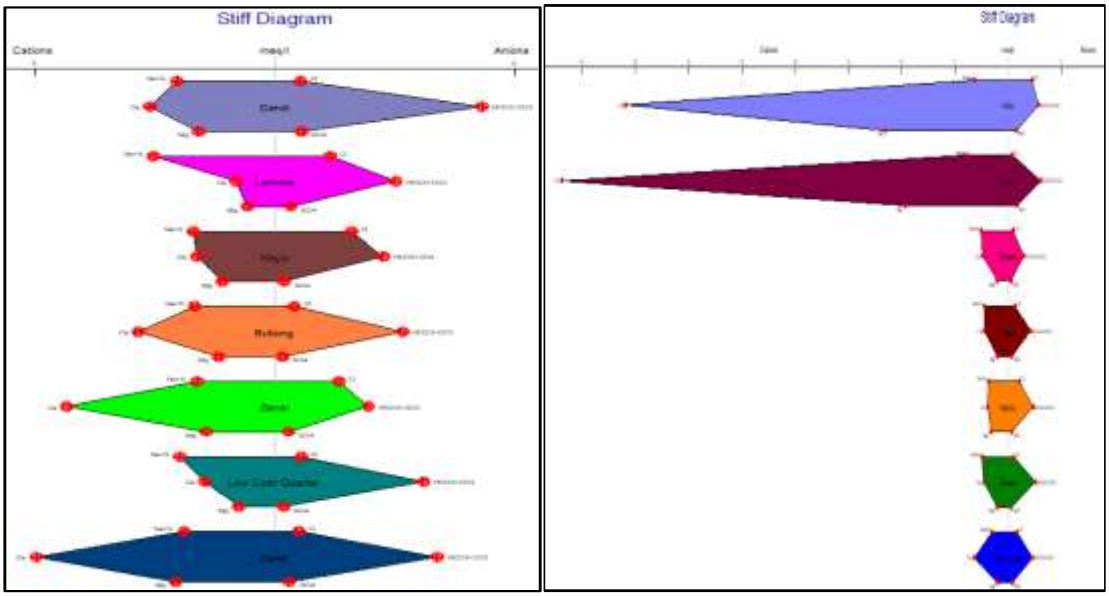

Samples No. ZGW/015-021 **Samples No. ZGW/022-028**

Figure 4.20: Stiff Plot of water sample of the study area

The piper diagram of the study area also displayed as Figure 4.21 infers that groundwater of the area is composed of four (4) water types and four (4) hydrochemical facies respectively. The groundwater types and hydrochemical facies showed 21 (75%) samples out of the 28 correspond to the earth alkaline water with prevailing HCO_3, 4(14.3%) samples conforming to alkaline water with prevailing HCO_3 while three (3) samples with

1 (3.6%) sample each corresponds to normal earth alkaline water with prevailing HCO_3 and SO_4 or Cl, earth alkaline water with prevailing SO_4 and Cl water respectively. Hydrochemical facies indicates four types with 20 (71.4%) samples corresponding to the Ca^{2+}-Mg^{2+}-HCO_3^- as the dominant facie, 4 (14.3%) samples corresponding to Na^+-K^+-HCO_3^- while 2 samples each fall corresponding to Na^+-K^+-$Cl^-SO_4^{2-}$ and Ca^{2+}-Mg^{2+}-Cl^--SO_4^{2-} respectively. The variations in the hydrochemical facies suggest possible groundwater evolution which could have been influenced by rock water interactions and residence time of groundwater.

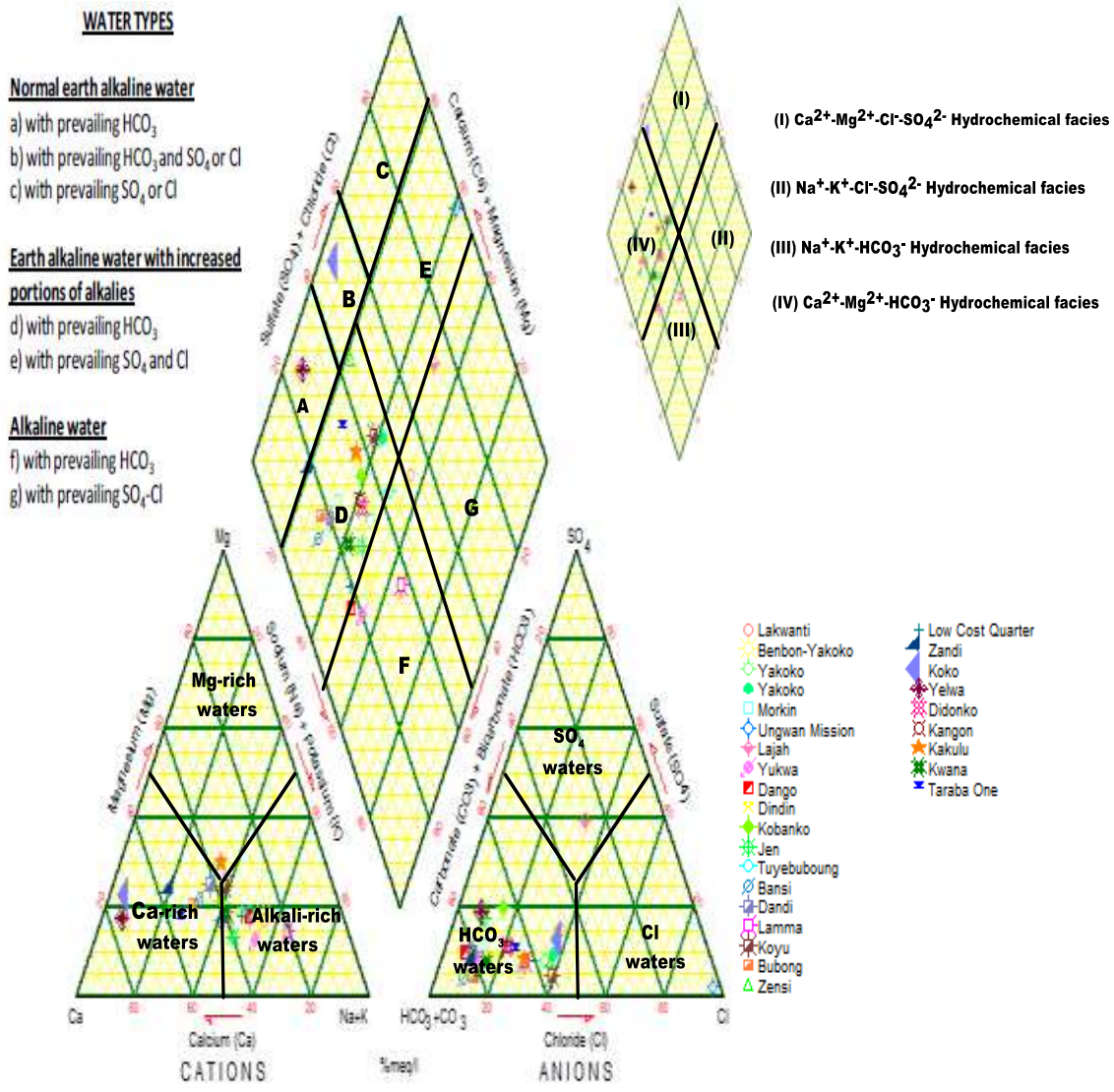

Figure 4.21. Piper Diagram of the study area

The Gibbs and Durov Plots as well as Source Rock Deduction and Reasoning is used to establish the geochemical processes influencing water chemistry including the origin and sources of measured parameters in the study area in Figure 4.22 suggests three distinct parameters namely, rock dorminance attributed to chemical weathering of rock forming minerals, precipitation and evaporation dorminance as the major driving force influencing groundwater chemistry of the study area. Statistical analysis of the Gibb's diagram(Figure 4.22 infers that 26 (92.8%) groundwater samples revealed rock dorminance attributed to rock water interaction with only 2(7.2%) samples depicting a combination of evaporation and precipitation dorminance (using the anions plot) . Consequently, using the cations, it indicated that 10(35.7%) of the groundwater samples are linked to rock dominance due to chemical weathering, 17(60.7%) samples revealed a combination of evaporation and precipitation while one (3.6%) sample showed precipitation dominance as the major force responsible for the chemistry of groundwater in the area. Consequently, the chemical weathering of the rocks and water rock interactions, evaporation and precipitation are the main major reasons for the poor water quality in few and most of the groundwater sampled in the area. The high concentration of ions in the groundwater system of the area could have been facilitated by evaporation processes.

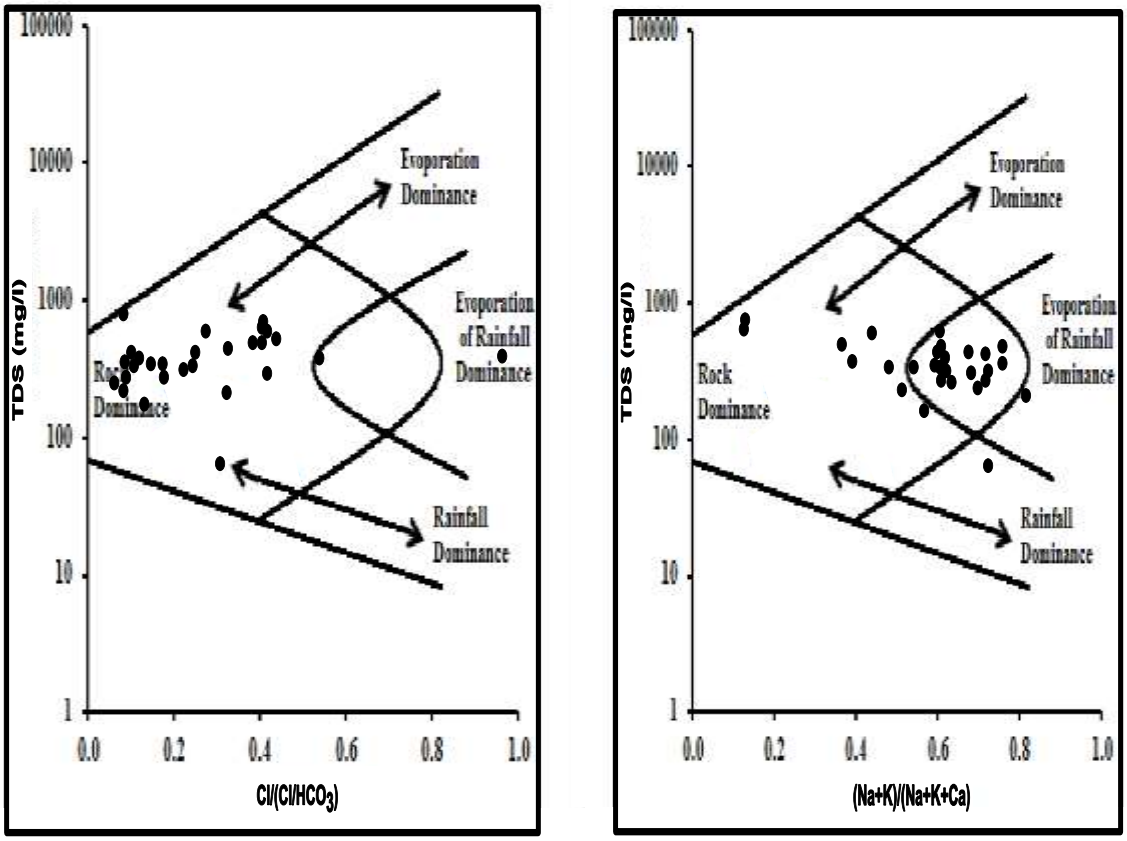

Figure: 4.22. Gibb's diagram of the study area

In a related development, the hydrogeochemical processes occurring in groundwater system of the study area revealed by Durov Diagram developed by Lloyd and Heathcoat (1985) as represented on figure 4.18 indicated that the reverse ion exchange reactions as shown in field 6, accounts for 17(60.7%) groundwater samples which is the most dorminant process within the aquifer matrixes. The effect is generally observed when sea water intrusion or oil field brine contamination occurs (Lloyd and Heatcote, 1995) . The reverse ion exchange reactions in groundwater of the area indicates the release of Ca^{2+} and occationally Mg^{2+} ion and decrease of Na^{+} and K^{+} ion concentration in the groundwater. The simple dissolution or mixing with 7(25%) groundwater samples aligning along the simple dissolution or mixing line on field 5, indicates recent recharge from precipitation whereas the 2(7.15%) samples each positioning on the axis of ion

exchange and reverse ion exchange respectively is an indication of the removal of Ca^{2+} and Mg^{2+} and replaced with Na^{+} thereby increasing Na^{+} over Cl- or reducing same respectively (Lloyd and Heatcoat (1995). Therefore, the disposition of groundwater samples of the area as revealed in Figure 4.23 revealed that the major hydrogeological processes influences the chemistry of groundwater in the study area are majorly, reverse ion exchange and simple dissolution or mixing occurring within the aquifer materials.

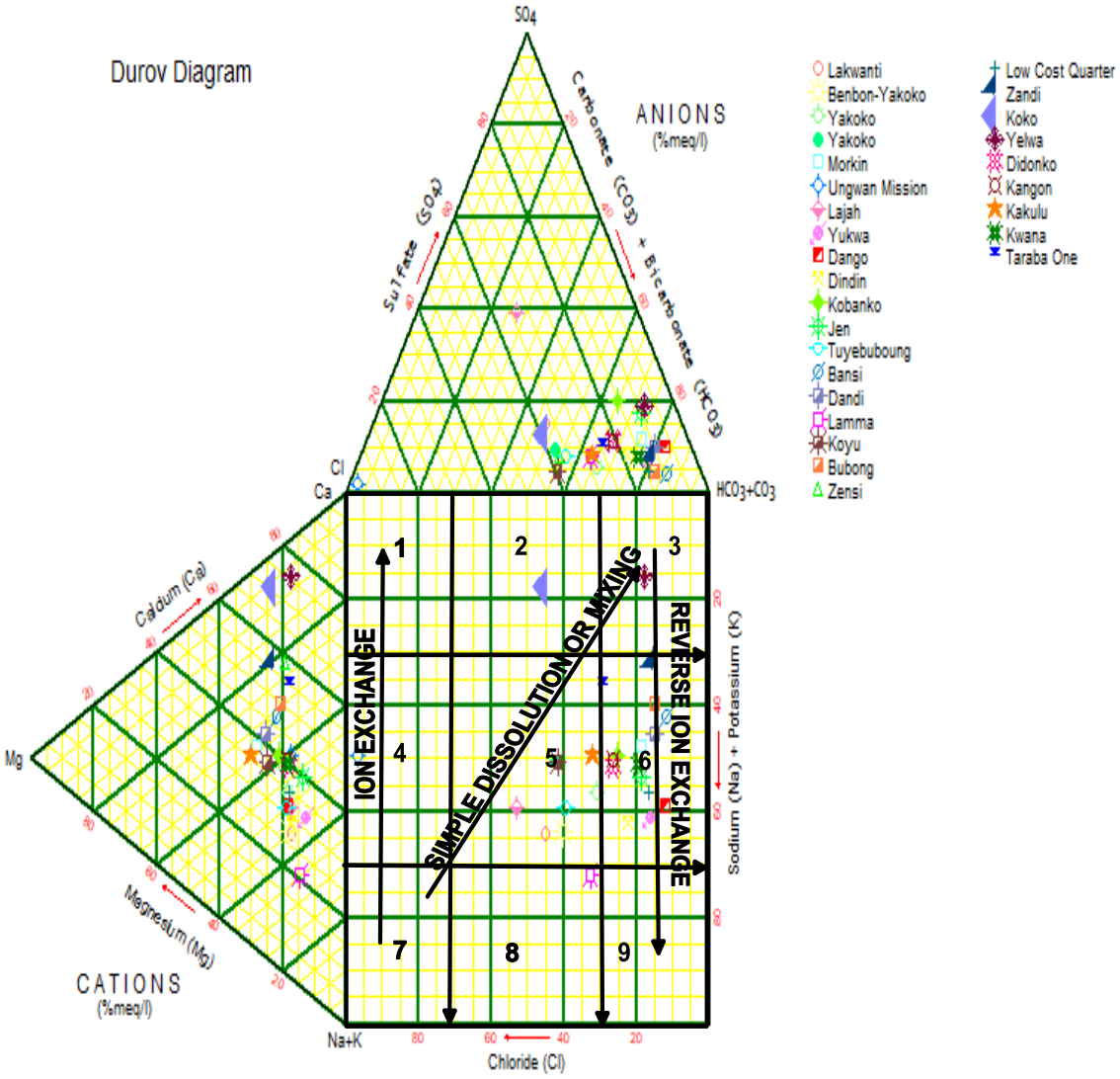

Figure 4.23. Durov diagram of the study area

The composition and groundwater quality of the study area was used to deduce source rock as shown in Table 4.12.

Table 4.12: Source rock deduction summary of reasoning (Hounslaw,1995)

Parameter((meq/l)	Value	Conclusion
$\frac{Na^+ + K^+ - Cl}{Na^+ + K^+ - Cl^- + Ca^{2+}}$	>0.2 and<0.8 <0.2 or >0.8	Plagioclase weathering possible Plagioclase weathering likely
$\frac{Na^+}{Na^+ + Cl^-}$	>0.5 = 0 < 0.5 TDS >500 <0.5 TDS < 500 >50 <0.5 TDS < 50	Sodium source other than halite-albite, ion exchange Halite solution Reverse softening Analysis error Rainwater
$\frac{Mg^{2+}}{Ca^{2+} + Mg^{2+}}$	=0.5 <0.5 >0.5 >0.5 <0.5	Dolomite weathering Limestone-dolomite weathering Dolomite dissolution, calcite precipitation, or sea water Ferromagnesian minerals Granite weathering
$\frac{Ca^{2+}}{Ca^{2+} + SO_4^{2-}}$	= 0.5 0.5 pH < 5.5 < 0.5 neutral >0.5	Gypsum dissolution Pyrite oxidation Calcium removal -Ion exchange or calcite precipitation Calcium source other than gypsum-carbonates or silicates
$\frac{Ca^{2+} + Mg^{2+}}{SO_4^{2-}}$	>0.8 and <1.2	Dedolomitisation
$\frac{Cl^-}{\text{Sum of Anions}}$	>0.8TDS>500 >0.8TDS<100 <0.8	Sea water, or brine, or evaporate Rainwater Rock weathering
$\frac{HCO_3}{\text{Sum of Anions}}$	>0.8 >0.8 sulphate high <0.8 sulphate	Silicate or carbonate weathering Gypsum dissolution Sea water or brine
TDS	>500 <500	Carbonate weathering Silicate weathering
Conclusion	Aquifer Mineralogy	
Conclusion	Reaction	

The results obtained from the application of source rock deduction and summary of conclusions as displayed in Tables 4.13 and 4.14 respectively indicated that the sources of chemical constituents in groundwater of the study area originated from the weathering of the rocks underlying the area confirmed by the geology of the present study. The concentration of chemical ions in the groundwater of the area therefore, could have been as a result of weathering of granites of sodium and calcium composition other than halite-albite, gypsum-carbonates or silicates and ion exchange processes (Table 4.14 ; equations 2 and 3). Furthermore, it could also have been as a consequent of weathering of plagioclase and silicate minerals from the granitic rocks of the area as confirmed in Table 4.7 and results of equations 1,3,6 and TDS value whose origin could have been from a sedimentary environment in view of the low sulphate (equation 7). Therefore, the overall chemistry of groundwater in Zing and its environs is linked to the elemental and mineralogical composition of the rocks underlaying the area confirmed by X-Ray Fluorescence and X-Ray Defraction results obtained from the rock analyses as well as the source rock deduction summary and reasoning including other hydrogeochemical processes which has facilitated the distribution and enrichment of ions in groundwater of the study area.

Table: 4.13: Results obtained from application of source rock deduction of the study area

Sample Code	$\frac{Na+K-Cl}{Na+K-Cl+C}$	$\frac{Na}{Na+Cl}$	$\frac{Mg}{Ca+Mg}$	$\frac{Ca}{Ca+Mg}$	$\frac{Ca+Mg}{SO4}$	$\frac{Ca}{Ca+SO4}$	$\frac{Cl}{Sum\ of\ Anions}$	$\frac{HCO3}{Sum\ of\ Anions}$	*TDS*
ZGW/001	0.6	1.8	0.4	1.3	5.3	1.2	0.0	0.0	359
ZGW/002	0.3	2.6	0.4	1.3	4.1	1.2	0.0	0.0	481
ZGW/003	0.5	2.1	0.4	1.4	9.8	1.1	0.0	0.0	415
ZGW/004	0.1	3.0	0.3	1.4	5.1	1.2	0.0	0.0	586
ZGW/005	0.6	1.5	0.4	1.6	6.0	1.2	0.0	0.0	163
ZGW/006	0.4	2.0	0.3	1.3	10.3	1.1	0.0	0.0	387
ZGW/007	0.9	1.3	0.4	1.4	6.8	1.1	0.0	0.0	293
ZGW/008	0.8	1.4	0.3	1.2	6.1	1.1	0.0	0.0	394
ZGW/009	0.8	1.3	0.4	1.4	5.5	1.2	0.0	0.0	239
ZGW/010	0.6	1.8	0.4	1.4	5.9	1.2	0.0	0.0	273
ZGW/011	0.7	1.5	0.4	1.5	5.1	1.3	0.0	0.0	336
ZGW/012	0.8	1.3	0.3	1.4	5.3	1.3	0.0	0.0	247
ZGW/013	0.3	2.6	0.4	1.3	4.7	1.2	0.0	0.0	63.1
ZGW/014	0.7	1.5	0.3	1.6	16.0	1.1	0.0	0.0	220
ZGW/015	0.7	1.5	0.4	1.8	7.7	1.3	0.0	0.0	337
ZGW/016	0.5	2.2	0.4	1.3	4.3	1.2	0.0	0.0	198
ZGW/017	0.2	2.6	0.4	1.6	14.2	1.1	0.0	0.0	469
ZGW/018	0.7	1.4	0.3	1.6	26.2	1.1	0.0	0.0	326
ZGW/019	0.3	2.3	0.2	1.7	20.7	1.1	0.0	0.0	476
ZGW/020	0.7	1.6	0.3	1.4	12.2	1.1	0.0	0.0	307
ZGW/021	0.7	1.5	0.3	2.1	24.0	1.1	0.0	0.0	357
ZGW/022	0.4	3.3	0.2	6.8	63.7	1.4	0.0	0.0	659

Table: 4.13: Continued

ZGW/023	0.9	1.4	0.2	5.9	65.1	1.4	0.0	0.0	740
ZGW/024	0.8	1.5	0.3	1.6	14.7	1.1	0.0	0.0	309
ZGW/025	0.7	1.6	0.3	1.5	9.7	1.2	0.0	0.0	317
ZGW/026	0.5	2.0	**0.5**	1.8	12.0	1.2	0.0	0.0	431
ZGW/027	0.7	1.5	0.3	1.6	13.4	1.1	0.0	0.0	273
ZGW/028	0.5	1.8	0.2	1.5	11.9	1.2	0.0	0.0	577

Table 4.14: Summary of findings from source rock deduction analyses of the study area

Parameter((mmol/l)	Value	Conclusion	Values of calculated Paramters of study area	Source rock deductions conclusions of the study area
$\frac{Na^+ + K^+ - Cl}{Na^+ + K^+ - Cl^- + Ca^{2+}}$	>0.2 and<0.8	Plagioclase weathering possible	>0.2 and< 0.8 shows 21(75%) samples	75% of plagioclase weathering eminent
	<0.2 or >0.8	Plagioclase weathering likely	<0.2 or >0.8 shows 7 (25%) samples	
$\frac{Na^+}{Na^+ + Cl^-}$	>0.5	Sodium source other than halite-albite, ion exchange	>0.5 shows 28 (100%)	Sodium source other than halite-albite, ion exchange
	= 0	Halite solution		
	< 0.5 TDS >500	Reverse softening		
	<0.5 TDS < 500	Analysis error		
	>50	Rainwater		
	<0.5 TDS < 50			
$\frac{Mg^{2+}}{Ca^{2+} + Mg^{2+}}$	=0.5	Dolomite weathering	= 0.5, 1(3.6%) sample	Granite weathering
	<0.5	Limestone-dolomite weathering	< 0.5, 27(96.4%) sample	
	>0.5	Dolomite dissolution, calcite precipitation, or sea water	> 0.5, 0 (%) sample	
	>0.5	Ferromagnesian minerals	>0.5, 0 (0%) sample	
	<0.5	Granite weathering	<0.5. 27(96.4%) sample	
$\frac{Ca^{2+}}{Ca^{2+} + SO_4^{2-}}$	= 0.5	Gypsum dissolution		
	0.5 pH < 5.5	Pyrite oxidation		Calcium source other than gypsum-carbonates or silicates
	< 0.5 neutral	Calcium removal -Ion exchange or calcite precipitation		
	>0.5	Calcium source other than gypsum-carbonates or silicates	>0.5, 28(100%) samples	

Table 4.14 Continued

$\frac{Ca^{2+}+Mg^{2+}}{SO_4^{2-}}$	>0.8 and <1.2	Dedolomitisation	>0.8 and <1.2; 11(39.3%) samples within >1.2 & above; 17(60.7%) samples	
$\frac{CL^-}{\text{Sum of anions}}$	>0.8TDS>500	Sea water, or brine, or evaporate		
	>0.8TDS<100	Rainwater		
	<0.8	Rock weathering	<0.8; 28(100%) samples	Rock weathering
$\frac{HCO_3}{\text{Sum of anions}}$	>0.8	Silicate or carbonate weathering		
	>0.8 sulphate high	Gypsum dissolution		
	<0.8 sulphate low	Sea water or Brine	<0.8 sulphate low; 28(100) samples	Sea water or Brine
TDS	>500	Carbonate weathering	>500; 4(14.3%) samples	More of silicate weathering
	<500	Silicate weathering	<500; 24(85.7%) sample	other than carbonate
Conclusion	Aquifer mineralogy			
Conclusion	Reactions			

CHAPTER FIVE

5.0 CONCLUSION AND RECOMMENDATIONS

5.1 CONCLUSION

The hydrogeochemical investigation of groundwater in Zing and its environs aimed at determining groundwater quality characteristics have been carried out. The study area is underlain by granites and granodiorites consisting of porphyritic granites, granodiorites, coarse-grained granite, fine-grained granite, gneiss and pegmatites in order of increasing abundance.

The rocks shows considerable enrichment in major elements such as aluminium and silicon including trace elements of strotium and barium compared to others. The bulk chemical composition of the rocks in weight (wt%) of SiO_2, Al_2O_3, K_2O and MgO indicates enrichment of felsic and mafic minerals with major minerals as quartz, albites, microcline and biotites. Other associated minerals are actinolites, annites, sinidine, zircon, kaolinites, magnetite and phlogopite.

Field observations, elemental and mineralogical composition as well as ore association of the rocks shows that they are of I-Type granitic rocks. The Chemical Index of Alteration(CIA) of the rock samples indicates that they are modederate to higly weathered rocks capable of mobilizing and discharging chemical elements into groundwater system.

The World Health Organization (WHO, 2017) and the Nigerian Standard for Driniking Water Quality (NSDWQ,2015) recommended values for drinking water compared with measured parameters in groundwater of the area suggests that all measured physicochemical parameters in the groundwater samples except EC, TDS, TH, Ca^{+2}, K^{+} Cl^{-}, F^{-}, Pb^{+2}**,** $Cr^{+3,}$ $Zn^{+2,}$ and Fe^{+2} in few and most of the sampled locations were above the prescribed permissible limits which could be of health risk to humans in the area. The

moderate to very hard water in the region could also be from dissolved calcium, magnesium and bicarbonate minerals in groundwater while the high levels of electrical conductivity and total dissolved solids in few wells could be as a result of mineralization of groundwater by the host rock at considerable depth.

The dorminant ions in the groundwater are the Ca^{+2} and HCO_3^2 with $Ca^{+2} > K^+ > Na^+ > Mg^{+2}$ or $Mg^{+2} < Na^+ < K^+ < Ca^{+2}$ for major cations while $HCO_3 > Cl^- > CO_3 > SO_4 > NO_3 > NO_2$ or $NO_2 < NO_3 < SO_4 < CO_3 < Cl < HCO_3^2$ for major anions which has facilitated the composition of four hydrochemical facies namely, Ca^{2+}-Mg^{2+}-HCO_3^-, Na^+-K^+-HCO_3^- ,Na^+-K^+-$Cl^-SO_4^{2-}$ and Ca^{2+}-Mg^{2+}-Cl^--SO_4^{2-} resulting from groundwater evolution due to rock-water interaction along its flow path over a period of time.

The climatic conditions of neutral to alkaline water, chemical weathering and geochemical processes such as rock dorminance, precipitation, evaporation, dissolution and ion exchange reactions withing the aquifer matrices could have aided the enrichment of chemical constituents in groundwater of the area.

Consequently, the sources and origin of chemical constituents in groundwater is derived from the composition of rock bearing minerals underlying the area and other associated minerals as revealed by rock geochemistry and source rock deduction and reasoning assessment.

Conclusively, the overall chemistry of groundwater of the study area is controlled by the geology rather than anthropogenic activities.

5.2 Recommendations

I. The communities particularly in fluoride rich areas above 1.5mg/l should use groundwater for bathing and laundry only while alternative source of potable water such as rainwater and surface water is being explored.

II. Cheaper and user frienly methods for treatment of groundwater should be explored by concerened authorities in the state to mitigate the health impact of chemical constituents whose concentration are above the permissible limits of WHO (2017) and NSDWQ (2015) at Zing and its environs

III. Further studies on health impact, bacteriological assessment of groundwater and treatment strategies is higly recommended.

IV. Further studies on the economic potential of rock forming minerals in the study area should be undertaken in view of the array of the revelation of mineral species from the rocks undelying the area

V. Routine monitoring and evaluation of groundwater quality needs to be carried out regularly by the State water quality and sanitation agency for management of water quality and chemical elements observed to be obnocious to human health.

5.3 **Contribution to Knowledge**

The research work has improved knowledge on the geology of the area as well as provided the needed geochemistry, mineralogical and hydrochemistry data for management of groundwater quality by relevant stakeholders in view of the increasing concentration chemical constituents in groundwater system of the study area.

REFERENCES

Abbas, G., Murtaza, B., Bibi, I., Shahid, M., Niazi, N.K., Khan, M.I., Amjad, M., Hussain M., & Natasha., K. (2018). Arsenic Uptake, Toxicity, Detoxification, and Speciation in Plants: Physiological, Biochemical, and Molecular Aspects. *International Journal of Environmental Resources and Public Health,* 15, 59-70.

Adedapo, J. O., & Fokolade, O. R. (2014). Groundwater Quality Assessment of Ekere Ekiti Artesian Well, Ekiti State, Nigeria. *Water Resources Journal of the Nigerian Association of Hydrogeologists*, 24, 34-36.

Adelana, S.M.A., & Olasehinde, P.I. (2003). High Nitrate in Water Supply in Nigeria: Implication for Human Health. *Water Resources,* 14, 1-11.

Adelana, S.M.A., Olasehinde, P.I., Vrbka, P., Edet, A.G. & Goni, I.B.((2008). An Overview of the Geology and Hydrogeology of Nigeria. In: S.M.A. Adelana and A.M. Mc Donald(Eds.), *Applied Groundwater Studies in Africa*, Leiden, Netherlands. CRS Press/Balkema.

Adelana, S.M.A., Olasehinde, P.I., & Vrbka, P. (2004). Hydrogeochemistry of Groundwater Resources in Sokoto Basin, Northwestern, Nigeria. Conference Proceedings of the 20th Colloquium of African Geology, Orleans, France,.

Adimalla, N., & Li, P. (2019). Occurrence, Health Risks and Geochemical Mechanisms of Fluoride and Nitrate in Groundwater of the Rock Dominant Semi-Arid Region, Telangana State, India. *Human Ecological Risk Assessment*, 25, 81–103.

Amadi, A.N., & Nwankwoala, H.O. (2013a). Evaluation of Heavy Metals in Soils from Enyimba Dumpsite in Aba, Southeastern Nigeria Using Contamination Factor and Geo-accumulation Index. *Energy and Environmental Research*, 3(1), 125-134.

Amadi, A.N., Olasehinde,,P.I., Okunlola,I.A., Dan-Hassan, M. A., & Jimoh, M.O. (2016). Occurrence of Fluoride and Some Heavy Metals in Groundwater from Shallow Aquifers Near Ogbomosho, North-central Nigeria. *Journal of Natural Science Research*, 6(13), 55-60.

Aminu, T., & Amadi A. N. (2014). Fluoride Contamination of Shallow Groundwater in parts of Zango Local Government Area of Katsina State, Northwest Nigeria. *Journal of Geosciences and Geomatics*, 2(4), 178-184.

Andy, N. M., & Silas, I. (2020). Evaluation of Physico-chemical Properties of Well Water Qualities in Selected Villages in Zing Local Government Area of Taraba State, Nigeria. *International Journal of Contemporary Research and Review*, 11(3), 20282–20288.

Anupam, S., & Rajamani, V. (2000). Weathering of Gneissic Rocks in the Upper Reaches of Cauvery River, South India: Implications to Neotectonics of the Region. *Chemical Geology*, 166, 203-223.

APHA(2020). American Public Health Association. Standard Methods for Examination of Water and Wastewater. 20th Edition, APHA, Washington DC.

Badafash,B.E.C.(1991). Consulting Engineers, Ibadan.

Bakari, A. (2014). Hydrochemical Assessment of Groundwater Quality in the Chad Basin around Maiduguri. *Nigeria Journal of Geology and Mining*, 6 (1), 1-12.

Banks, D., Rhor-Torp, E., & Skarphargen, H. (1994). Groundwater Resources in Hard Rock: Experiences from the Hvaler Study, Southeastern Norway. *Applied Hydrogeology*, 233-242.

Brindha, K. & Elango, L. (2011). Fluoride in Groundwater: Causes, Implications and Mitigation Measures. In: Monroy, S.D. (Ed.), Fluoride Properties, Applications and Environmental Management, 111- 136.

Bura, B., Goni, I.B., Sheriff, B.M., & Gazali, A. K. (2018). Occurrence and Distribution of Fluoride in Groundwater of Chad Formation Aquifers in Borno State, Nigeria. *International Journal of Hydrology*, 2(4), 527-536.

Carter, J.D., Barber, W., & Tait, E.A. & Jones, G.P. (1963). The Geology of Parts of Adamawa, Bauchi and Bornu Provinces in Northeastern..*Geological Survey of Nigeria* Bulletin, 30, 108.

Chae, G. T., Yun, S. T., Mayer, B., Kim, K. H., Kim, S. Y., Kwon, J. S., Kim, K., & Koh, Y. K. (2007). Fluorine geochemistry in Bedrock Groundwater of South Korea. *Science of the Total Environment,* 385, 272-283.

Chakraborti, D., Rahman, M.M., Mukherjee, A., Alauddin, M., Hassan, M., Dutta, R.N., Pati, S., Mukherjee, S.C., Roy, S., Quamruzzman, Q., Rahman, M., Islam, T., Sorif, S., Selim, M.D., Islam, M.R., & Hossain, M.M. (2015). Groundwater Arsenic Contamination in Bangladesh—21 years of Research. *Journal of Trace Element and Medical Biology*, 31, 237-248.

Chapman, D., & Kimstach, V. (1996). Selection of Water Quality Variables. .In: Chapman D (Ed.), Water Quality Assessment, A Guide to Use of Biota, Sediments and Water in Environmental Monitoring (2nd Edition).

Chappell, B.W., & White, A.J.R. (1978). Granitoids from the Moonbi District, New England batholiths, Eastern Australia. *Journal of Geological Sciences*, Australia, 25, 267-283.

Chilton, P.J. & Foster, S.S.D. (1995). Hydrogeological Characterization and Water Supply Potential of Basement Aquifers in Tropical Africa. *Hydrogeology Journal*, 3, 36-49.

Cox, K.J., Bell, J.D., & Pankhurst,R.J.(1969). The Interpretation of Igneous Rocks. London: George Allen and Unwin, 450p.

Dahlgaard, H., Eriksson, M., Nielsen, S.P., & Joensen, H.P. (2004). Levels and Trends of Radioactive Contaminants in the Greenland Environment. *Journal of Science and Environ,* 331, 53–67.

Dash, S. (2003). Occurrence of Groundwater in Hard Rock Terrains of Sundargarh District, Orissa, India. In: J. Krasny, Z. Hrkal & J. Bruthan(Eds.). Proceedings of

IAH Internal Conference on Groundwater in Fractured Rocks, Prague, Czech Republic, 47-48.

Dibal, H.U., Schoeneick, K., Garba, I., Lar, U.A., & Bala, E.A.(2012). Overview of Fluoride Distribution in major aquifer units of Northern Nigeria. *Journal of Environmental Health Sciences*. 4(12), 1287-1294.

Du Preez, J.W., & Barber, W. (1965). The Distribution and Chemical Quality of Groundwater in Northern Nigeria. *Geological Survey of Nigeria Bulletin*, 36 (32), 93p.

Ekwueme, B.N. (1987). Structural Orientations and Precambrian Deformation Episodes of Uwet Area. Oban Massif. *Precambrian Research*, 34, 269-285.

Elumalai, V., Nethononda, V.G., Manivannan, V., Rajmohan, N., Li, P., & Elango, L. (2020). Groundwater Quality Assessment and Application of Multivariate Statistical Analysis in Luvuvhu Catchment, Limpopo, South Africa. *Journal of Africa Earth Science,*171,103967.

Farnbauer, B., & Teiz, H. (2000). The Individuality of Laterites Developed on the Jos, Plateau, Central Nigeria (in deutsch). *Journal of Geology and Peleotology*, 5(6), 509-525.

Feenstra, L.,Vasak, L., &Griffioen,J.(2007). Fluoride in Groundwater: Overview and Evaluation of Removal Methods. *International Groundwater Resources Association Centre Report,* 2007(1),1-21.

Foster, S.S.D., Tuinhof A, & Garduno, H. (2008), Groundwater in Sub Sahara Africa – A Strategic Overview of development issues. In Adelana, S.M.A. & MacDonald, A.M. (eds) Applied Groundwater Studies in Africa. IAH Selected Papers on Hydrogeology. 13, CRC Press/Balkenia, Leiden, The Netherlands**.**

Gibbs, R. J. (1970). Mechanisms Controlling World Water Chemistry. *Journal of Science*, 17, 1088–1090.

Giridharan L., Venugopal T., & Jayaprakash M. (2008). Evaluation of the Seasonal Variation on the Geochemical Parameters and Quality Assessment of the Groundwater in the Proximity of River Cooum, Chennai, India. *Environmental Monitoring and Assessment*, 143(1), 161-178.

Grant, N.K. (1971). A Compilation of Radiometric Age from Nigeria. *Journal of Mining Geology*, 6,37-54.

Hanna (2019). Hanna Instrument Instruction Manual., Highland Industrial Park, 584 Park East Drive, Woosocket, RI 02895, USA.

Hansen, B., Thorling, L., Schullehner, J., Termansen, M., & Dalgaard, T. (2017). Groundwater Nitrate Response to Sustainable Nitrogen Management. Journal of Science, 7, 8566 -8568.

Haruna, I.V., Orazulike , D.M. & Ofulume, A.B. (2010). Preliminary Geological and Radiometric Studies of Granitoids of Zing-Monkin Area. Adawawa Massif, North Eastern, Nigeria. *Global Journal of Geological Sciences*, 9(2), 123-134.

Hashim, MA., Mukhopadhyay, S., Sahu, J.N., & Sengupta, B. (2011). Remediation Technologies for Heavy Metal Contaminated Groundwater. *Journal of Environmental Management*, 92, 2355–2388.

He, X., & Li, P. (2020). Surface Water Pollution in the Middle Chinese Loess Plateau with Special Focus on Hexavalent Chromium (Cr^{6+}): Occurrence, Sources and Health Risks. *Journal of Heath Sciences*, 12, 385–401.

Hem, J.D. (1985). Study and Interpretation of the Chemical Characteristics of Natural Water. United States Geological Survey Water Supply Paper 2254, 2258.

Henrinksen, A., & Braathen, A. (2006). Effects of Fracture Lineaments and in-situ rock stresses on groundwater flow in hard rocks: A case study from Sunnfjord, Western Norway**,** *Hydrogeology Journal***,** 14, 444-461.

Hounslaw W. (1995). Water Quality Data: Analysis and Interpretation Press, Boca Raton, 71-127.

Huang, C., Lin, T., Chiao, L., & Chen, H. (2012). Characterization of Radioactive Contaminants and Water Treatment Trials for the Taiwan Research Reactor's Spent Fuel Pool. J. Hazard Mater. 233–234, 140–147.

International Association of Hydrogeologists (IAH,2020). Groundwater— More About the Hidden Resource. https://iah.org/education/general-public/groundwater-hidden-resource. Accessed 13 Nov 2020.

Ishaku, J.M., Kwada , I.A., & Adekeye, J.I.D. (2009). Hydrogeological Characterization and Water Supply Potential of Basement Aquifers in Taraba State, N.E. Nigeria. *Nature and Science*, 7(3), 75-83.

Jenifer, M.A., & Jha, M.K. (2018). Comprehensive Risk Assessment of Groundwater Contamination in a Weathered Hard Rock Aquifer System of India. *Journal of Clean Product*, 201, 853–868.

Ji, Y., Wu, J., Wang, Y., Elumalai, V., & Subramani, T. (2020). Seasonal Variation of Drinking Water Quality and Human Health Risk Assessment in Hancheng City of Guanzhong Plain, China. *Journal of Health*, 12, 469–485.

JICA (2011). Japan International Cooperation Agency Final Report on the Preparatory Survey on Project Improvement on Water Supply. Yachiyo Engineering Co., Ltd. 234-390.

Jones, H.A., & Hockey, R.D. (1964). The Geology of Southern Nigeria. *Geological Survey of Nigeria Bulletin*, 31, 101.

Kana, M.A., Schoeneich, K., & Garba.,L.A (2014). Suitability of Groundwater for Domestic and other Uses in Nasarawa Town and Environs, North Central Nigeria.

Water Resources Journal of the Nigerian Association of Hydrogeologists ,24, 55-74.

Karunanidhi, D., Aravinthasamy, P., Subramani, T., Wu, J., & Srinivasamoorthy, K. (2020). Potential Health Risk Assessment for Fluoride and Nitrate Contamination in Hard Rock Aquifers of Shanmuganadhi River basin, South India. *Human Ecological Risk Assessment*, 25, 250–270.

Kogbe, C.A. (1989). The Cretaceous and Paleogene sediments of southern Nigeria. *In:* C.A.Kogbe (ed.), Geology of Nigeria. Rock View Nigeria Limited, Jos, Nigeria, 324-334.

Li, P., Tian, R., Xue, C., & Wu, J. (2017a). Progress, Opportunities and Key Fields for Groundwater Quality Research under the Impacts of Human Activities in China with a Special Focus on Western China. *Environmental Science Pollution Resources,* 24, 3224–13234.

Li, P., Wu, J., & Qian, H. (2016). Preliminary Assessment of Hydraulic Connectivity between River Water and Shallow Groundwater and Estimation of their Transfer Rate during Dry Season in the Shidi River, China. *Environmental Earth Sciences,* 75, 99.

Lloyd, J. A., & Heathcote, J. A. (1985) Natural inorganic hydrochemistry in relation to groundwater: An introduction. Oxford Uni. Press, New York , 296.

Longe, E.O., Malomo, S., & Olorunniwo, M.A. (1987). The Hydrogeology of Lagos Metropolis. *Journal of Africa Earth Sciences, 6,* 1*63-174.*

Lytle, D.A., Sorg, T., Wang, L., & Chen, A. (2014). The Accumulation of Radioactive Contaminants in Drinking Water Distribution Systems. *Journal of Water Resources,* 50, 96–407.

Mac Donald., A.M., Davies, J., & Carlow., R.C. (2008). African Hydrogeology and Rural Water Supply. In: S.M.A. Adelana and A.M McDonalds (Eds.).*Applied Groundwater Studies in Africa*. 125-145, London, CRC Press.

Mac Donald, J.A., & Kavanaugh, M.C. (1994). Restoring Contaminated Groundwater: An Achievable Goal. *Environmental Science and Technology*. 28(8), 362A–368A.

Macleod, W.N., Turner, D.C., & Wright, E.P. (1971). The Geology of the Jos Plateau. *Geolology of Nigeria Buttetin*, 32, 18.

Maspalma, S.S.,Okunola, I.A., Amadi, A.M.,Olasehinde, P.I., & Okoye, N.A.(2016). Geospatial and Temporal Distribution of Fluoride in Groundwater and Health Impacts in Hong Area, North Eastern Nigeria. *Journal of Natural and Applied Sciences*, 5 (1), 82-93.

McCurry, P. (1976). A Generalized Review of the Geology of the Precambrain to Lower Paleozoic Rocks, Northern Nigeria: In Kogbe, C.A. (ed), Geology of Nigeria, Elizabethan Press, Lagos, 13-38.

Middilemost, E.A.K.(1994). Naming Materialsin the Magma and Ingneous Rock System. *Earth Science Reviews*. 37, 215-244

Montcoudiol N. (2015). Contribution de l'hydrogéochimie à la Compréhension des écoulements d'eaux souterraines en Outaouais, Québec, Canada (Doctoral dissertation, Université Laval).

Msonda, K. W. M., Masamba, W. R. L., and Fabiano, E. (2007). A Study of Fluorides Groundwater Occurrence in Nathenje, Lilongwe, Malawi. *Physics and Chemistry of the Earth*, 32, 1178-1184.

Mthembu, P.P., Elumalai, V., Brindha, K., & Li, P. (2020). Hydrogeochemical Processes and Trace Metal Contamination in Groundwater: Impact on Human Health in the Maputal and Coastal Aquifer, South Africa. *Journal of Expo Health*, 12, 403–426.

National Population Commission (NPC,2006). Population Figures for Zing Local Government Area, Taraba State.

Ndolo, V. (2002). Examination of Water Availability, Access and Quality in Drought-Prone Areas in Balaka District Malawi. MSc Thesis. University of Malawi, Chancellor College, Zomba**.**

Nelson, A. (2015). Physical Geology Notes (EENS1110) on Mountains and Deformation of Rocks.http//www.tulane.edu/-sanelson/eens110/deform.pdf.

Nesbitt, H. W., & Young, G. M. (1982). Early Proterozoic Climates and Plate Motions Inferred from Major Element Chemistry of Lutites. *Nature*, 299, 715–717.

Nesbitt, H. W., & Young, G. M. (1984). Prediction of some Weathering Trends of Plutonic and Volcanic Rocks Based on Thermodynamic and Kinetic. *Geochim. Cosmochin. Acta*, 48, 1523-1534.

Njuguna, S.M., Makokha, V.A., Yan, X., Gituru, R.W., Wang, Q., & Wang, J. (2019). Health Risk Assessment by Consumption of Vegetables Irrigated with Reclaimed Wastewater: A Case Study in Thika, Kenya. *Journal of Environmental Management*, 231, 576–581.

NSDWQ (2007). Nigerian Standard for Drinking Water Quality. Nigerian Industrial Standards , 18-25

NSDWQ (2015). Nigerian Standard for Drinking Water Quality. Nigerian Industrial Standards, 16-22.

Offodile, M.E. (2002). Hydrogeology. Groundwater Study and Development in Nigeria, Second Edition. Published by Mecon Engineering Services Ltd, Jos, Nigeria. 239 – 345.

Offodile, M.E. (2014). Hydrogeology. Groundwater Study and Development in Nigeria, Third Edition. Published by Mecon Engineering Services Ltd, Ratya, Jos, Nigeria.

Ogezi, E.A. (2002). ‘‘Geology’’ In Africa Atlases, Nigeria. Les Editions J.A., Paris, France. 60-61.

Okosun., E.A. (1998). Review of the Early Tertiary Stratigraphy of Southwestern Nigeria. *Journal of Mining and Geology, 34,* 7-35.

Okunlola, I. A., Amadi, A. N**.,** Idris-Nda, A., Agbasi, K. & Kolawole L. L. (2014). Assessment of Water Quality of Gurara Water Transfer from Gurara Dam to Lower Usuma Dam for Abuja Water Supply, FCT, Nigeria. *American Journal of Water Resources,* 2(3), 74 – 80.

Okunola, I.A., Amadi, A.N., Olasehinde, P.I., Maspalma,S.S & Okoye, N.O. (2016). Quality Assessment of Groundwater from Shallow Aquifers in Hong Area, Adamawa State, Northeastern Nigerian. *Ife journal of Science,*1891,267-283.

Olasehinde, P. I., & Amadi, A. N. (2009). A Review of Borehole Construction, Development and Maintenance Techniques around Owerri and its Environs, Southeastern Nigeria. *Journal of Science, Education and Technology,* 2(1), 310-321.

Olasehinde, P.I.(2010). The Groundwaters of Nigeria: A Solution to Sustainable National Water Needs. Inaugural Lecture Series 17, Federal University of Technology, Minna, Nigeria

Olasumbo, M., & Olufemi, I. (2020). Essentials of Practical Water Quality Studies. First Edition, published by University Press PLC. ISBN 978- 978-940-747- 7.

Olufemi,V.O., Joseph, O.A., Samson, B.O., Salome, H.A., Amobi, C.E., Degree, N.U., & Sylvester, W.O. (2019). Hydro- chemical Characteristics of Quality Assessment of Groundwater from Fractured Albian Carbonaceous Shale Aquifers around Enyigba-Ameri, Southeastern Nigeria. *Environment Monitoring Assessment*, 191, 125..

Oluyide, P.O., Nwajide, C.S., & Oni, A.O. (1998). The Geology of Ilorin Area with Explanation on the 1:250,000 Series, Sheet 50 (Ilorin). *Geological Survey of Nigeria Bulletin,* 42,1-84.

Oruonye, E.D., & Abbas, B. (2011). The Geography of Taraba State, Nigeria. LAP Publishing Company, Germany.

Oruonye,E.D., & Bange,E. (2015). Challenges of Water Resources Development in Zing Town, Taraba State, Nigeria. *Journal of Advance Humanities,* 4(1), 355-360.

Oyawoye, M.O. (1972). The Basement Complex of Nigeria. In: T.F.J. Dessavagie and 1A.J. Whiteman (Eds). African Geology (66-102). Ibadan, University of Ibadan Press.

Pandey, H.K., Duggal, S. K., & Jamatia, A. (2016). Fluoride Contamination of Groundwater and its Hydrological Evolution in District Sonbhadra (U.P.), India. *Proceedings of the National Academy of Sciences, 70,* 2250-2258

Pascual, B., Gold-Bouchot, G., Ceja-Moreno,V., & Del Ri'o-Garrci'a, M. (2004). Heavy Metals and Hydrocarbons in Sediments from three Lakes from San Miguel,Chiapas, Mexico. *Environmental and Contamination and Toxicology Bulletin* ,73,762-769.

Piper, A.M. (1944). A Graphical Procedure in the Geochemical Interpretation of Water Analyses. *American Geophysical Union, Transactions,* 25, 914 – 923.

Rahaman, M.A. (1989). Review of the Basement Geology of Southern Nigeria. In: C.A. Kogbe (Ed.). Geology of Nigeria (2nd ed.) Ibadan Rock View (Nig) Ltd.

Ray,H.H., & Yusuf, M.B. (2011). The incidence of soil erosion in Zing Local Government Area of Taraba State, Nigeria. *Ethiopian Journal of Environmental Studies and Management,* 4(2), 9-16.

Reyment, R.A.(1965). *Aspect of the Geology of Nigeria*. Ibadan, University of Ibadan Press.

Rebelo, F.M., & Caldas, E.D. (2016) Arsenic, Lead, Mercury and Cadmium: Toxicity, Levels in Breast Milk and Risks for Breastfed Infants. *Environmental Resources,* 51, 671–688.

Sawyer, G.N., & McCarthy, D.L. (1967). *Chemistry of Sanitary Enginneers* (2nd Ed). (M). McGraw Hill, New York. 518p

Schillinger, J., Özerol, G., Güven-Griemert, Ş., & Heldeweg, M, (2020), Water in War: Understanding the Impacts of Armed Conflict on Water Resources and their Management. WIREs Water 7: e1480. https:// doi.org/10.1002/wat2.1480.

Schoeller, H. (1955). *Géochimie des eauxsouterraines, application aux eaux des gisements de pétrole*. Revue de L'InstitutFrançais du Pétroleet An. de Combustibles Liquides, 213p.

Schroeter, H.A. (1966). Municipal Drinking Water and Cardiovascular Death Rate. *Journal of American Medical Association,* 195, 81-85.

Serio, F., Miglietta, P.P., Lamastra, L., Ficocelli, S., Intini, F., De Leo, F., & De Donnon, A. (2018). Groundwater Nitrate Contamination and Agricultural Land Use: A Grey Water Footprint Perspective in Southern Apulia Region (Italy). *Science Total Environment,* 645, 1425–1431.

Srinivasa, R.Y., Reddy, T.V.K. and Nayudu, P.T. (2000). Groundwater Targeting in a Hard Rock Terrain Using Fracture Pattern Modeling, Niva River Basin, Andr. Pradesh, India. *Hydrogeology Journal*, 8 (5), 494-502.

Stiff Jr, H. A. (1951) "The Interpretation of Chemical Water Analysis by Means of Patterns. "J. Petrol. Technol., 3, 15-161951.

Su, Z., Wu, J., He, X., & Elumalai, V. (2020). Temporal Changes of Groundwater Quality within the Groundwater Depression Cone and Prediction of Confined Groundwater Salinity using Grey Markov Model in Yinchuan Area of Northwest China. *Expo Health*, 12, 447–468.

Subba Rao, N., Ravindra, B., & Wu, J. (2020). Geochemical and Health Risk Evaluation of Fluoride Rich Groundwater in Sattenapalle Region, Guntur district, Andhra Pradesh, India. *Humanities and Ecological Risk Assessment,* 26, 2316–2348.

Tatti, F., Papini, M.P., Torretta, V., Mancini, G., Boni, M. R & Viotti, P. (2019). Experimental and Numerical Evaluation of Groundwater Circulation Wells as a Remediation Technology for Persistent, Low Permeability Contaminant Source Zones. *Journal of Contaminant Hydrology*, 222, 89–100.

Teng, Y., Hu, B., Zheng, J., Zhai, Y., & Zhu, C. (2018). Water Quality Responses to the Interaction between Surface Water and Groundwater along the Songhua River, NE China. *Hydrogeology Journal*, 26, 1591–1607.

Tirumelesh, A., Shivanna, A., & Jalihal, A. (2007). Isotope Hydrochemical Approach to Understand Fluoride Release into Groundwater of IIkal Area, Bagalkot District, Karnataka, India. *Hydrology Journal*, 15, 589-598.

Todd, D.K., (1980). Groundwater Hydrology, 2nd (ed.) J. Wiley and Sons, New York, 2nd Edition, 524p

Turner, D.C. (1964). Notes on Fieldwork on the Basement Rocks of 1:250,000, Sheets 7 & 8. *Geological Survey of Nigeria Report*. No. 5503.

Vojtech, J., Colin, M. F., & Vojtech, E. (2006). Interpretation of Whole-Rock Geochemical Data in Igneous Geochemistry: Introducing Geochemical Data Toolkit (GCDkit). *Journal of Petrology,* 47(6), 1255-1259

Wang, D., Wu, J., Wang, Y., & Ji, Y. (2020). Finding High Quality Groundwater Resources to Reduce the Hydatidosis Incidence in the Shiqu County of Sichuan Province, China: Analysis, Assessment, and Management. *Journal of Health*, 12, 307–322.

Waziri, S.H., Waziri, N.M., Tijani, A., Okunlola, A.I., & Umar, A. (2016). Assessment of Chemical Quality of Water from Shallow Alluvial Aquifers in and Around Badaggi, Central Bida Basin. *Journal of Earth Sciences and Geotechnical Engineering* ,6(3), 133-145.

Waziri, S.H., Abdullahi, N.I., & Adeniji, M.A. (2019). Geology and Chemical Characterization of Groundwater in Kafin-Koro and its Environs, North central Nigeria. *Journal of Mining and Geology*, 55(1), 83-89.

WHO (2006). Guidelines for Drinking Water Quality, Volume 1, Recommendations, Geneva, Switzerland.

WHO (2009). Guidelines for Drinking Water Quality, Third Edition, Volume 2. Health Creteria and other Supporting Information.WHO,Geneva Switzerland, 234-235.

WHO (2011). Guidelines for Drinking Water Quality, Fourth Edition. A Publication of World Health Organization, Gutenberg, 468-475.

WHO (2017). Guidelines for Drinking Water Quality: Fourth Edition Incorporating the First Addendum, Geneva, Switzerland. 469-474a.

World Bank (1997). Selecting an Option for Private Sector Participation in Water and Sanitation, Toolkits for Private Participation and Sanitation, No.1. The World Bank Publication, Washington, DC.

Wright, E.P. & Burgess, W.G (eds). (1992). The Hydrogeology of Crystalline Basement Aquifers in Africa. Geological Society, London. Special Publications 66.

Wu, J., & Sun, Z. (2016). Evaluation of Shallow Groundwater Contamination and Associated Human Health Risk in an Alluvial Plain Impacted by Agricultural and Industrial Activities, Mid-West China. *Expo Health,* 8, 311–329.

Wu, J., Li, P., & Qian, H. (2015). Hydrochemical characterization of drinking groundwater with special reference to fluoride in an arid area of China and the Control of Aquifer Leakage on its Concentrations. *Environmental Earth Sciences*, 73,8575–8588. .

Wu, J., Li, P., Qian, H., & Fang, Y. (2014). Assessment of Soil Salinization Based on a Low-Cost Method and its Influencing Factors in a Semi-Arid Agricultural Area, Northwest China. *Environmental Earth Sciences*, 71(8) ,3465–3475.

Wu, J., Zhang, Y., & Zhou, H. (2020). Groundwater Chemistry and Groundwater Quality Index Incorporating Health Risk Weighting in Dingbian County, Ordos Basin of Northwest China. *Geochemistry*, 80(4), 25607-125615.

Yuan, Y., Xiang, M., Liu, C., & Theng, B.K.G. (2019). Chronic Impact of an Accidental Wastewater Spill from a Smelter, China: A Study of Health Risk of Heavy Metal (loid)s via Vegetable intake. *Ecotoxicology and Environmental Safety* 182, 109401

Zhang, Y., Wu, J., & Xu, B. (2018). Human Health Risk Assessment of Groundwater Nitrogen Pollution in Jinghui Canal Irrigation Area of the Loess Region, Northwest China. Environmental Earth Science, 77, 273.

Zhou,Y., Li, P., Chen, M., Dong, Z., & Lu, C. (2020). Groundwater Quality for Potable and Irrigation uses and Associated Health Risk in Southern Part of Gu'an County, North China Plain. *Journal of Environmental Geochemistry and Health*, 50(23), 1250-1280

APPENDIX A

WATER SAMPLE FIELD DATA SHEET FOR POSTGRADUATE PROJECT ON HYDROGEOCHEMICAL INVESTIGATION OF GROUNDWATER QUALITY IN ZING AND ENVIRONS, PART OF JALINGO SHEET 236NE, NORTH EASTERN NIGERIA.

1. LOCATION NAME……2. ALTITUDE……(m)a.m.s.l 3.DATE OF SAMPLE COLLECTION ……

4. SAMPLE CODE/ NUMBER…… 5. LOCAL GOV'T AREA…… 6. STATE…… …

7. COORDINATES N…… E…… ……. 8. TIME OF COLLECTION…… ……

9. SOURCE OF WATER

i) PRECIPITATION……. ii) NAME OF RIVER/IMPOUNDED RESERVOIR……

iii) NAME OF WELL/BOREHOLES…… iv) WELL, /BOREHOLE IDENTIFICATION NO. /NAME OF OWNER…….

v) USE OF WELL/BOREHOLE……. vi) STATIC WATER LEVEL……. (m)

vii) TOTAL DEPTH OF WELL/BOREHOLE……..…(m) viii) AQUIFER NAME/LITHOLOGY…… ……..

10. IN-SITU MEASUREMENTS OF PHYSIOCHEMICAL PARAMETERS:

i) COLOUR**……** ii) ODOUR**……** ii**)** TASTE…… iv) pH**……**

v) ELECTRICAL CONDUCTIVITY……(µs/cm) vii) TEMPERATURE…**……**O^c viii) TOTAL DISSOLVE SOLIDS (TDS**) ……**ppt

X) DESCRIPTION OF TYPE OF SAMPLE COLLECTED FOR ANALYSES AND SAMPLING ENVIRONMENT……

APPENDIX B

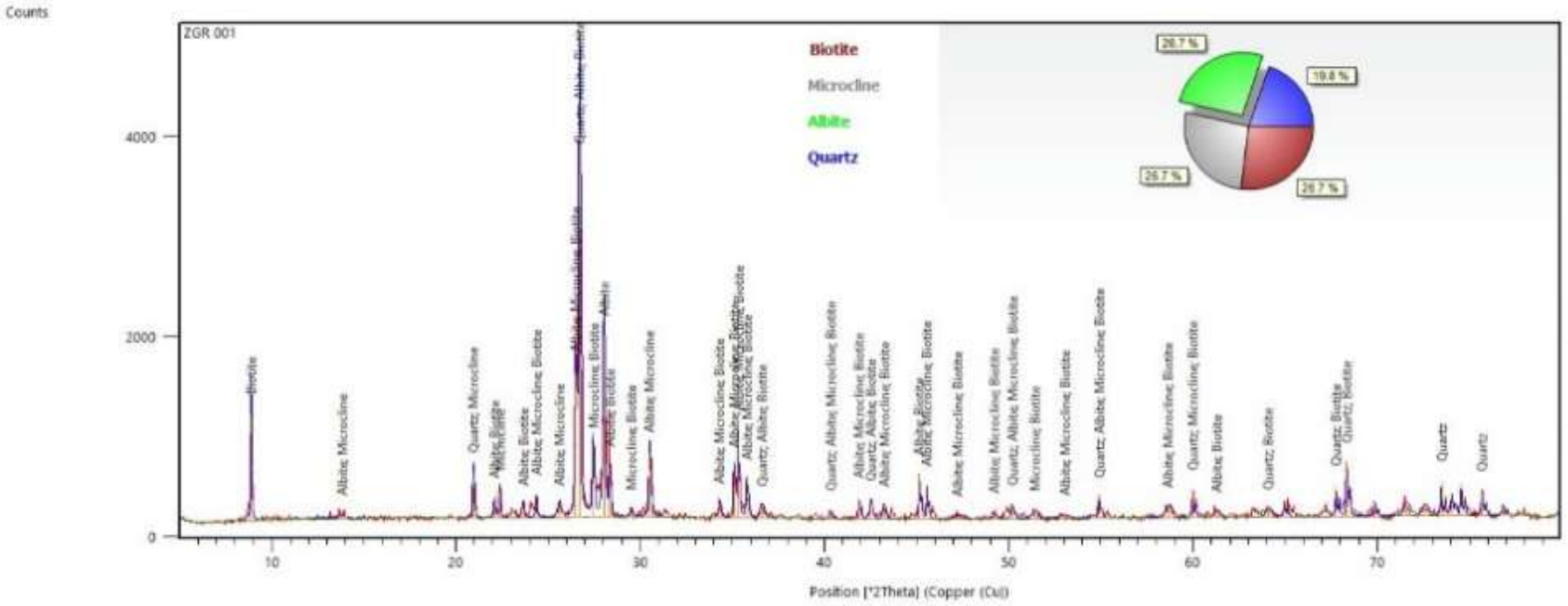

Figure 4.9j. Diffractogram of Rock sample, **ZGR/001**with **Biotite,** Microcline**,** **Albite** and **Quartz** as dominant minerals.

APPENDIX C

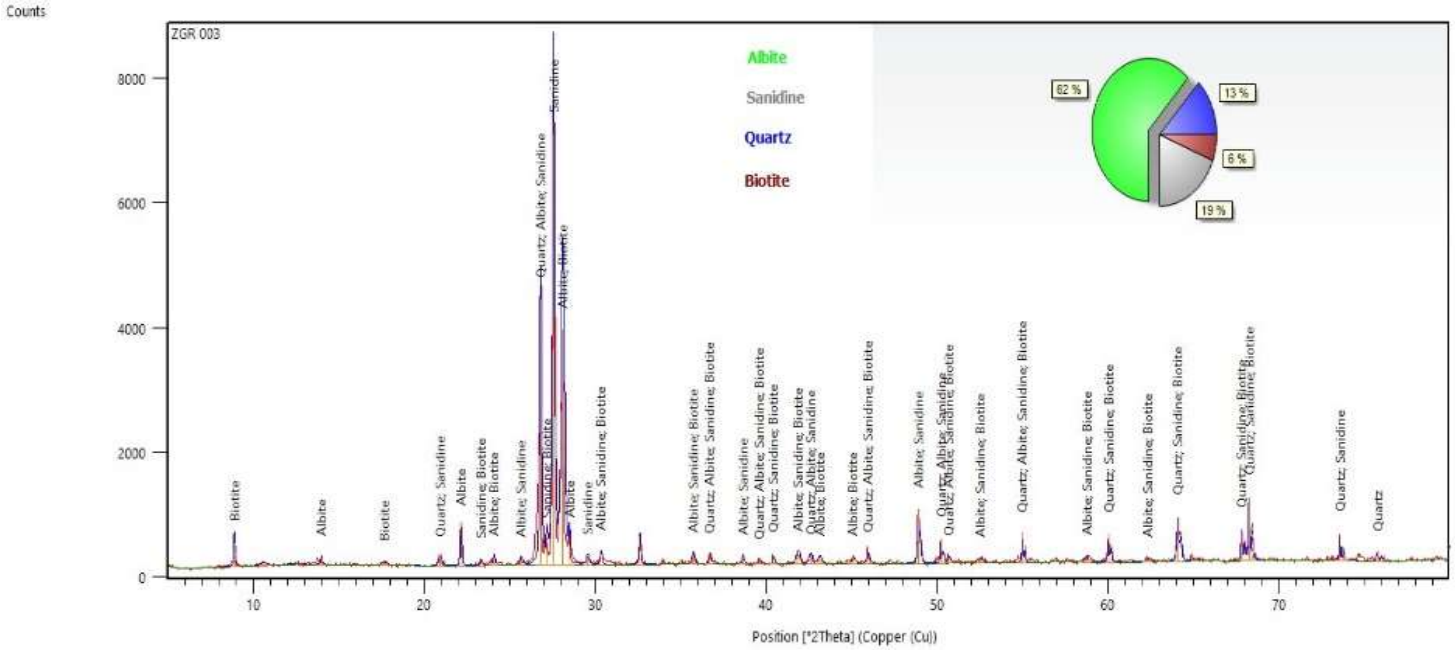

Figure 4.9k. Diffractogram of Rock sample, **ZGR/003** with **Albite, Sinidine, Quartz** and **Biotite** as dominant minerals.

Figure 4.9k. XRD chart of Rock sample 003

APPENDIX D

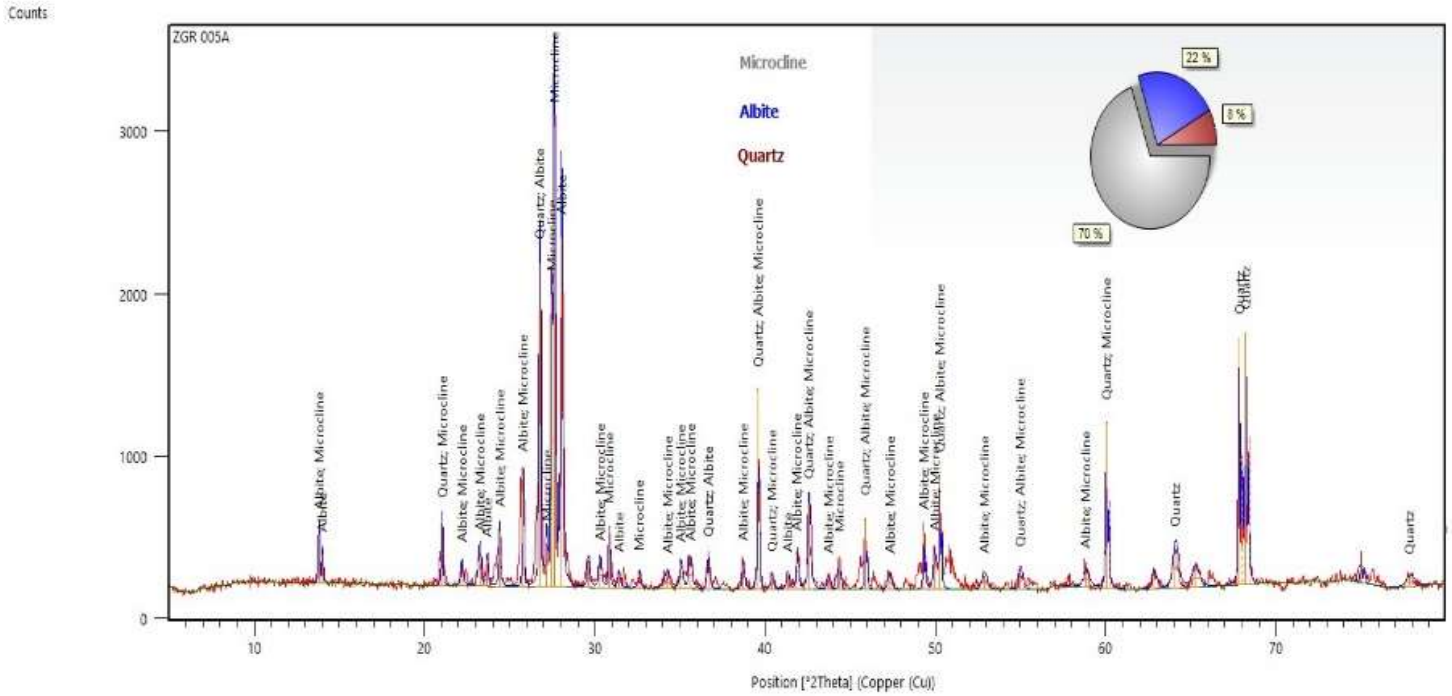

Figure 4.9k. Diffractogram of Rock sample, **ZGR/005A** with **Microcline, Albite** and **Quartz** as dominant minerals.

APPENDIX E

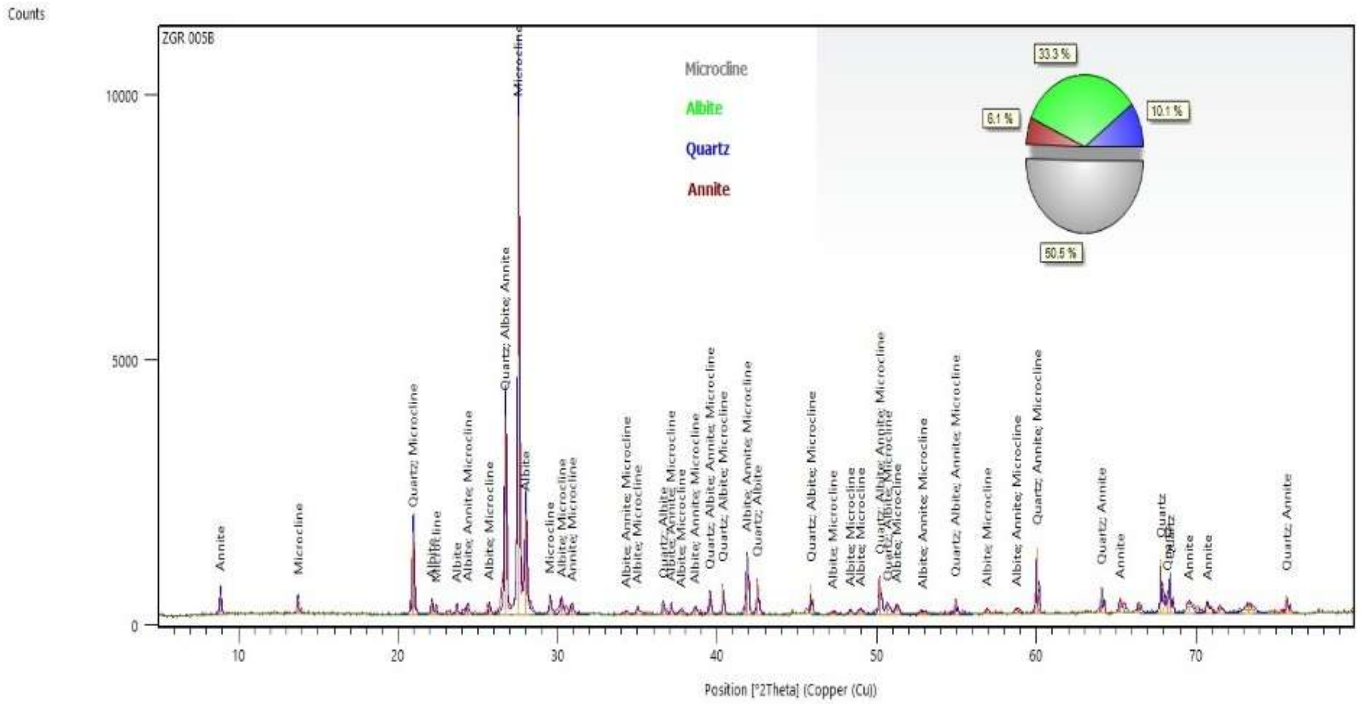

Figure 4.9m. Diffractogram of Rock sample, **ZGR/ 005B** with **Microcline, Albite, Quartz and Annite** as major minerals.

APPENDIX F

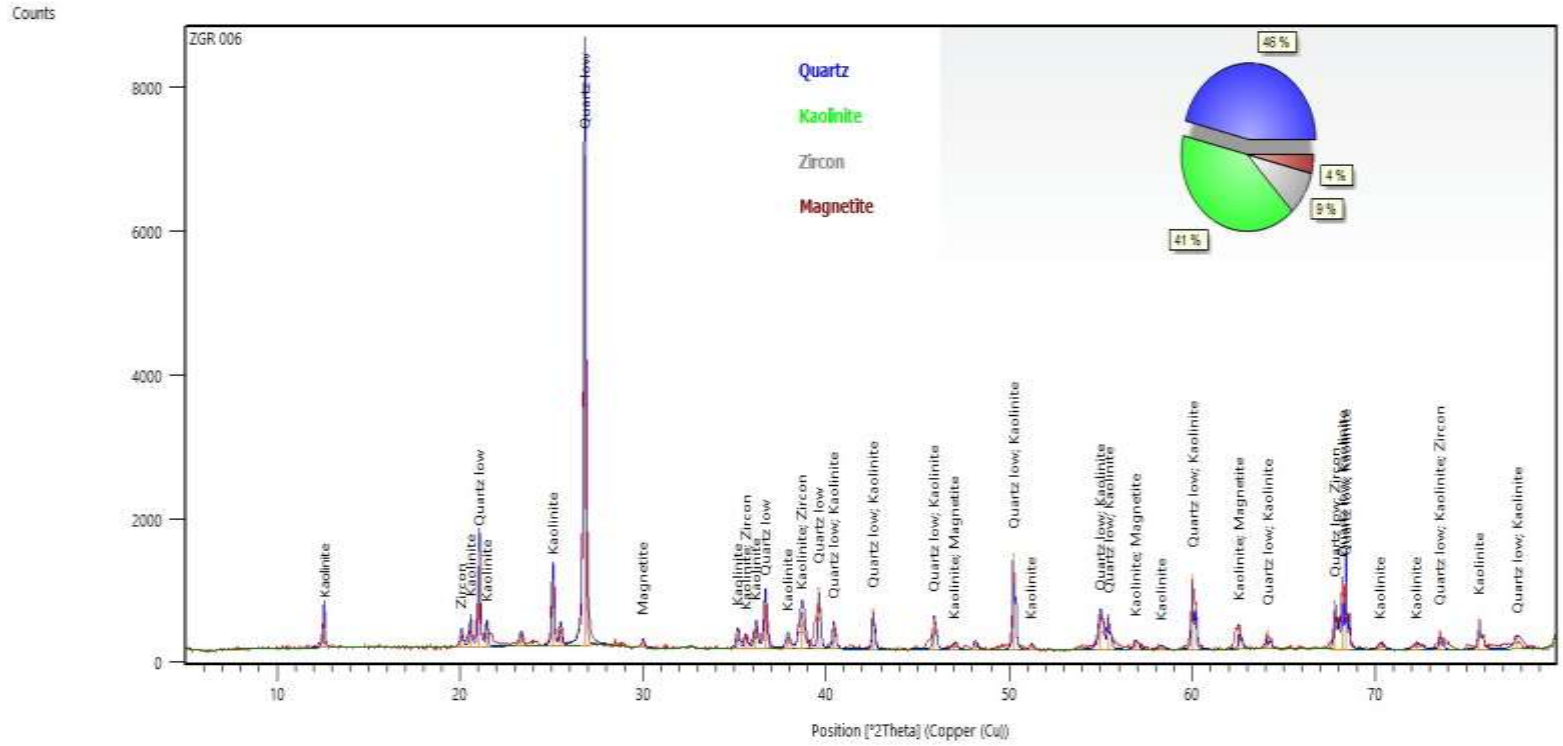

Figure 4.9m. Diffractogram of Rock sample, **ZGR/006** with **Quartz, Kaolinite, Zircon** and **Magnetite** as the major mineral

APPENDIX G

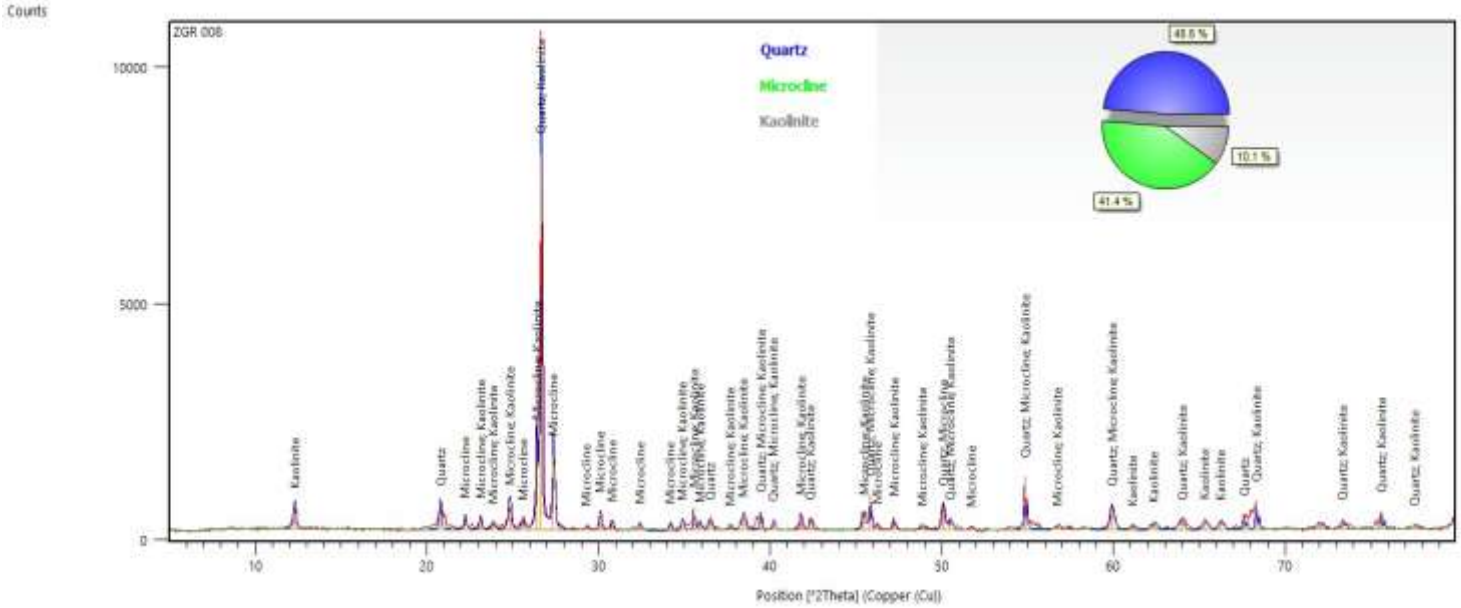

Figure 4.9n. Diffractogram of Rock sample **ZGR/008**, with **Quartz, Microcline** and **Kaolinite** as major minerals

APPENDIX H

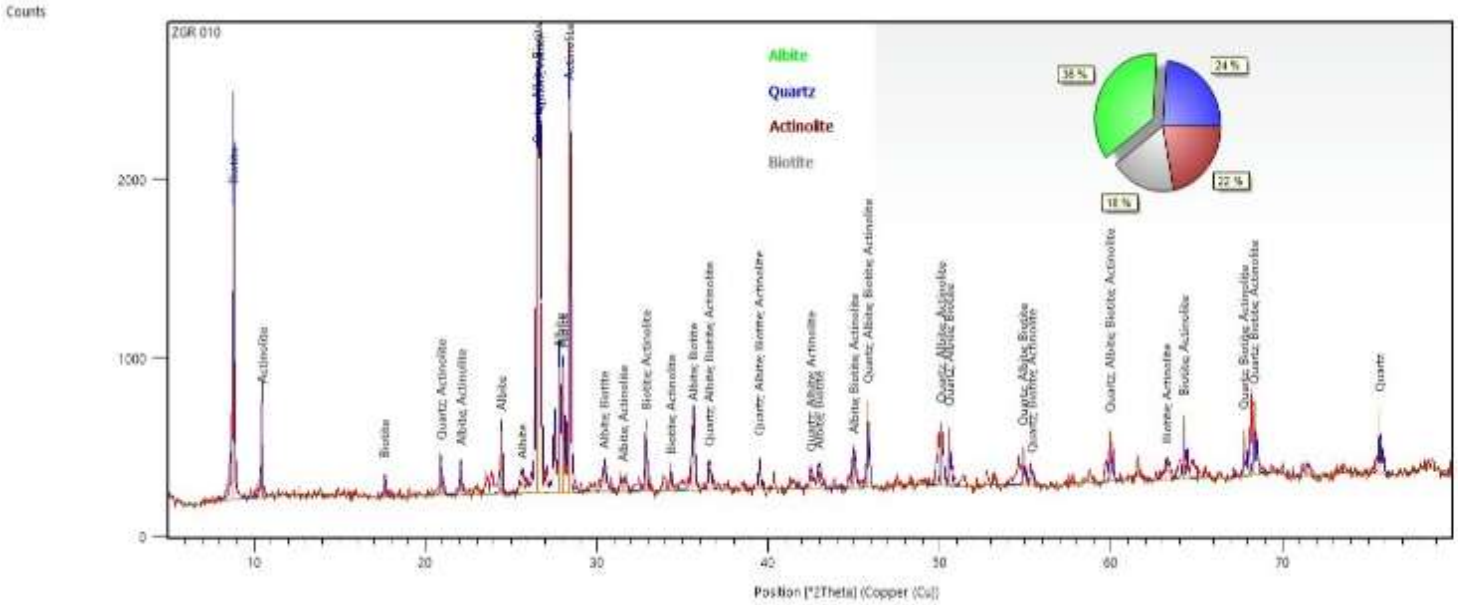

Figure 4.9o. Diffractogram of Rock sample **ZGR/010**, with **Albite**, **Quartz, Actinolite** and **Biotite** as the major minerals

APPENDIX I

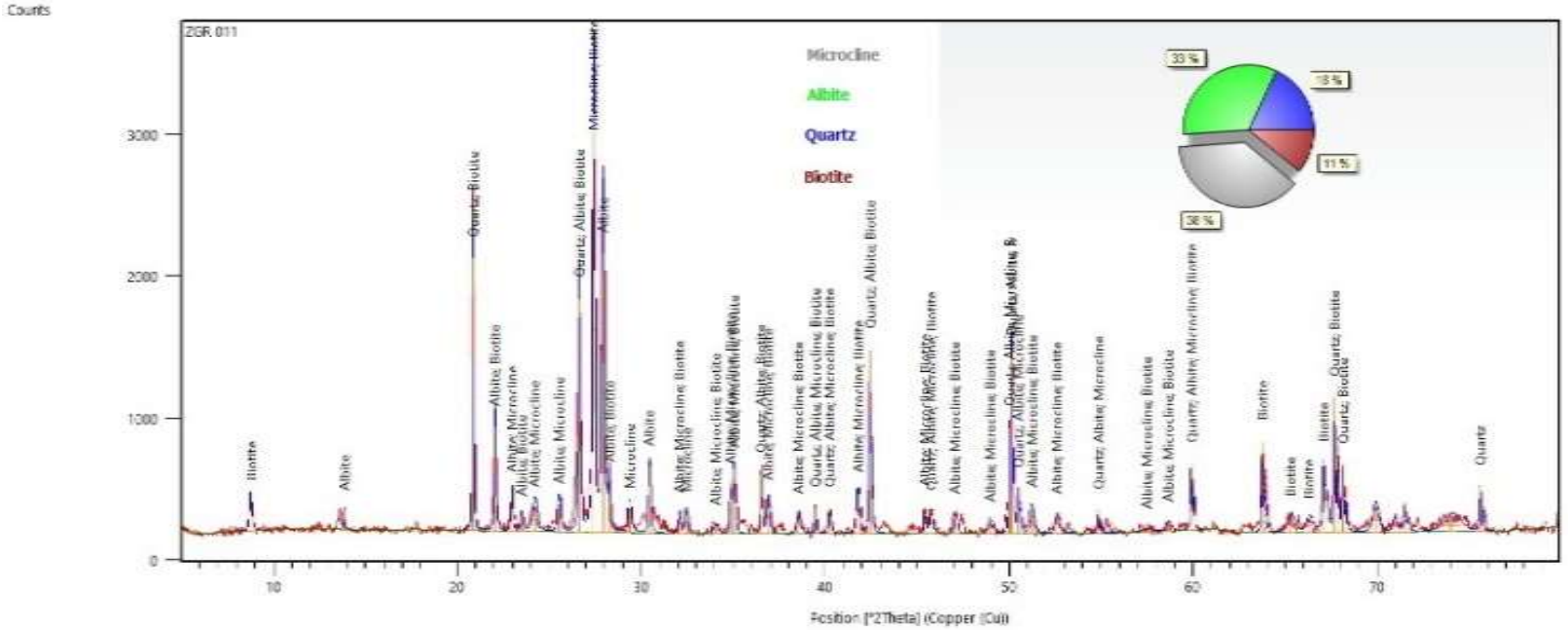

Figure 4.9p. Diffractogram of Rock sample **ZGR/011**, with **Microcline**, **Albite**, **Quartz** and **Biotite** as major minerals

APPENDIX J

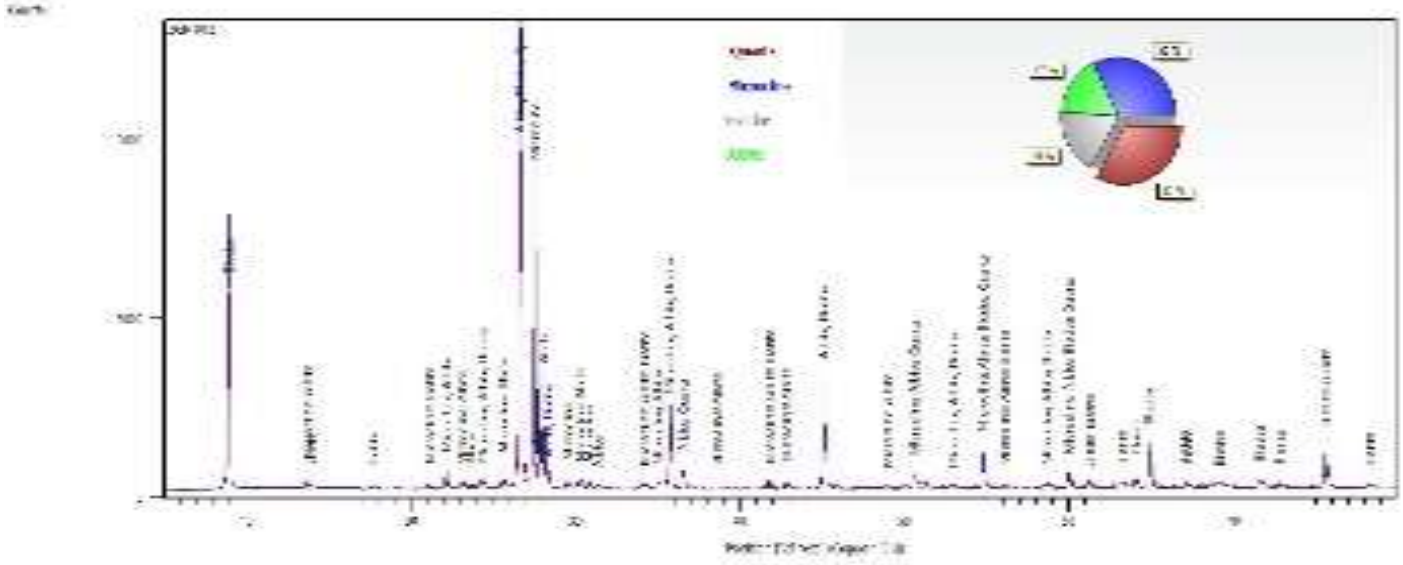

Figure 4.9q. Diffractogram of Rock sample ZGR/012 with **Microcline**, **Albite**, **Quartz** and **Biotite** as major minerals

APPENDIX K

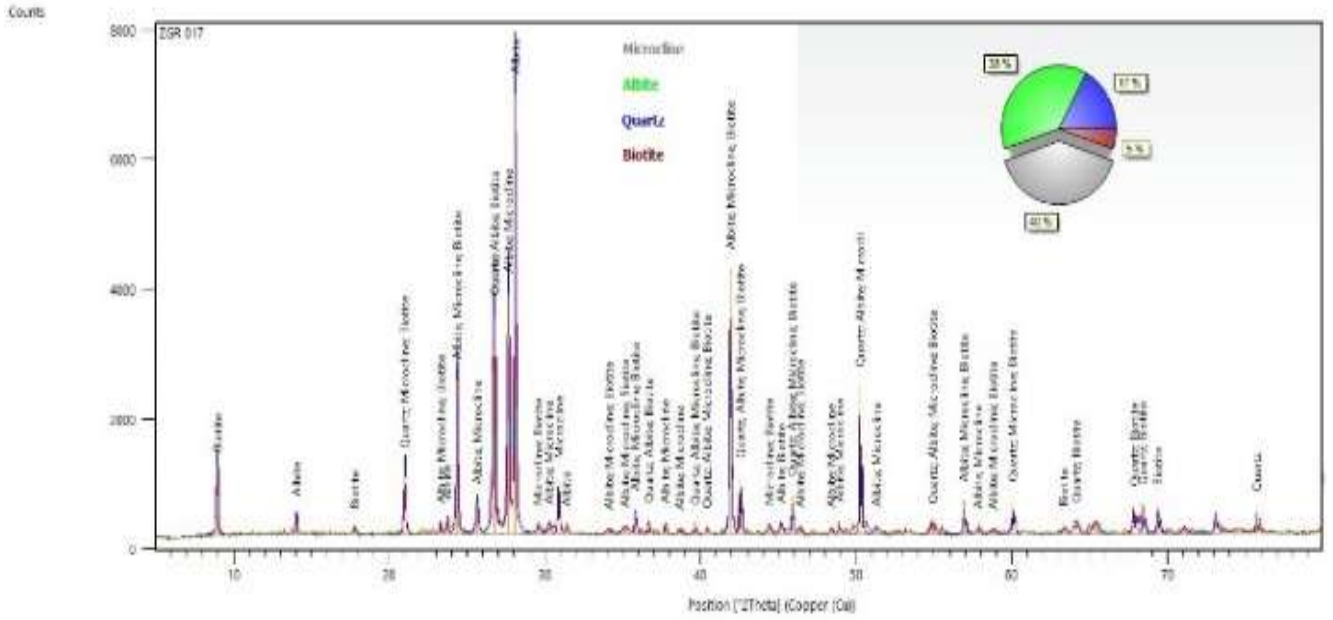

Figure 4.9r. Diffractogram of Rock sample **ZGR/017** with **Microcline**, **Albite**, **Quartz** and **Biotite** as major minerals

APPENDIX L

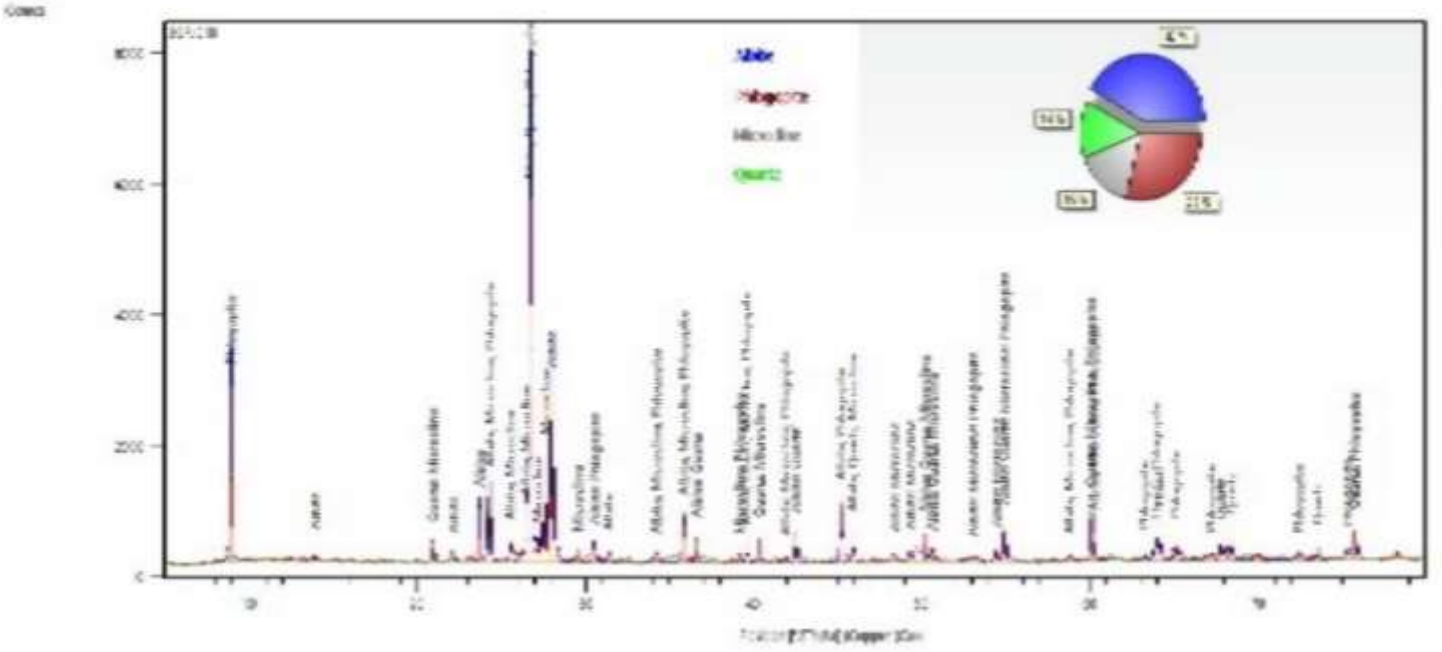

Figure 4.9s. Diffractogram of Rock sample **ZGR/018,** with **Albite, Phlogopite**, Microcline and **Quartz** as the major minerals

APPENDIX M

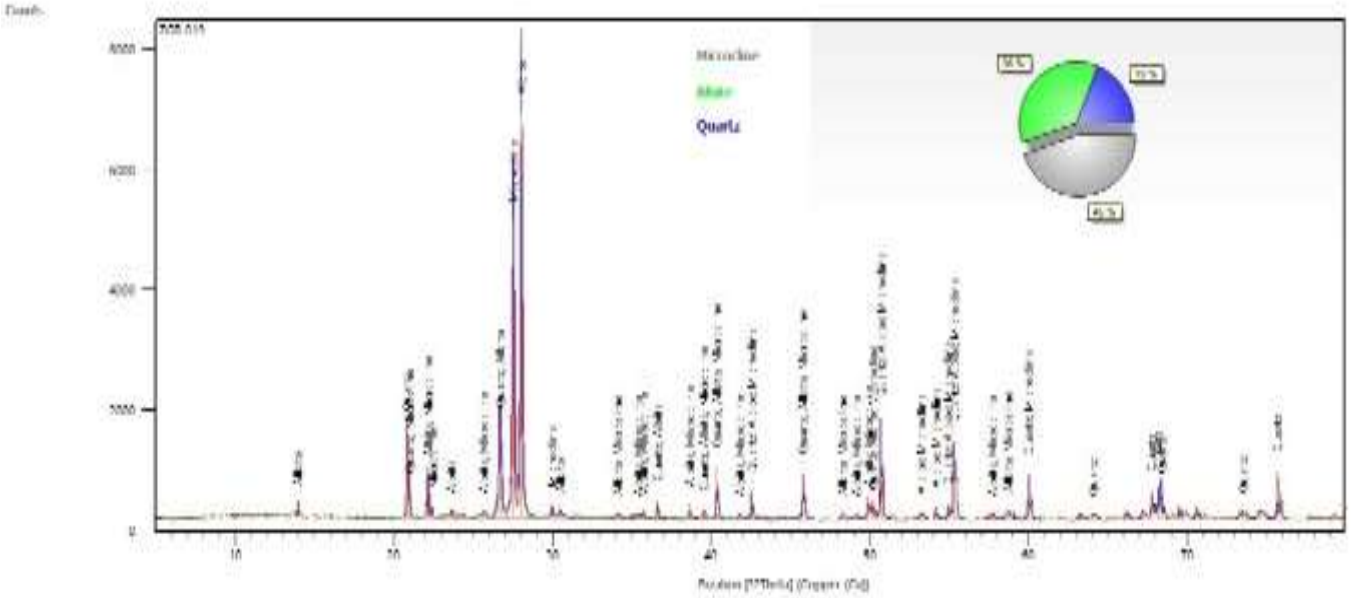

Figure 4.9t. Diffractogram of Rock sample, **ZGR/019** with **Albite, Microcline** and **Quartz** as major minerals